

AALBORG UNIVERSITY

WIRELESS COMMUNICATION SYSTEMS 9-10

**Enabling the Spectral Efficient
Coexistence of Device to Device
and Device to Infrastructure
communications through
Opportunistic Interference
Cancellation**

Authors:

Enrique Saez Gil
Andrés Buendía Gil

Supervisors:

Nuno Kiilerich Pratas
Germán Corrales Madueño

MASTER THESIS



AALBORG UNIVERSITET

Department of Electronic Systems Electronic Engineering

Fredrik Bajers Vej 7
9220 Aalborg Ø
Telefon 99 40 86 00
<http://es.aau.dk>

Title:

Enabling the Spectral Efficient Coexistence of Device to Device and Device to Infrastructure communications through Opportunistic Interference Cancellation

Subject:

Interference cancellation for radio access technologies with focus on the GSM system

Project period:

WCS 9-10, 2013-2014

Group:

Group 952

Authors:

Enrique Saez Gil
Andrés Buendía Gil

Supervisors:

Germán Corrales Madueño
Nuno Pratas

Copies: 5

Page count: 111

Appendix: 5

Completed: June 4th, 2014

Synopsis:

This Thesis addresses the main challenge associated to the deployment of new generation cellular systems: spectrum limitations. The goal is to test the feasibility of the coexistence of two different radio access systems working in the same frequency. For this purpose and taking into account the existent literature, an interference cancellation scheme is proposed. Both simulation and implementation models are developed to test the performance of the proposed interference cancellation scheme and its applicability in a real life scenario.

To conclude the proposed solution is rendered to be very valuable if implemented in one or both ends of the communication link providing a significant capacity gain and achieving the initial goal for the coexistence of two different radio access systems under a single frequency. Finally a perspective on future developments and improvements are suggested.

Preface

This Master Thesis is the result of the work conducted as part of the curriculum for the 9th and 10th semesters in the Wireless Communication Systems master's programme at the Department of Electronic Engineering, Aalborg University. The Thesis deals with “Enabling the Spectral Efficient Coexistence of Device to Device communications and Device to Infrastructure through Opportunistic Interference Cancellation” and spans from September 7th, 2013 to June 4th, 2014. It was supervised by Dr. Nuno Kiilerich Pratas and Phd. Fellow Germán Corrales Madueño.

Reading guide

Readers of this report, are expected to have prior knowledge with accordance to first three semesters of WCS, or higher.

References to literature is done using a numerical notation, enclosed in square brackets, e.g. [1].

Attached to this report is a CD containing Matlab code developed for the simulations as well as other bibliography.

Andrés Buendía Gil

Enrique Saez Gil

Contents

1	Introduction	1
1.1	Spectrum considerations	2
1.2	Implementation considerations	3
1.3	Motivation	4
2	Problem Definition	5
2.1	Scenario	5
2.2	Delimitations	8
2.3	Problem Formulation	8
2.4	Objectives	9
3	State of the art	10
3.1	D2D/M2M communications overview	10
3.2	Interference cancellation state of the art	10
3.2.1	Interference suppression as a means to enhance system performance	11
3.2.2	Controlled interference as a means to enhance system performance	12
3.2.3	Capture Effect	12
4	Method Description	14
4.1	Scenario recap	14
4.1.1	Interference modeling	16
4.2	Fundamentals of Capture Effect	16
4.3	Iterative SIC Algorithm	17
4.3.1	Synchronous link level model	18
5	Simulations	22
5.1	Physical Level Simulations	23
5.1.1	SIC reference case	23
5.1.2	SIC for OFDM and GMSK, reference cases	24
5.1.3	Implementation of an iterative SIC Algorithm	30
5.2	Link level Simulations	33
5.2.1	Influence of coding in the FSR	34

5.2.2	Frame Success Rate (FSR) for OFDM and GMSK using SIC, reference cases	36
5.2.3	Analysis of the iterative SIC algorithm at the Link level	37
5.3	System level Simulations	38
5.3.1	System level simulation for Orthogonal Resources . . .	39
5.3.2	System level simulation for Shared Resources	41
5.4	Throughput comparison for a system using orthogonal versus shared resources	45
5.5	Simulations using the guidelines of the METIS project	47
5.5.1	System performance from the eNodeB perspective . .	48
5.5.2	System performance from the perspective of the D2D UE	53
5.5.3	Results discussion for the METIS simulations	59
6	Implementation	60
6.1	Hardware requirements	60
6.2	Software tools	61
6.3	Setup Description	61
6.3.1	GMSK modulation and demodulation	65
6.3.2	Synchronization considerations	66
6.3.3	Bandwidth and Rate considerations	67
6.4	Interference cancellation process	68
6.4.1	Interference regeneration	68
6.4.2	Amplitude matching	69
6.5	Initial interference cancellation scheme	69
6.5.1	Initial interference cancellation results	70
6.6	Proposed interference cancellation scheme	70
6.6.1	De-compensation of the sampling clock shift	71
6.6.2	Proposed interference cancellation scheme results . . .	71
6.7	Experimental results discussion	73
7	Conclusion	76
7.1	Summary	76
7.1.1	Research contributions	77
7.1.2	Expected applications	77
7.2	Future outlook	78
A	Cellular Networks	80
A.1	Channel Considerations	80
A.2	Frequency Division Duplex and Time Division Duplex	82
A.2.1	Frequency Division Duplexing	82
A.2.2	Time Division Duplexing	82
A.3	Multiple Access Techniques	83
A.3.1	Frequency Division Multiple Access	83

A.3.2	Time Division Multiple Access	83
A.3.3	Code Division Multiple Access	84
A.4	Cellular Network planning	84
A.4.1	Signal to Noise Ratio and Signal to Interference Ratio considerations	86
B	Basic Principles of GSM Physical Channel	87
B.1	GMSK	87
B.2	Multiple Access Scheme	88
B.2.1	GSM Data Burst	89
C	Basic Principles of LTE Physical Channel	90
C.1	Principles of OFDM	90
C.1.1	Peak average power ratio (PAPR)	91
C.2	Frame structure	92
C.3	Downlink Transmissions	93
C.3.1	Throughput calculations	93
D	USRP2 Architecture	95
D.1	USRP2 Basic Description	95
D.1.1	Daughterboard	95
D.1.2	Field Programmable Gate Array (Field Programmable Gate Array (FPGA))	96
	Acronyms	97
	List of figures	101
	List of tables	105
	Bibliography	107

Chapter 1

Introduction

The surge in the number of mobile terminals and the ever-increasing capacity demanded by each of them have placed the network operators in a difficult position in which they must service their wireless customers in an "anything-anywhere-anytime" manner [1]. At the same time Over The Top (OTT) service providers are profiting from the deployment of advanced network infrastructures while pushing the network operators aside to play a secondary role in the telecommunications business relegating them to being the so called "dumb pipes". However, the rise of Machine to Machine (M2M) communications and the possibilities associated to Device to Device (D2D) communications provide the network operators with the chance to regain a central role in the industry by leading the innovation in this field and by establishing appropriate business models. One of the plausible business models to be implemented is the operators controlled D2D communications in LTE-Advanced networks [2].

D2D communications refer to technologies that enable devices to communicate directly without an infrastructure of access points or base stations [2]. Traditional D2D technologies available to consumers such as Bluetooth or WiFi working in the unlicensed Industrial Scientific and Medical (ISM) radio band face many technical limitations like uncontrolled interference or limited range. The alternative proposed by the operators controlled D2D (OC-D2D) communications in LTE-Advanced revolves around the idea of devices communicating with each other under the control of the cellular network or the network operator with a guaranteed quality of service [2] as opposed to traditional D2D techniques. Depending on the level of operator control over the D2D communication two categories can be defined [2]:

- Fully controlled D2D mode: the D2D link shares the cellular licensed band with the other cellular connections being the network in full control over the D2D connection.

- Loosely controlled D2D mode: the network operator simply authenticates the different D2D devices which can establish D2D connections and communications autonomously by using the unlicensed band or by using a dedicated carrier on the licensed band.

The fully controlled OC-D2D communications paradigm will be adopted as the basis for this Thesis. Therefore it is assumed that the Base Station (BS) is in charge of control plane functions such as connection setup and maintenance, and data plane functions like resource allocation [2]. The many technical challenges associated with this paradigm will be discussed in Chapter 3.2.3.

This Thesis will investigate the possibility of improving the network performance through digital signal processing techniques that would require only a hardware and software upgrade in the BS as later explained in Section 1.3.

1.1 Spectrum considerations

The telecommunications industry is a regulated sector. Each geographic region has its own regulatory agency such as the Federal Communications Commission (FCC) in the United States (US) or its counterpart in Europe, the European Conference of Postal and Telecommunications Administrations (CEPT). These agencies regulate different aspects of the telecommunications industry including the radio frequency spectrum allocation.

Different frequency bands are allocated by the regulatory agencies for specific services. Thereafter, the national governments and regulators allocate the spectrum to network operators commonly through auctions [3]. Initially new frequency bands could be progressively allocated to keep up with the increasing demand but the radio frequency spectrum is a scarce and costly resource and its implications are of paramount importance during the design of a cellular radio system. In order to overcome the limited spectrum available for each operator and maximize its Return over Investment (ROI) different approaches have been adopted, the most common being frequency reuse [4].

Network operators can service entire geographical regions thanks to frequency reuse by dividing them into smaller regions (clusters) which are allocated all the frequencies at the disposal of the operator. These clusters, which are again divided into cells, populate the entire geographical network to be serviced. Network planning is determined by two factors:

- Reuse distance: refers to the minimum distance that must exist between two cells using the same frequency.

- Reuse ratio: refers to the number of cells that cannot use the same frequency for transmission.

As the number of terminals to be served and more importantly, the demand of each terminal increases, the reuse ratio tends to be smaller in order to cope with the increased demand yielding network scenarios where the interference becomes more and more limiting to system performance [5].

An alternative solution to this problem is enabling the coexistence at the same frequency of traditional Device to Infrastructure (D2I) communications with D2D communications (to be referred throughout this Thesis as primary and secondary systems respectively). [6] defines four types of gain related to D2D.

- Proximity gain, the short range inherent to D2D communications allows for high data rate, low delay and low power consumption.
- Hop gain, traditional D2I communications uses two hop instead of one for D2D using less resources.
- Reuse gain, D2D and D2I nodes are able to coexist in same frequency band.
- Pairing gain, a device can choose to work in D2I or D2D mode.

There are many technical challenges associated with the deployment of the aforementioned OC-D2D network infrastructure such as power control, resource allocation and interference management [1] as later detailed in Chapter 3. However, as outlined in Chapter 2, this Thesis will be focused exclusively on the interference manipulation in both ends of the communication link, the BS and the User Equipment (UE). This is a crucial issue in order to achieve a solid coexistence between the D2D and the D2I communication flows.

1.2 Implementation considerations

Power consumption is closely related to computational complexity. In a mobility scenario an increased power consumption might be a deterrent for the deployment of computationally demanding solutions. Nonetheless, it is assumed that overcoming the adverse interference conditions which might lead to an increased power consumption is preferred over a poor service or not service at all.

Additionally, the rapid adoption of smartphones and innovative solutions such as "Cloud run" for BSs result in a staggering increase of the computational power available at both ends of the communication link. Taking advantage of this technological trend in which performance prevails

over computational complexity, this Thesis will be focused on developing a software-based solution.

Hence, it is considered very relevant the exploration of emerging solutions such as Software Defined Radio (SDR) that provides a highly customizable platform for development and research in mobile communications. An example of a cutting-edge applications that takes full advantage of these features is OpenBTS that offers a limited but functional Free and Open-Source Software (FOSS) implementation of the publicly available Global System for Mobile Communications (GSM) standard.

1.3 Motivation

When confronting the challenges described throughout this Chapter, network operators are at crossroads. Legacy cellular networks are not suitable nor designed to cope with the constantly increasing capacity demand or with the forecast huge increase in the number of connected devices. However, it is in the interest of network operators to invest and research for alternatives that allow these new users to be serviced with the minimum infrastructure investment.

In order to keep up with the increasing demand, network operators gradually deploy new radio access technologies that, among other advantages, offer improved frequency efficiency. These upgrades eventually force the deployed and widely adopted radio access technologies, such as GSM, to be removed from the market.

Considering the described background, this Thesis will attempt to prove that:

- A complementary solution to frequency reuse can be implemented in software for maximizing the capacity and quality of the cellular network under the constraint imposed by the limited number of frequencies allocated to each operator.
- Traditionally, network planning is based on a radio-electric study. However, this study needs to be complemented with the interference cancellation capabilities of the serviced devices and the radio access infrastructure to enable the successful coexistence of two different radio access systems in the same frequency.
- The withdrawal of the legacy technologies might not prove as beneficial as enabling its coexistence along the new solutions.
- The coexistence of two different radio access technologies under the same frequency is possible if the interference between both systems is handled adequately.

Chapter 2

Problem Definition

2.1 Scenario

As stated in the previous Chapter even though network operators are deploying new generation networks to satisfy the increased capacity demand and number of connected devices they are inherently constrained by the limited radio spectrum. A concise and graphical representation of the forecast transition from traditional D2I to D2D networks can be seen in Figure 2.1 where it can be observed the following¹:

- On the left half of the figure, a traditional D2I network in which the UE requires the BS for all its communication purposes within the network.
- On the right half of the figure, a D2D communication network can be seen in which different technologies coexist under the supervision of the eNodeB.

In this scenario the D2D communication is considered as an underlay to the cellular system using the same resources and being controlled by the eNodeB as in the OC-D2D scenario mentioned in Chapter 1. The UE is served by the eNodeB and may communicate directly with other UEs over the D2D links under the control of the eNodeB that allocates the resources used for the cellular communications and the D2D links [7]. The eNodeB sets the constraints of the transmit power of the D2D transmitters to limit the interference experienced at the cellular receivers [7]. As explained in Appendix A.4 on page 84 cellular systems divide areas into cells. The cells are grouped into clusters and within the cluster each cell is assigned a unique group of channels. By reusing the same channels from cluster to

¹In this Thesis it is assumed that the Base Station, that serves the legacy users, and the Evolved Node B or E-UTRAN Node B (eNodeB), that serves the D2D users, are placed in the same position and their control is centralized. Hence, there is no noticeable difference between them with regards to the work to be conducted in this Thesis. Consequently, throughout this document the Base Station will be noted as eNodeB

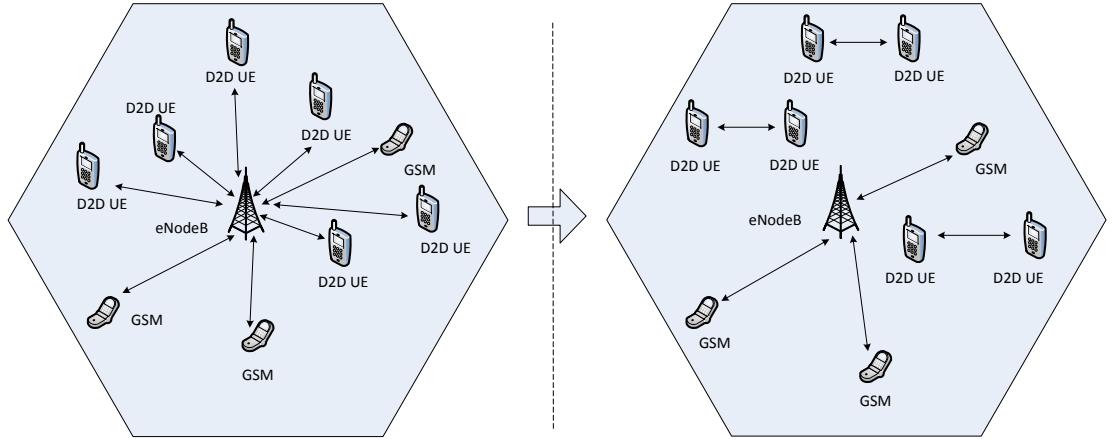


Figure 2.1: *Transition from D2I system to a D2D system. Figure adapted from [6].*

cluster, entire geographical areas can be serviced at the expense of cochannel interference. However, this Thesis will be limited to the study of a single cell and interference from neighbouring cells will not be taken into account.

A more detailed representation of the scenario depicted in the right-side of Figure 2.1 can be seen in Figure 2.2. The most relevant elements in this scenario and its functions are:

- The eNodeB: controls both the UEs and D2D links.
- The legacy user (Device 1): communication has higher priority than the D2D users. The legacy communication is based on Frequency Division Duplex (FDD), making use of different frequencies for uplink and downlink.
- The D2D users (Device 2 and Device 3): both devices establish a communication link between them reusing the frequency of the legacy user's Uplink.

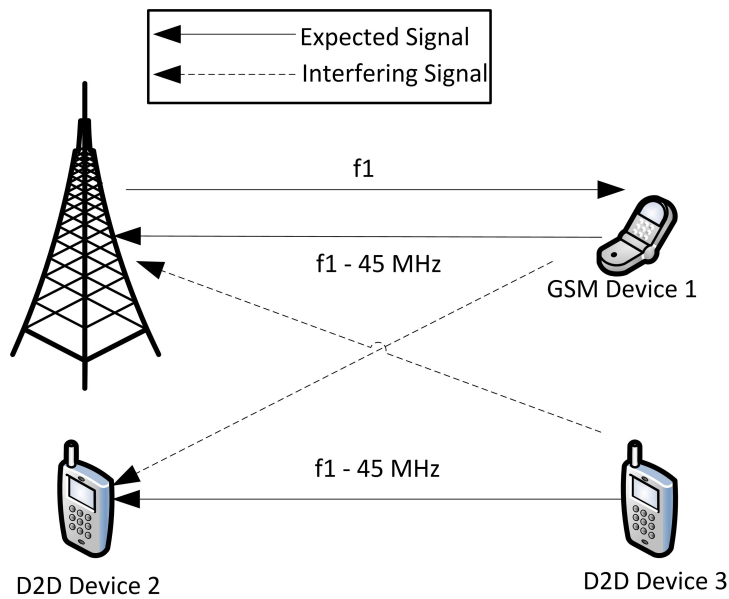


Figure 2.2: Reference scenario: a legacy device coexisting with a D2D link in the same frequency uplink.

The scenario depicted in Figure 2.2 will serve as the reference for this Thesis.

Throughout this document it will be assumed that the legacy system employs the GSM technology and the D2D system uses Long Term Evolution (LTE) downlink. It should be remarked that the D2D link will be modelled as Time Division Duplex (TDD). Furthermore it will be assumed that at any given instant, only one of the D2D UEs is transmitting in the same frequency as the legacy link. Furthermore, the D2D pair is set to work in the frequency corresponding to the uplink of the legacy system for the following reasons:

- The proposed solution should be transparent for the legacy user.
- The eNodeB does not have the power constraints of the mobility user associated to an increased computational effort required by interference cancellation.
- The eNodeB has access to more side information than the UE. As explained in Chapter 1 in this Thesis it has been assumed that the network is in full control of the D2D operations and therefore it is also in control of the interference produced by these connections.

In the aforementioned scenario two different study cases for the interference cancellation should be considered:

- Interference cancellation at the eNodeB: it can be assumed to have access to certain amount of side information, such as the expected interference levels produced by the D2D, modulations, operational frequencies.
- Interference cancellation at D2D devices: the access to side information is more restricted. Nevertheless, it is assumed that the eNodeB will send enough side information to the D2D pair to establish a efficient communication without interfering with the legacy system.

2.2 Delimitations

This section will summarize the delimitations taken into account in this Thesis. It should be noted that as mentioned in the previous section, the scenario under consideration is a fully controlled D2D mode. Although some of the limitations have been already mentioned previously in this chapter, they will be further explained:

- The technical challenges associated to power control, resource allocation and interference management are considered out of the scope of this Thesis. As mentioned in Section 1.3 the objective of this Thesis is related to the cancellation of the existing interference in the UE and the eNodeB.
- A single cell with no interference from neighbouring cells is assumed.
- The receiver is able to perform a perfect estimation of the channel.
- The receiver is assumed to stay in the same position, therefore no Doppler effect has been taken into account.
- Furthermore some of the potential simplifications proposed by [5] are included:
 - No Adjacent Channel Interference will be taken into consideration based on the potential simplifications.
 - Only a synchronous system simulation will be developed due to the complexity constraints associated to asynchronous networks. Therefore the receiver is assumed to be able to perfectly synchronize regardless of decoding the desired or the interfering signal.

2.3 Problem Formulation

As previously stated, the Thesis will be based on the Operator Controlled D2D (OC-D2D) paradigm in which it is investigated if a secondary system (D2D) can operate along the primary system (D2I) using the same frequency.

The eNodeB is assumed to control the primary and secondary systems. Under these assumptions the challenges faced by the network are:

- The BS has to cope with the interference caused by the operation of the D2D system.
- The secondary receiver has to cope with the interference caused by the primary transmitter.
- The limited power available to the secondary transmitter (set by the eNodeB) constraints the capacity of the D2D communication link.

Considering the aforementioned challenges and the delimitations enumerated in the previous section, the following issues can be formulated:

- Considering a single cell scenario, is it possible through signal processing and related techniques to guarantee a minimum quality of service in a D2D system reusing the same frequency of the D2I system albeit the existent interference between both systems?
- Considering a single cell scenario, is it possible to manipulate the interference suffered by both the BS and the UE in such a way that results in an increased system capacity by allowing more traffic to be routed through the D2D communication links?

2.4 Objectives

The ultimate goal of the work here presented is to design a solution that would allow two different wireless systems to coexist in the same frequency, working under a heavier interference and consequently increasing the capacity and reliability of the network. For this purpose a digital signal processing solution, capable of cancelling an interfering signal with a minimum amount of previous information about it, will be developed. Moreover it is of interest to analyze the implementation issues related to the deployment in a real system. Hence the following issues will be addressed:

- The design and development of a Single Antenna Interference Cancellation (SAIC) scheme.
- Measurement of the performance of the proposed interference cancellation scheme.
- Measurement from a system level perspective of the performance of two different technologies coexisting the selected algorithm.
- Implementation of the proposed algorithm in a real setup.

Chapter 3

State of the art

3.1 D2D/M2M communications overview

The D2D communications is a technique that aims for providing wireless peer-to-peer services and enhance spectrum utilization in the LTE-Advanced networks. The user equipments (UEs) are allowed to directly communicate between each other by reusing the cellular resources rather than using uplink and downlink resources in the cellular mode when communicating via the base station[6].

3.2 Interference cancellation state of the art

Interference has been considered until recently as a negative factor for the performance of cellular radio systems. In particular co-channel interference is a fundamental topic in the relevant literature; [8], [9] and a key design aspect because of its influence on spectral efficiency. Two models for interference are assumed in research [10] :

- Protocol model: concurrent transmissions within a given range of the receiver will cause a collision resulting in packet loss.
- Physical model: packet loss occurs when the Signal to Interfering Noise Ratio (SINR) falls below a given threshold.

This Thesis will deal with interference assuming the physical model. Recent approaches suggest that interference can be regarded as advantageous under the adequate circumstances and the gains obtained from exploiting it are not to be disregarded as insignificant. Consequently in this section the previous work related to interference management will be classified into two main groups depending on whether it is considered as positive or negative regarding its influence on system performance.

3.2.1 Interference suppression as a means to enhance system performance

A traditional approach to overcome the limits inherent to interference is interference cancellation and a wide background is available in this field. Depending on whether the cancellation technique is at the transmitter side or at the receiver side the interference cancellation techniques can be classified as follows [9]

- Pre-IC: This technique is established in the transmitter side and revolves around the precoding of the information to be sent based on the channel state information exchanged via signalling. Perfect channel state information is very difficult to accomplish and errors introduced in the precoding phase increase the signalling overhead and the system inefficiency.
- Post-IC: This technique is established in the receiver side. The basis of the Post-IC techniques is the decoding of the desired information and using this information along channel estimates to cancel a fraction of the received interference from the original signal.

Post-IC techniques are regarded to fit best the requirements derived from the project goal and the scenario under consideration. The available Post-IC techniques can be further classified into:

- Techniques that make use of a generic algorithm [8], [9], [11]: based on decoding the desired and interfering signals using either SAIC, Single user decoding (SUD) or joint decoding schemes. According to [5] SAIC is "a generic name for techniques which attempt to cancel or suppress interference by means of signal processing without the use of multiple antennas". Most SAIC algorithms can only cancel one interferer and the effectiveness is dependent on the remaining interfering signals. Currently SAIC is considered as a "viable and feasible technology that will support voice capacity gains for both asynchronous and synchronous networks when applied to Gaussian Minimum Shift Keying (GMSK) modulation" [5]. [11] and [12] investigate the use of power control along SAIC and show that a higher throughput can be achieved. The previous research dealing with interference cancellation for multiple antenna systems [13], is considered out of the scope of this Thesis as discussed in Chapter 2.
- Techniques that make use of specific solutions for previously known modulations [14]: these solutions are mainly focused on GMSK signals. In [15] it is shown how to approximate a GMSK signal into its linearized form. [14] takes advantage of this approximation to recover an 8-Phase Shift Keying (PSK) signal. Additionally [16]

proposes an algorithm to create a virtual antenna from which an extra diversity grade can be obtained. Other techniques focused on GSM interference cancellation like [17] propose a joint demodulation for a burst-synchronous GSM/Enhanced Data Rates for GSM Evolution (EDGE) system to cancel a dominant cochannel interferer. In [18] it is proposed a Constant Modulus Single Antenna Interference Cancellation (CM-SAIC) along with multiple channel estimation.

3.2.2 Controlled interference as a means to enhance system performance

An alternative proposal is using the interference to enhance the communication system. As detailed in [19] the transmission of the secondary transmitter can be precoded in such a way that it allows constructive interference to the primary user. However, this approach requires knowledge of channel state information along with the redefinition of the estimator to determine the interfering symbols and the constructive interference sectors. Hence, it will not be further considered.

3.2.3 Capture Effect

In [20] capture effect is defined as "the ability of certain radios to receive a signal from one transmitter despite interference from another transmitter" allowing gains through recovery of the stronger packet from collisions. This ability is studied in [10] by setting up a testbed in which two nodes transmit simultaneously. One of the nodes transmits with a fixed power while the power of the other node is varied. The results, featured in Figure 3.1, exhibit that at the receiver three different regions can be distinguished in the curve of packet reception rate as a function of the SINR:

- White regions: in these regions one of the sources is assured reception even in presence of the other concurrent transmission.
- Black region: in this region neither of the transmissions is received.
- Grey regions: in these regions packet reception is intermittent.

The opportunistic decoding scheme from [10] provides a valuable foundation for the work to be conducted. However, [21] goes beyond by including a cancellation scheme, detailed in section 4.2, that consists on:

- Opportunistically demodulating the stronger signal.
- If the interfering signal is much stronger than the desired signal, the result of the demodulation is used to reconstruct the interfering signal with the help of the estimated channel impulse response. The reconstructed signal is subtracted from the received signal to reveal the desired signal.

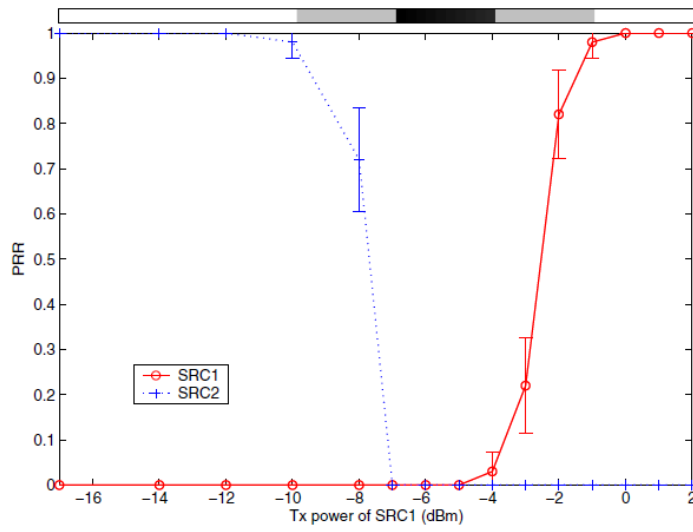


Figure 3.1: *Transmission Power level to packet recognized at the receiver (PRR) [20].*

Taking into account the existing work in relation to interference cancellation outlined throughout this Chapter, the opportunistic decoding scheme proposed by [20] and the cancellation scheme proposed by [21] are considered the most relevant for the scenario under consideration and will be further studied.

Chapter 4

Method Description

4.1 Scenario recap

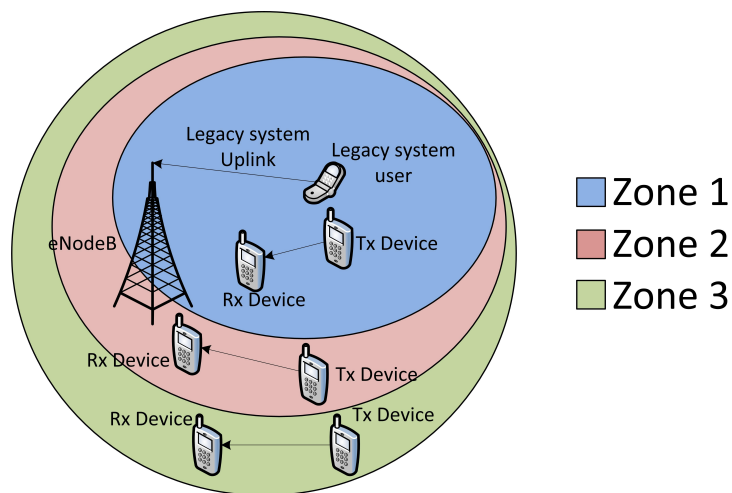


Figure 4.1: Representation of the different SIR zones for the reference scenario of Figure 2.2 on page 7.

Assuming that the interference cancellation process takes place at the D2D pairs and considering the signal from the D2D system as the desired signal and the signal from the legacy user as the interfering signal, the reference scenario for this Thesis, depicted on Figure 2.2 on page 7, can be represented as in Figure 4.1. Three different zones can be identified as a function of the SIR level at the receiving device.

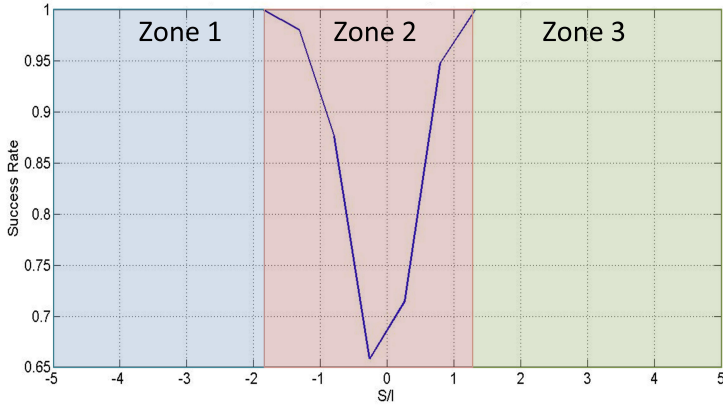


Figure 4.2: *Example of zone delimitation as a function of the SIR.*

Figure 4.1 should be considered together with Figure 4.2. For both figures the difference in power between the interfering and the desired signals, as a consequence of the different distances between the active D2D UE and the GSM user determine the SIR. These figures can be interpreted as follows:

- Zones 1 and 3: the power level of one of the signals (either the interfering signal or the desired signal) is much higher than the power of the other signal, resulting in a considerably high or considerably low SIR that allows the exploitation of a capture effect.
- Zone 2: the power level of the interfering signal and the desired signal is approximately the same.

The boundaries for Zone 2 are defined as the SIR value that allows a bit success rate of 0.999 [22], in accordance with the minimum system requirements of GSM. As detailed in the Section 4.2 the manipulation of the interference is different based on the SIR level. Therefore, the delimitation of the different zones is fundamental in terms of the designed interference cancellation solution.

In [23] it is proposed a solution to dynamically share the spectrum between GSM and LTE by reserving a small number of resources blocks for the GSM channels. In our current scenario [23] provides the possibility of disabling the subcarriers of LTE in cases where the SIR levels are comprehended between the boundaries of Zone 2, Figure 4.3.

As mentioned in Chapter 2, the interference cancellation process at each end of the communication link differs depending on the amount of side information available. Although the method described in section 4.3 can be implemented in both ends of the communication link, throughout this Chapter the proposed interference cancellation solution will disregard the

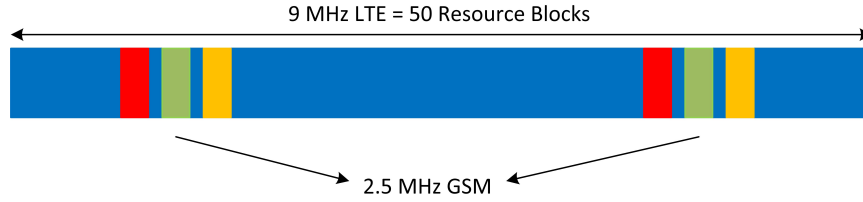


Figure 4.3: *Example of sharing spectrum for LTE and GSM.*

different advantages achievable with extra-side information. Further more in this document the interference cancellation process will be studied from the the eNodeB and from the D2D point of view, however no advantages related to side information have been taken into account in the studied cases.

4.1.1 Interference modeling

This section details how the power of a wideband signal will be measured with relation to a narrowband one in this document. These considerations are relevant because the classic definition of SIR that compares signals' power without taking into account the bandwidth are not valid in the context of this Thesis. In order to analyse signals with different bandwidths, the SIR will refer to the difference of the power spectral density instead of the subtraction of the total signal power as is typically defined.

4.2 Fundamentals of Capture Effect

In this section the capture effect technique will be described . This technique is the baseline for the algorithm shown in section 4.3.

The received sampled signal can be expressed as the summation of the desired signal, the interfering signal, and a noise component as:

$$r(n) = s(n) + i(n) + n(n) \quad (4.1)$$

Where $r(n)$ is the received signal, $s(n)$ is the desired signal, $i(n)$ is the interfering signal and $n(n)$ is Additive White Gaussian Noise (AWGN).

The Successive Interference Cancellation (SIC) technique is based on operating differently according to the difference in power of the desired and interfering signals. Two scenarios can be distinguished:

- The power level of the desired signal is higher than the interfering signal: in this case the desired signal can be directly decoded considering the interfering signal as noise. The SINR can be defined as follows;

$$\frac{S}{I + N} = \frac{S/N}{I/N + N/N} = \frac{\gamma_S}{\gamma_I + 1} \quad (4.2)$$

Being; S the received signal power, I the interfering signal power, N the noise power and γ_S , γ_I the SNR and INR respectively. This operation mode will be applied when the SINR is higher than a certain threshold, Γ_s ;

$$\frac{\gamma_S}{\gamma_I + 1} \geq \Gamma_s \quad (4.3)$$

The selection of the threshold depend on various factors such as the signals under consideration, the characteristics of the communication channel, among others.

- The power level of the desired signal is lower than the power level of the interfering signal: in contrast to the previous case, the desired signal is considered as noise so the interfering signal can be decoded and subtracted from the received signal. The result of this subtraction is used to attempt the decoding of the desired signal.

$$\frac{I}{S + N} = \frac{I/N}{S/N + N/N} = \frac{\gamma_I}{\gamma_S + 1} \quad (4.4)$$

In the same way as in the previous reasoning, this operation mode will be carried out if;

$$\frac{\gamma_I}{\gamma_S + 1} \geq \Gamma_i \quad (4.5)$$

Therefore the probability of decoding the desired signal is given by the sum of the probabilities of the two modes;

$$P_s = P\left(\frac{\gamma_S}{\gamma_I + 1} \geq \Gamma_s\right) + P\left(\gamma_S > \Gamma_s \mid \frac{\gamma_I}{\gamma_S + 1} > \Gamma_i, \frac{\gamma_S}{\gamma_I + 1} < \Gamma_s\right) \quad (4.6)$$

Bearing in mind the considered scenario, shown in Figure 4.1, two zones where the SIC technique can be applied can be clearly distinguished. The next section elaborates on this distinction as well as the inherent properties of the desired signal and the interfering one.

4.3 Iterative SIC Algorithm

As explained in Section 4.1 depending on the difference in the power level of the interfering and desired signals, for the scenario under investigation in this Thesis, two different zones can be distinguished. This distinction is crucial for the applicability of the algorithm based on the SIC technique detailed in the previous section.

Therefore, as shown in Figure 4.2, two different zones are clearly distinguished attending to the difference in the power level of the desired and interfering signals:

- High difference in power level between the interfering and the desired signals: in zone 1 and zone 3 the high difference in power level of the contending signals allows the application of a capture effect and as explained in [21] a SIC technique will be used.
- Small difference in power level between the interfering and the desired signals: in zone 2 it does not exist an efficient solution to decode the interfering signal or the desired one, therefore this zone will be assumed to be in most cases, avoidable through solutions like power control [11], or as proposed in [23] subcarrier disabling.

4.3.1 Synchronous link level model

As stated in Chapter 2 for the reference scenario of this Thesis, Figure 2.2 on page 7, it is studied the feasibility of the coexistence of two communication links using two different technologies, LTE and GSM. LTE employs Orthogonal Frequency Division Multiple Access (OFDMA) as an access scheme, while GSM uses Time Division Multiple Access (TDMA) with subcarrier division. A detailed description of the LTE and GSM access schemes can be found in Appendix B and C.

In this section, it will be assumed that independently of the SIR, the synchronization of both signals, GMSK for GSM and OFDMA for LTE is perfect. This might be challenging especially when the SIR is very low. However, there are several methods to achieve this target [24].

The sampled transmitted OFDMA signal can be expressed as follows;

$$x(n) = \sqrt{P_{tx}} \sum_{k=0}^{N-1} X(k) e^{j2\pi kn/N} \quad (4.7)$$

Where N is the total number of sub-carriers, $X(k)$ is the mapped symbol of the k th subcarrier and P_{tx} is the transmitted power. Considering a multipath channel $h(l)$ with L_{OFDMA} delays and assuming that the maximum delay is lower than the cyclic prefix, the output would be;

$$y(n) = \sqrt{P_{rx}} \sum_{l=0}^{L_{OFDMA}-1} h(l) x(n - D_l) \quad (4.8)$$

Being P_{rx} the received power and D_l the delay of the l th tap.

In the frequency domain the received OFDMA signal can be expressed as:

$$Y(k) = \sqrt{P_{rx}} X(k) \sum_{l=0}^{L_{OFDMA}-1} h(l) e^{-j2\pi k D_l/N} = \sqrt{P_{rx}} X(k) H(k) \quad (4.9)$$

Similarly, the GMSK signal can be expressed as:

$$s(n) = \sum a_m g(n - mT) \quad (4.10)$$

Being $s(n)$ a linearized GMSK, where a_m is the differential data, $g(n)$ is the pulse shaping filter and T is the symbol period. Noting as $h'(n)$ the multipath channel with L_{GMSK} delays seen by the GMSK signal, then the received signal would be;

$$z(n) = \sqrt{P_{rx}} \sum_{l=0}^{L_{GMSK}-1} h'(l) s(n - lT) \quad (4.11)$$

The aforementioned link level model in which a GMSK signal and an OFDMA signal use the same frequency can be represented from a spectral point of view as shown in Figure 4.4, where the GMSK signal is interfering with K OFDMA subcarriers. The difference in the signal characteristics leads to an important distinction that is the key to explain the gain obtained from using a SIC algorithm:

- In time domain the GMSK symbols are structured data carrying information, while the OFDMA signal behaves as white noise. Therefore the received signal in sampled time domain can be expressed as follows;

$$r(n) = z(n) + \sum_{k=0}^{N-1} Y(k) e^{j2\pi kn/N} + w(n) \quad (4.12)$$

- In frequency domain the OFDMA signal carries structured data and the GMSK can be considered as coloured noise. The received signal in frequency domain can be expressed as:

$$R(k) = Y(k) + \sum_{k=0}^{N-1} z(n) e^{-j2\pi kn/N} + W(k) \quad (4.13)$$

Where $w(n)$ is AWGN and $W(k)$ is its Fourier transform.

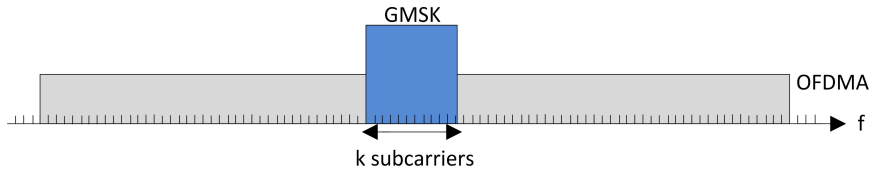


Figure 4.4: *OFDMA and GMSK in frequency.*

Implemented SIC algorithm for Zones 1 and 3

This section addresses a detailed description of the implemented algorithm for zones 1 and 3 from Figure 4.1 in which a high enough or low enough SIR justifies the application of a SIC technique (leading to capture effect).

As detailed in Section 3.2.2 on page 12 due to the similarity with this Thesis, the proposed algorithm in [21] has been selected to deal with the interference in zones 1 and 3.

The fundamental idea of the algorithm is to improve the interference cancellation through successive iterations of a common SIC algorithm. The algorithm requires as its input the estimation of either the GMSK signal, noted as $\hat{z}(n)$, or the OFDMA signal, noted as $\hat{Y}(k)$. Two cases should be distinguished depending on which signal is used as the input for the algorithm:

- If the GMSK power level is high enough to give a positive result in the energy detector then;

$$\hat{z}(n) = \sum_{k=0}^{N-1} R(k)e^{j2\pi kn/N} \quad (4.14)$$

Otherwise

$$\hat{Y}(k) = R(k) \quad (4.15)$$

Assuming that the the energy detector is able to distinguish the GMSK signal, the GMSK signal is demodulated, regenerated and subtracted from the received signal in the frequency domain;

$$\hat{Y}(k) = R(k) - \sum_{n=0}^{N-1} \hat{z}(n)e^{-j2\pi kn/N} \quad (4.16)$$

Similarly to the previous procedure, the OFDMA signal is demodulated, regenerated and subtracted from the received signal in time domain as follows;

$$\hat{z}(n) = r(n) - \sum_{k=0}^{N-1} \hat{Y}(k)e^{j2\pi kn/N} \quad (4.17)$$

It should be born in mind that the key of the algorithm is that even if $\hat{z}(n)$ may contain errors, they will be spread through many samples in the frequency domain. Similarly, for $\hat{Y}(k)$ a symbol error will be spread through many samples in time domain. Consequently, an error in one domain does not necessarily lead to an error in the reciprocal transformed domain. In Figure 4.5 it is shown a flowchart of the implemented algorithm adapted from [21].

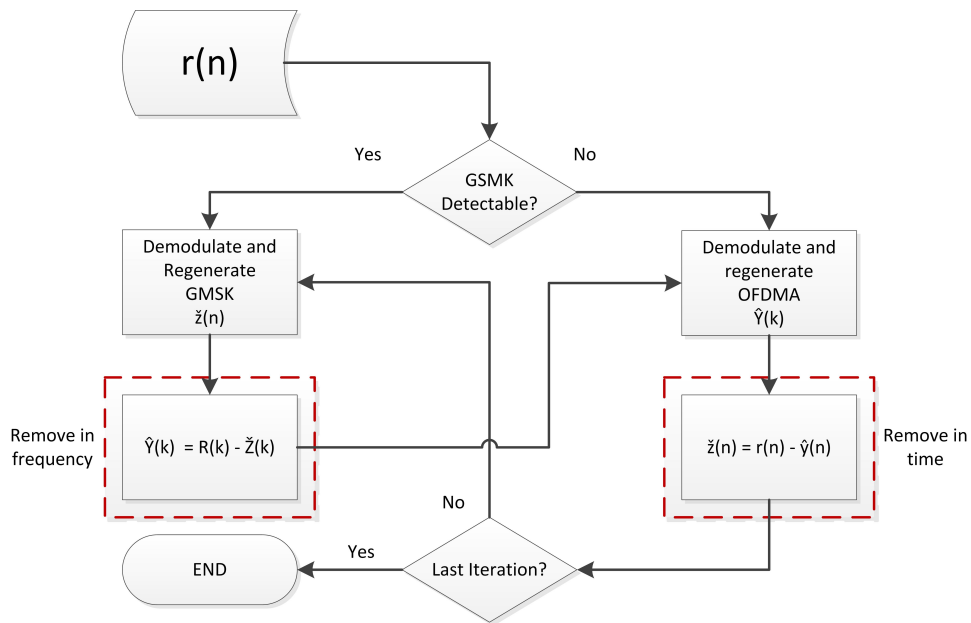


Figure 4.5: Algorithm flowchart.

Chapter 5

Simulations

This chapter provides a detailed account of the simulations performed in order to:

- Establish a reference model for the scenario detailed in Chapter 2.
- Validate the SIC technique
- Evaluate the performance of the SIC algorithm detailed in Chapter 4
- Build a Physical Level Simulator
- Build a Link Level Simulator
- Build a System Level Simulator
- Compare the throughput of a system using orthogonal resources, when the LTE and GSM spectrum is divided, against the throughput of the same system using shared resources.
- Measure the performance of the proposed interference cancellation method within the guidelines of the Mobile and wireless communications Enablers for the Twenty-twenty Information Society (METIS) project.

First a basic simulation that shows the improvements achieved by using a SIC technique when two equally modulated signals interfere each other is provided. Then the parameters associated to the systems described in the scenario of the Thesis are introduced and the influence of the SIR in the bit success rate, successfully decoded bits, is studied to provide a reference case. Next the influence of the SIC algorithm is studied and the effect of different modulations in the Orthogonal Frequency Division Multiplexing (OFDM) subcarriers analysed to build a Link Level Simulation. Finally the System Level simulation is described and its results discussed.

It should be noted that two different systems each with a different bandwidth are analyzed. In order to make a valid comparison, as explained in subsection 4.1.1, the SIR level will be related to power spectral density [$W/hertz$]. As detailed in Appendix C on page 90, LTE is a wideband system compared to GSM. Additionally as discussed in Section 4.3 increasing the OFDM bandwidth yields a performance improvement in the interfering cancellation results. To validate the SIC technique, the OFDM bandwidth is set to 180 KHz according to [25] against the 200 KHz of GSM [4] in order to compare both systems when their working bandwidths are as similar as possible.

5.1 Physical Level Simulations

This section and its subsections, contain the physical level simulations for the systems under consideration. The simulation setup is explained and its results are described. In this section the bit success rate is calculated taking into account only the SIR and Signal Noise Ratio (SNR) levels. As discussed in the previous chapter the selected systems are LTE and GSM. The following assumptions have been made for the physical level simulations:

- Only one primary and one secondary user are considered.
- The LTE system, as stated in the previous point, has been modelled with only one user. Therefore the access method of LTE OFDMA is modeled as OFDM. It has been assumed that the differences between both methods is not relevant for the objectives of these simulations.

5.1.1 SIC reference case

In this subsection the results of some simple examples of SIC are shown. The basics of the SIC technique are explained in Section 4.2 on page 16. The objective is to analyze the influence of the SIR in the symbol success rate and measure the any improvement achieved by the SIC technique in a simple case.

The desired and the interfering signals are GMSK modulated. The parameters used in this simulation are shown in Table 5.1.

The obtained results can be observed in Figure 5.1:

- The blue curve represents the bit error rate for a perfect knowledge of the received signals power level.
- The red curve shows the bit error rate for a simple detection of the desired GMSK.

Parameter	Value
SNR	30 dB with relation to the desired signal
Channel model	AWGN
SIR	-5 dB to 5 dB
Number of repetitions	100
Symbols per transmission	10
Samples per symbol	8

Table 5.1: Parameters of the simulation.

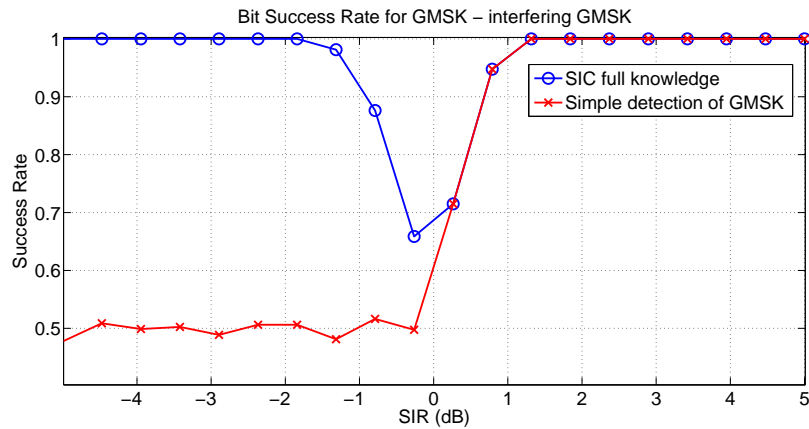


Figure 5.1: Bit success rate for GMSK with one GMSK interfering signal over a AWGN channel.

In Figure 5.1 it can be observed the dependency of the bit success rate on the SIR. It can also be seen the improvement achieved by using SIC for low SIR levels. Finally it should be remarked that for SIR levels close to 0 dB the bit success rate decreases. The described behaviour matches those found in literature [9], [21].

5.1.2 SIC for OFDM and GMSK, reference cases

The purpose of this section is to create a reference model, that allows to measure the improvement achieved by the implemented SIC algorithm adapted from [21]. The parameters used for this simulation are shown in Table 5.2.

Parameter	Value
SNR	15 dB with relation to the desired signal
Channel model	AWGN
SIR	-10 dB to 10 dB
Number of repetitions	100
OFDM Parameters	
Number of resource blocks	1
Subcarriers per resource block	12
Subcarrier separation	15 KHz
Symbols per subcarrier	1
Subcarrier modulation	QPSK
GMSK Parameters	
GMSK Symbols per transmission	18
GMSK Samples per symbol	113

Table 5.2: *Parameters of the reference cases simulation.*

Detecting OFDM and GMSK in presence of one interfering signal

This subsection deals with the simulations of the simplest cases considered in this Thesis:

- The bit success rate for a OFDM encoded signal when the interfering signal is GMSK modulated.
- The bit success rate for a GMSK modulated signal when the interfering signal is OFDM encoded.

The parameters used are those of Table 5.2. The results can be observed in Figures 5.2 and 5.3.

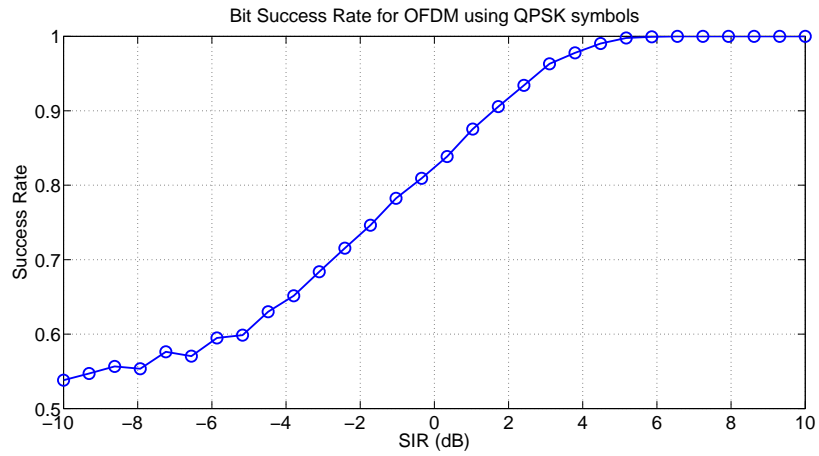


Figure 5.2: *Bit success rate for OFDM with one GMSK interfering signal over a AWGN channel.*

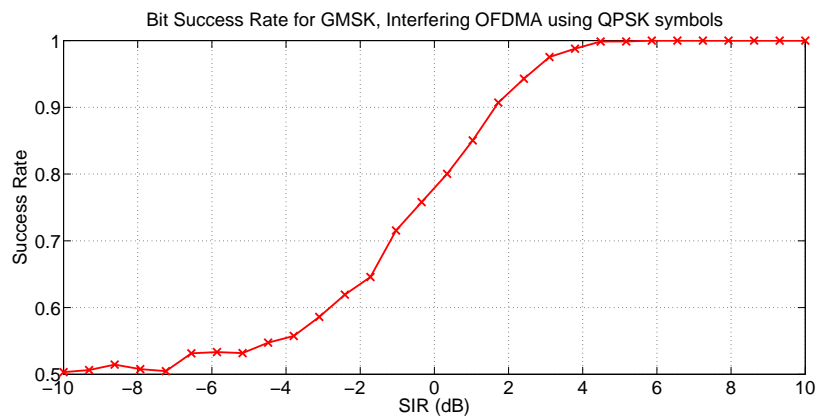


Figure 5.3: *Bit success rate for GMSK with one OFDM interfering signal over a AWGN channel.*

Figures 5.2 and 5.3 reveal that the bit success rate increases on par with the SIR. This is an expected behaviour if compared with the previous literature [26], [27].

Simple SIC for OFDM and GMSK in presence of one interfering signal

This subsection, similarly to the previous one, features the results of the simulations of a simple SIC algorithm, as described in Section 4.2. The parameters used in this simulation are shown in Table 5.2. The results are shown in Figures 5.4 and 5.5. The SIC algorithm assumes that there is no information about the power of the received signals. The algorithm works as follows:

- The receiver attempts to decode the desired signal.
- If the desired signal can not be decoded successfully, the interfering signal is decoded and subtracted from the received signal.
- The receiver decodes the remaining signal.

Two cases are analyzed:

- The bit success rate for an OFDM encoded signal when the interfering signal is GMSK modulated.
- The bit success rate for a GMSK modulated signal when the interfering is OFDM encoded.

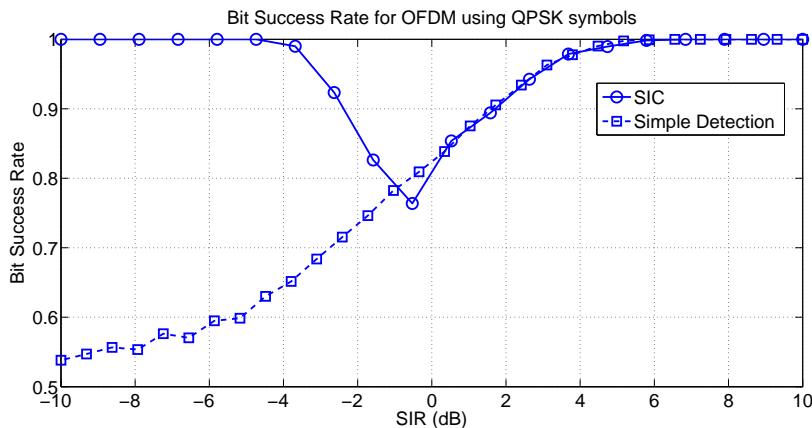


Figure 5.4: *Bit success rate for a OFDM signal using QPSK modulated subcarriers under the interference of a GMSK signal over a AWGN channel after applying SIC.*

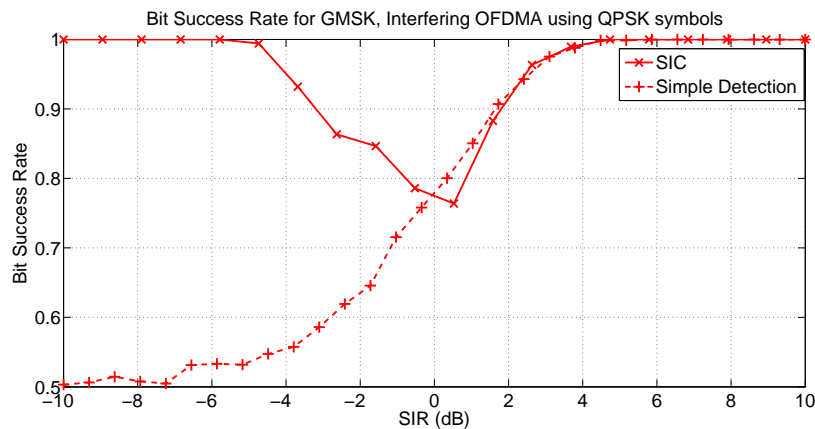


Figure 5.5: *Bit success rate for a GMSK signal under the interference of a OFDM signal using QPSK modulated subcarriers over a AWGN channel after applying SIC.*

In Figures 5.4 and 5.5 it can be observed the improvement achieved by the SIC technique over the simple detection of the OFDM and the GMSK signals respectively. In both Figures:

- The solid line curve represents the case in which SIC is applied.
- The dashed line curve is the simple detection case.

Analyzing both Figures it can be seen that the SIC curve is behaving as expected according to the results from [21]:

- The bit success rate decreases when the SIR approaches to zero.
- The SIC algorithm performs better for a low or high SIR.

Comparing Figures 5.4 and 5.5 with Figure 5.1 it can be observed that the symmetry of the SIC curve from the latter is not observed in the other figures. This asymmetry is related to the multiple domain circumstances: In Figures 5.4 and 5.5 two different signals are considered. Since the data of the GMSK signal is in time domain and in the OFDM signal is in frequency domain, decoding at least a fraction of the interfering signal can contribute to improve the desired signal quality. Conversely Figure 5.1 considers two GMSK signals whose data is exclusively in time domain. Furthermore it should be highlighted the different slopes of the curves at each side of the zero SIR value. This is due to the fact that for negative SIR values, the desired signal is decoded only in presence of noise after the removal of the interfering signal. For positive SIR values the desired signal is directly decoded in presence of noise and interference.

To study the effect that using a higher modulation might have in the bit success rate a new simulation is performed . The OFDM signal is encoded

with 64QAM symbols. The results are depicted in Figures 5.6 and 5.7. On the other hand the constellation symbols are closer, leading to a lower tolerance to SNR and SIR. Therefore, for the same symbol rate it is expected a degradation in the bit success rate.

It should also be mentioned that for the SIR values close to 0 dB it is more efficient not to perform the SIC technique since not properly decoding the interfering signal adds an extra impairment to the desired signal [20].

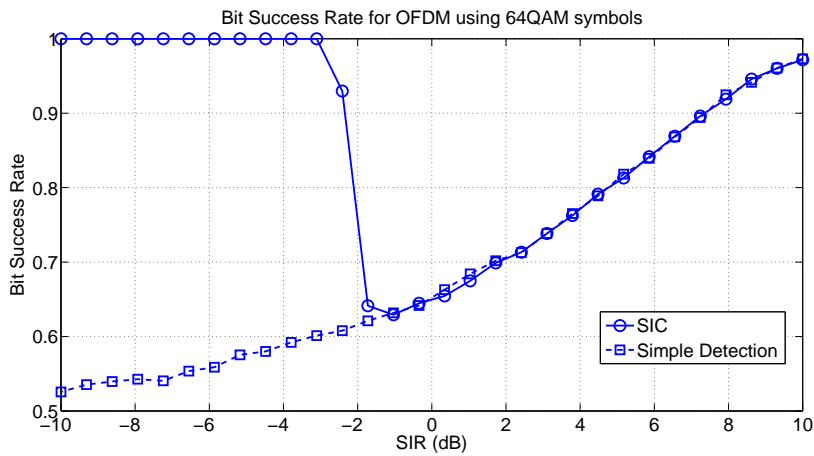


Figure 5.6: Bit success rate for a OFDM signal using 64-QAM modulated subcarriers, under the inference of a GMSK signal over a AWGN channel after applying SIC.

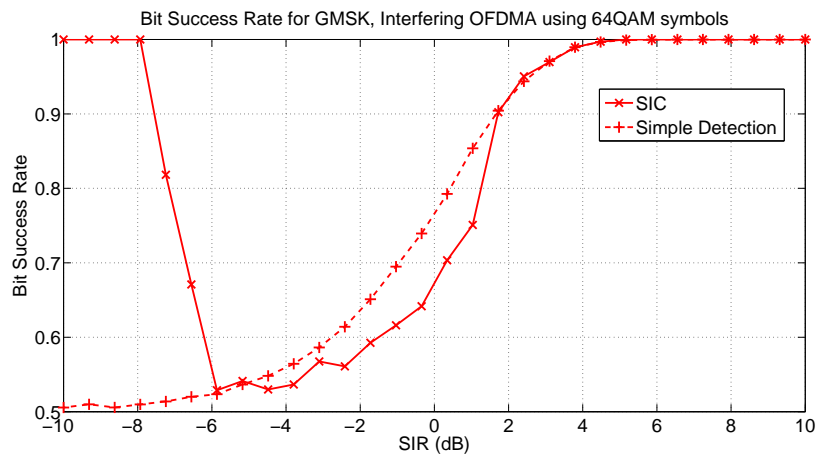


Figure 5.7: *Bit success rate for a GMSK signal under the interference of a OFDMA signal using 64-QAM modulated subcarriers over a AWGN channel after applying SIC.*

5.1.3 Implementation of an iterative SIC Algorithm

This section addresses the simulations of the iterative SIC algorithm described in Section 4.3 on page 17. While [21] makes use of an energy detector to differentiate the signals of interest, [28] discusses a method to mathematically distinguish between two modulations. However modulation detection is regarded as out of the scope of this work. Therefore it will be assumed that the received power levels of the interfering and desired signals is known at the receiver. The same parameters as in the previous section, shown in Table 5.2, are used to compute the simulations, the results shown in Figures 5.8 and 5.9.

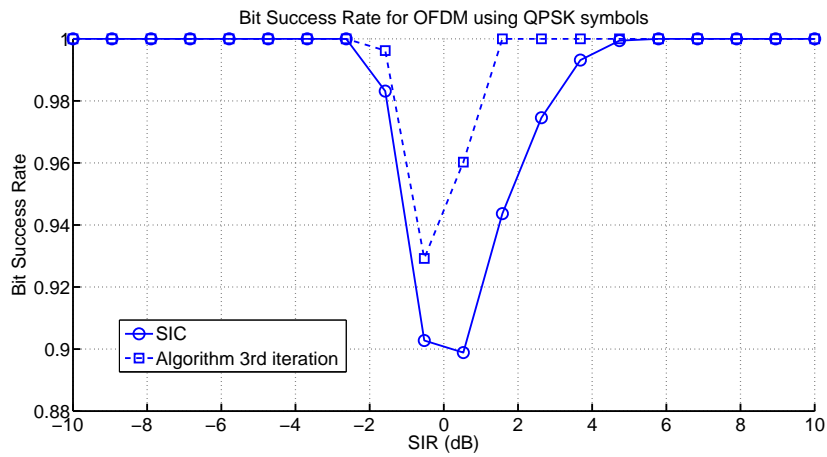


Figure 5.8: Bit success rate for OFDM with one GMSK interfering signal over a AWGN channel using the proposed algorithm

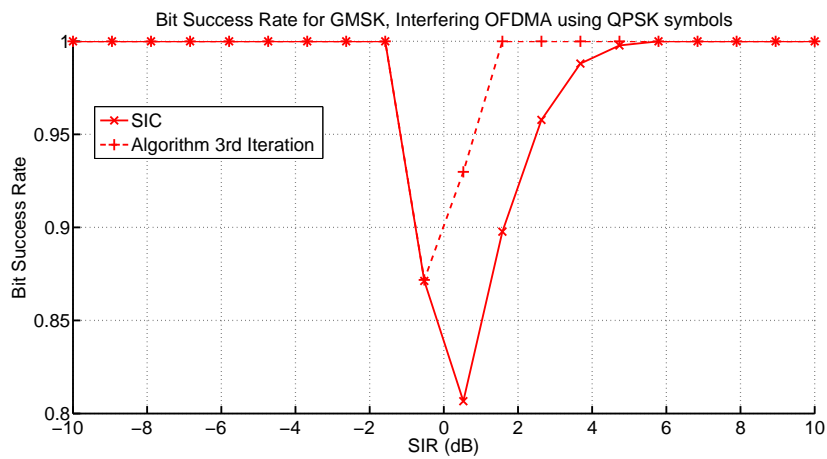


Figure 5.9: Bit success rate for GMSK with one OFDM interfering signal over a AWGN channel using the proposed algorithm.

In Figures 5.8 and 5.9:

- The solid curve represents bit success rate of applying the SIC technique.
- The dashed curve represents bit success rate computed after three iterations of the algorithm.

Figures 5.8 and 5.9 exhibit that if the input for the iterative SIC algorithm is chosen optimally, the curves representing a three-iteration algorithm provide a considerable improvement in the regions when the SIR value is a small but positive. In the SIC case when the SIR value is a small positive, the desired signal is demodulated in presence of a strong interference. However when the algorithm is applied the interfering signal is removed for such cases. This is a relevant point because as detailed in section 4.2 on page 16 the SIC technique requires a significant difference in the power level of the signals to be subtracted.

It is also considered of interest to analyze the impact that different subcarrier modulations in the OFDM signal might have in the performance of the iterative SIC algorithm. Following the same procedure detailed at the beginning of this section, but using 64QAM symbols instead of QPSK for the OFDM subcarrier modulation, a degradation in the bit success rate is anticipated. The results can be seen in Figures 5.10 and 5.11.

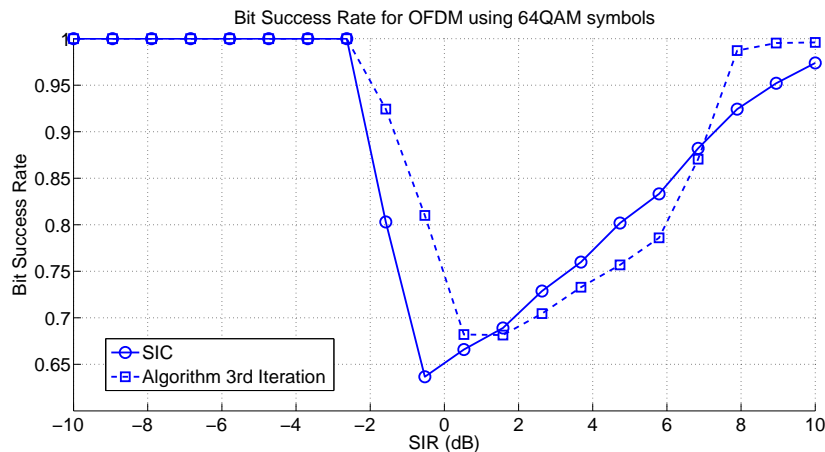


Figure 5.10: *Bit success rate for GMSK with one OFDM interfering signal with 12 subcarriers over a AWGN channel using the proposed algorithm.*

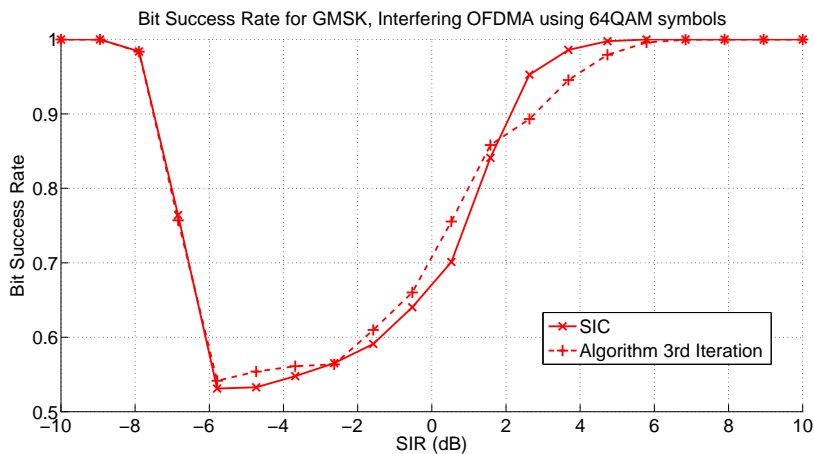


Figure 5.11: *Bit success rate for GMSK with one OFDM interfering signal with 12 subcarriers over a AWGN channel using the proposed algorithm.*

Comparing Figures 5.10 and 5.11 with Figures 5.10 and 5.10 the anticipated and significant degradation in the bit success rate can be observed. It can be also noticed that for some SIR values the algorithm performs worse than the SIC. This is a consequence of having a high modulation order, since the 64QAM can not be decoded properly, the algorithm iterations degrade the GMSK quality. The results featured in this section indicate that the OC-D2D paradigm is suitable for a network scenario where service availability is more important than throughput. This reasoning is in accordance with the initial purpose of this Thesis in which the coexistence of both systems has preference against throughput.

5.2 Link level Simulations

In this section, the link level simulations carried out according to the scenario described in Chapter 2 are detailed. These simulations differ from the Physical Level Simulations of the preceding section in the fact that the smallest unit of communication considered is the packet instead of a single bit. Consequently the FSR is analyzed, as a function of the SIR and SNR. The simulations described in this section will be used as a platform to build the System level simulations on top. Additionally the effect of using the iterative SIC algorithm described in section 4.2 on page 16 at the Link level is studied. In order to match as closely as possible a communications link in a real scenario, throughout these simulations the information to be transmitted is coded. The bits transmitted in the GMSK signal are coded using a convolutional code and the bits transmitted in the OFDM signal are coded using a turboencoder according to [29] and [4]. The simulations

performed for this section assume that the frame is only composed of traffic data, hence no signalling bits are included. A detailed explanation of the selected coding techniques can be found in [30].

5.2.1 Influence of coding in the FSR

Similarly as done in section 5.1.2, this subsection contains a set of reference cases. The results obtained in this subsection will be used in section 5.3.1 for system level simulations. First it is discussed the influence of coding in the FSR dependency on the SNR for the GMSK and OFDM signals. To analyze this dependency, a simulation is built in which the success rates for coded and uncoded frames is compared. The parameters used for this simulation are those of Table 5.3 and the results are shown in Figures 5.13 and 5.12 on the next page.

Parameter	Value
SNR	-10 dB to 15 dB
Channel model	AWGN
SIR	-10 dB to 10 dB
Number of repetitions	100
Packet length	700 bits
OFDM Parameters	
Number of resource blocks	1
Subcarriers per resource block	12
Subcarrier separation	15 KHz
Symbols per subcarrier	1
Subcarrier modulation	QPSK
The turbo encoder rate	1/7
Turbo encoder's trellis structure (octal numbers)	[11 13 15 17]
GMSK Parameters	
Symbols per transmission	18
Samples per symbol	113
Convolutional encoder rate	1/7
Convolutional encoder's Trellis structure (octal numbers)	[171 137 145 165 133 155 150]

Table 5.3: *Parameters of the simulation.*

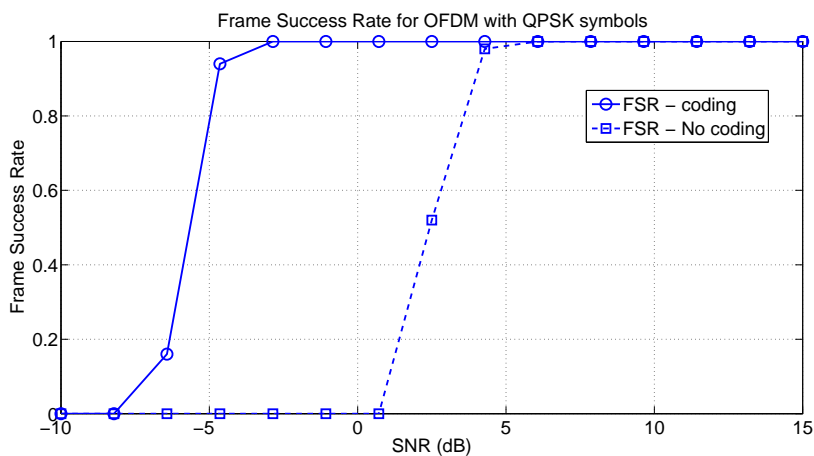


Figure 5.12: *FSR for OFDM over a AWGN channel.*

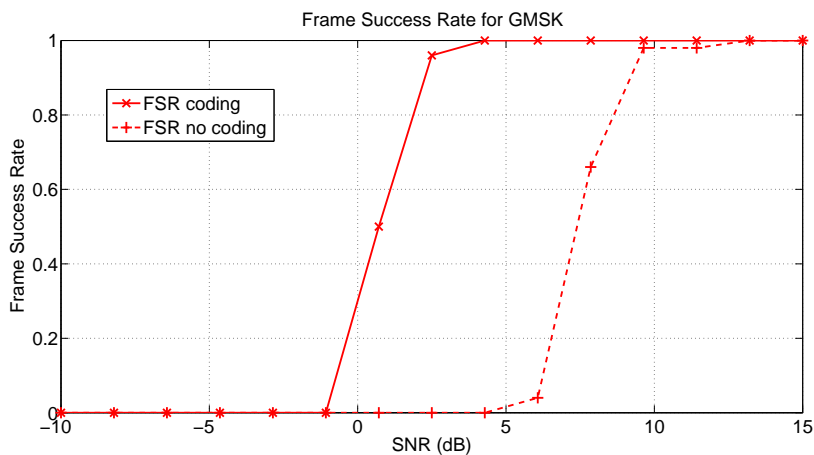


Figure 5.13: *FSR for GMSK over a AWGN channel.*

Analyzing the graphs shown in Figures 5.13 and 5.12, it can be concluded that the curves behave as expected, since the frame success rate increases for higher SNR levels, being the FSR of the coded signal significantly smaller than the FSR of the uncoded signal. Comparing both Figures it should be remarked that the OFDM signal seems more robust against the effect of noise. This robustness will be observed in posterior SIC curves as an asymmetry. A reason for the increased robustness of the OFDM signal against noise may be the superior performance of the turbo encoder over the convolutional encoder.

5.2.2 FSR for OFDM and GMSK using SIC, reference cases

To measure the FSR in presence of interference, the SIC technique outlined in Section 4.2 is applied for a range of SIR values. The parameters used are noted in Table 5.3. The results of these simulations are shown in Figures 5.14 and 5.15. It should be remarked that the bandwidth used in these simulations is 200 KHz for the GMSK signal and 180 KHz for the OFDM signal.

Additionally it is considered of interest to study the impact that the OFDM signal bandwidth has in the FSR. A last set of simulations is provided in this subsection in which the same parameters as in the previous simulation are used with the exception of the number of subcarriers in the OFDM signal, increased from 12 to 24 effectively doubling the bandwidth of the OFDM signal. The results are shown overlaid in Figures 5.14 and 5.15. From both Figures it can be extracted that a higher bandwidth results in an improved performance. This is expected, as explained in [21], since the GMSK signal interferes with a smaller percentage of the OFDM signal. Thus, the number of correctly decoded symbols is higher and the subtraction of the OFDM is more accurate.

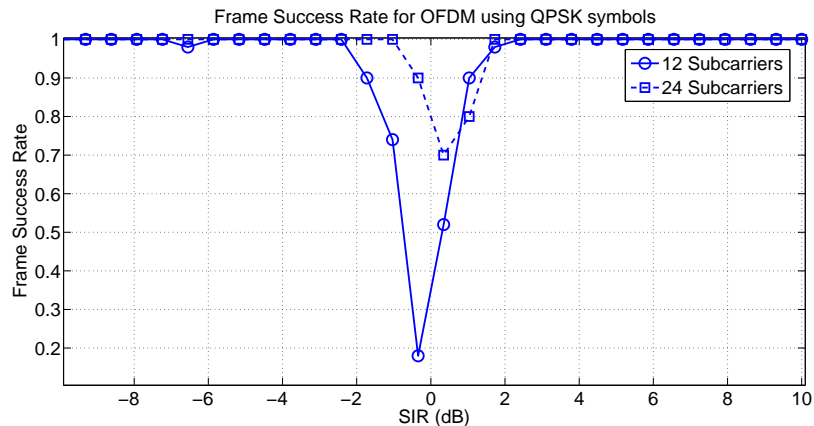


Figure 5.14: FSR for OFDM over a AWGN channel with a OFDM interfering signal.

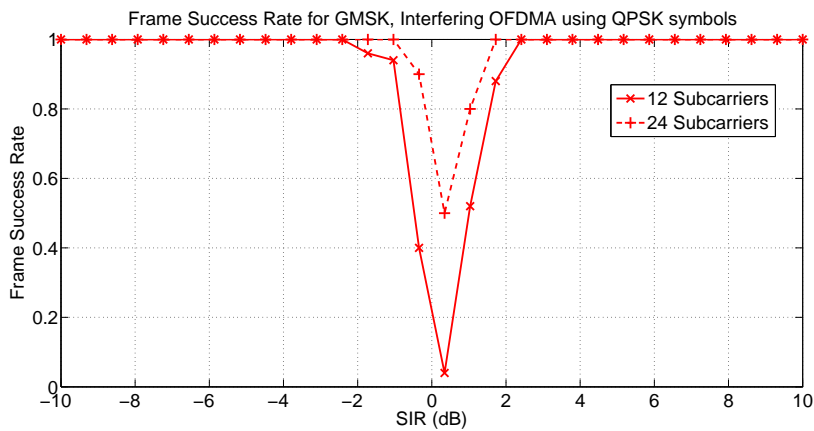


Figure 5.15: *FSR for GSMK over a AWGN channel with a GSMK interfering signal.*

5.2.3 Analysis of the iterative SIC algorithm at the Link level

In this subsection the impact of the iterative SIC algorithm described in Section 4.3 is analyzed at the Link level. The goal of this section is to compare the possible improvement that results from the application of the iterative SIC algorithm against the results obtained by applying the simple SIC technique detailed in the previous section.

The number of iterations of the algorithm is set to three. The parameters used in this simulation, the same as in the previous subsection, can be found in Table 5.3. The results are shown in Figures 5.16 and 5.17.

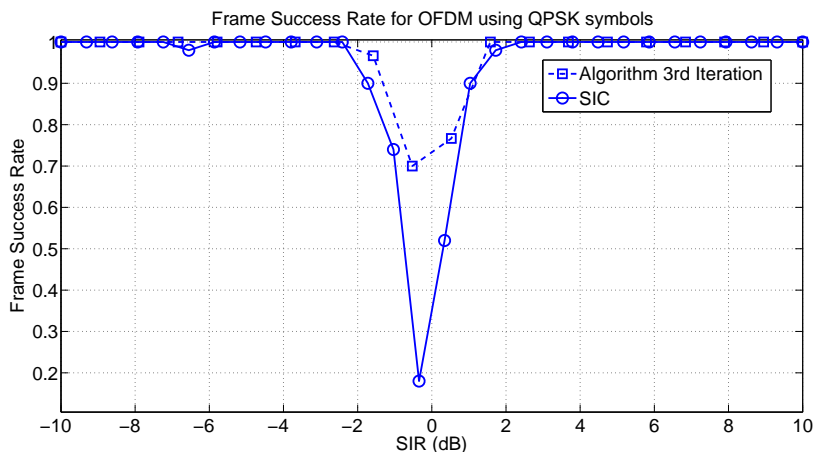


Figure 5.16: *FSR for OFDM over a AWGN channel with a GSMK interfering signal using the proposed algorithm.*

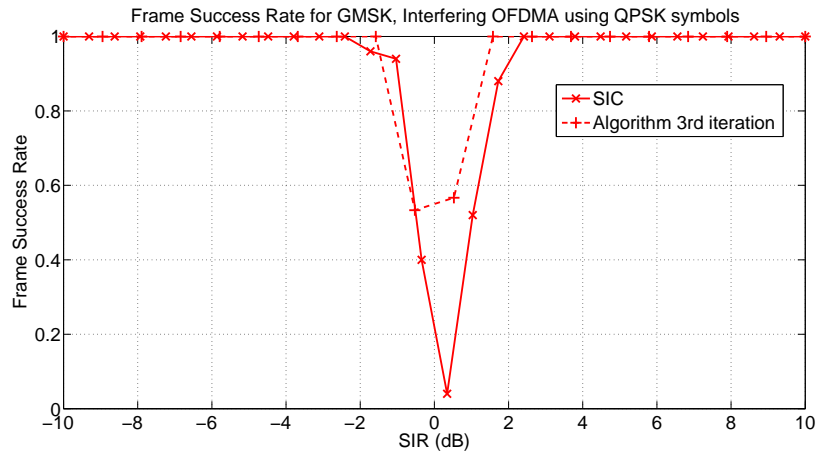


Figure 5.17: *FSR for GSMK over a AWGN channel with a OFDM interfering signal using the proposed algorithm.*

The gain derived from applying the algorithm in both cases is visible in particular for SIR levels close to 0 dB.

5.3 System level Simulations

This section addresses the system level simulations. The simulations are built upon the Link Level Simulations described in the previous section. In order to build a reasonably accurate model a set of link level simulations with different SNR have been computed. The SNR goes from -10 dB to 15 dB, with a step of approximately 1.5 dB. Therefore taking into account the previously modelled communications link a complete communications scenario is simulated. Two different cases are studied:

- The FSR when both systems are using orthogonal resources, i.e. each system uses a different frequency.
- The FSR when both systems are using shared resources, i.e. both systems operate in the same frequency.

Based on the premises detailed in Chapter 2, the scenario under study in this Thesis will be modelled as a single cell with the following parameters:

- Cell radius R_c : 1000 meters.
- GSMK maximum transmitting power: 33 dBm.
- OFDM maximum transmitting power: 23 dBm.
- Attenuation constant of the medium: $\alpha = 4$.

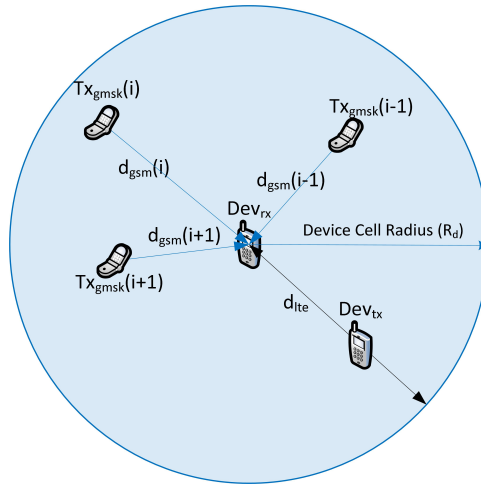


Figure 5.18: *Simulated System Level Scenario from the device point of view.*

The Link parameters are set in accordance to those of the previous section, shown in Table 5.3. It should be remarked that the transmitting power will be divided over the complete band that the device is operating in. The bandwidths considered in this simulations are, 180 KHz in the OFDM case [25] and 200 KHz in the GMSK case [4].

5.3.1 System level simulation for Orthogonal Resources

In this subsection it is considered the traditional approach for D2I networks, in which different radio access systems are allocated to different bands to avoid interference. The data to compute the results in this subsection has been taken from Figures 5.12 and 5.13.

Two communication links have been modeled: the first one over a AWGN channel and the second one over a fading channel with a maximum Doppler shift of 1 KHz. Although it was previously stated that the devices are static, it is considered of interest to study the performance of the proposed system under fading. For each communication link two different cases are analyzed:

- The FSR at the eNodeB for the GMSK link as a function of the distance between the GMSK transmitter and the eNodeB. Considering that the eNodeB is located in the center of the cell, Figure 5.19.
- The FSR at the UE for the OFDM link as a function of the distance between the two UE that are part of the communication link, Figure 5.18.

As depicted in Figure 5.18 the distance considered in the GMSK case varies from 0 to 1000 meters in accordance to the radius of the hexagonal cell in a urban scenario [31]. For the OFDM link the maximum distance

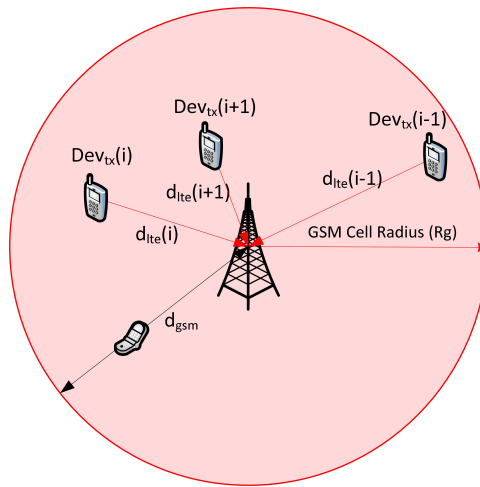


Figure 5.19: *Simulated System Level Scenario from the Base Station point of view.*

between devices can be twice the radius of the cell, 2000 meters. However, to simplify the simulations, it is assumed that the receiving device is placed in the center of a cell, and the transmitting devices are placed uniformly in that cell.

In both cases the procedure is the following:

- For each possible distance within the cell, the SNR is computed.
- Taking into account the SNR the FSR is obtained following the same procedure as shown in the previous section 5.2.
- The throughput is calculated taking into account that for GSM the maximum throughput is 270.833 Kbits [4] per second and 14000 Symbols per second [25] for OFDM.

The results are shown in Figures 5.20 and 5.21.

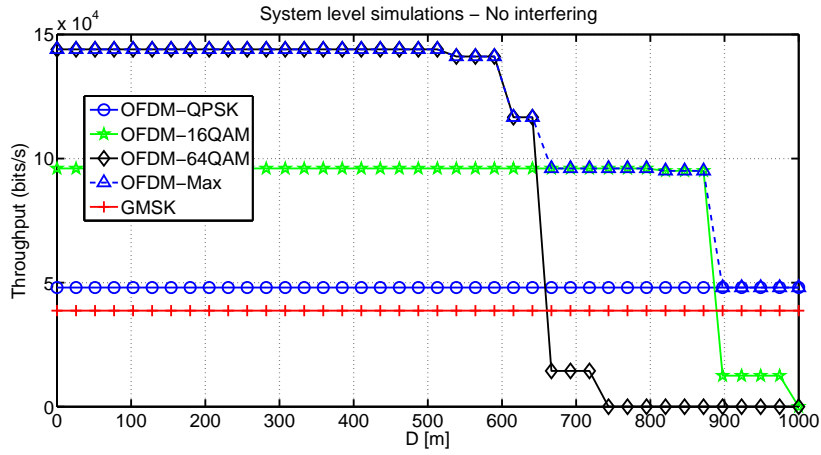


Figure 5.20: Throughput for OFDM and GSMK over a AWGN channel.

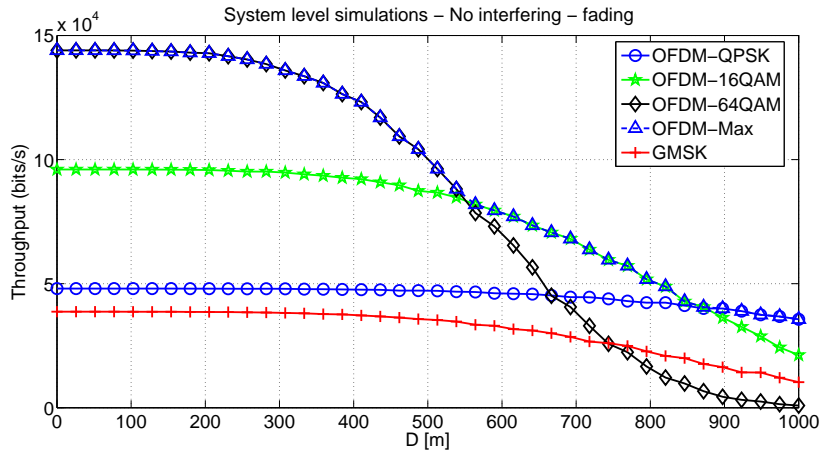


Figure 5.21: Throughput for OFDM and GSMK over a fading channel.

From Figure 5.21 it can be seen that throughput decrease as a function of the distance. It can also be remarked that depending on the distance there is an optimum modulation to achieve the highest throughput for OFDM noted in the figure as OFDM-Max.

5.3.2 System level simulation for Shared Resources

This subsection analyzes the packet success rate when both systems share the resources, i.e. operate in the same frequency. Similarly to the case from the previous section in which the system uses Orthogonal Resources, two cases are analyzed:

- The FSR at the eNodeB for the GSMK link as a function of the distance

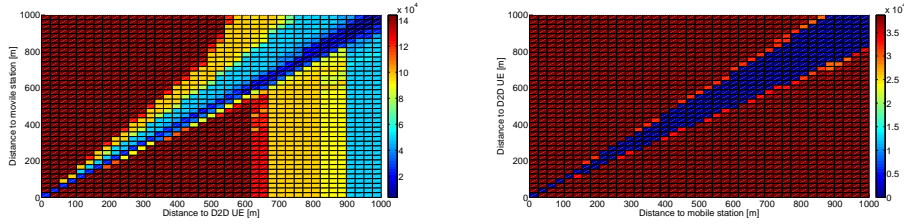
between the GMSK user and the eNodeB.

- The FSR at the receiving UE for the OFDM link as a function of the distance to the transmitting UE.

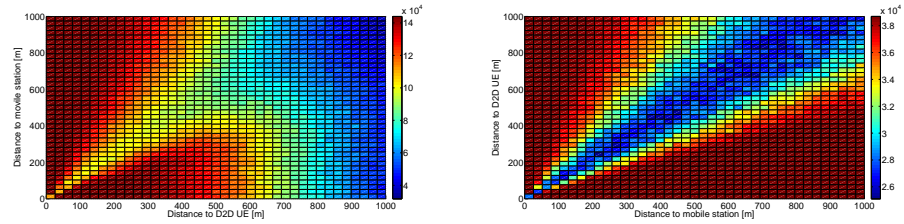
In both cases the procedure is the following:

- The data to compute the simulations in this subsections is taken from Figures 5.14 and 5.15 on page 37.
- For each distance the SNR is computed, and a interfering device is randomly placed in the cell in order to calculate the SIR. The packet success rate is calculated for every distance according to the simulated data from the figures mentioned in the previous point. In the OFDM case it has been chosen the modulation that produce the highest throughput for a certain SIR and SNR.
- The throughput is calculated taking into account that for GSM the maximum throughput is 270.833 Kbits [4] per second and 14000 Symbols per second [25] for OFDM. Hence the throughput for the latter would be dependent on the used modulation order.

In Figure 5.22 the deterministic results are shown.



(a) *Throughput for OFDM, using QPSK symbols, with a GMSK interfering signal and a AWGN channel.* (b) *Throughput for GSMK with a OFDM interfering signal, using QPSK symbols and a AWGN channel.*



(c) *Throughput for OFDM, using QPSK symbols, with a GMSK interfering signal and a fading channel.* (d) *Throughput for GSMK with a OFDM interfering signal, using QPSK symbols and a fading channel.*

Figure 5.22: *Throughput for OFDM and GSMK for a deterministically placed interfering source.*

It should be remarked that these simulations are computed from the results obtained in the Link Level simulation, subsection 5.2.2 on page 36, featured in Figures 5.14 and 5.15 on page 37.¹ Additionally it is important to notice the offset in both Figures produced by the difference in the system's bandwidth and transmitted power, leading to a variation in the spectral power difference of the two systems under consideration and affecting the results of the SIC technique.

Throughput of a system using shared resources for randomly positioned users

In order to have an estimate of the expected throughput with relation of the separation distance, between the eNodeB and the device for the GSM case, and between the D2D pair for the OFDM case, a new simulation set is built. For each evaluated distance the expected packet success rate is obtained by randomly placing the interfering sources along the cell. The results of this

¹It has to be noted that since the minimum SNR taken into account in the Link Level simulation is only -10 dB, the distances comparable to the cell radius may experience lower SNR values. Therefore it can be anticipated that the results from this simulation in the area close to the end of the cell are not reliable and it will not be further discussed.

simulation are shown in Figure 5.23 for a AWGN channel and Figure 5.24 for a fading channel with a maximum Doppler shift of 1 KHz.

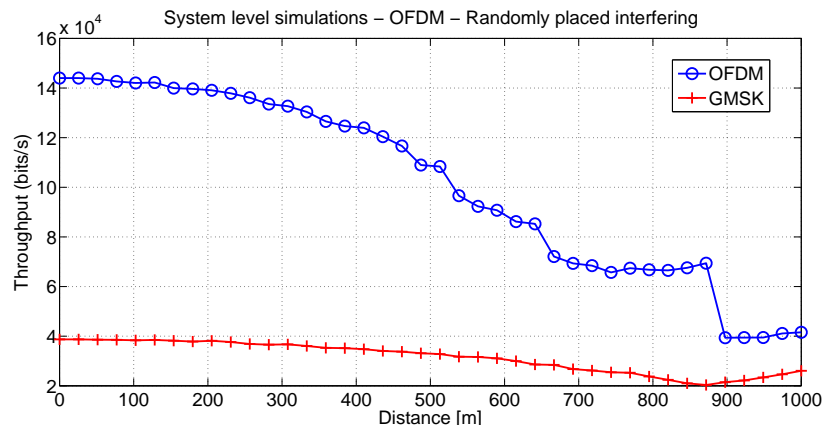


Figure 5.23: *Throughput for OFDM and GSMK, randomly placing the source of the interference signal when the channel is considered AWGN.*

It has to be noticed that in Figure 5.23, the red graph representing the GSMK signal shows an unexpected increase starting at 900 meters. This can be justified as follows:

- It can be observed that the distance where both graphs reach their minimum, matches with the distance where the area with a low packet success rate is maximum.
- It can also be seen that from the distance where both graphs reach their minimum, the previously mentioned area decreases, consequently increasing the packet success rate.

In addition it is also remarkable the GSMK behavior is less affected by large distances than the OFDM.

Regarding the curves shown in Figure 5.24, it has to be pointed out that:

- The data from which this figure is computed does not take into account the noise levels lower than -10 dB and the derived calculations when the channel exhibits a deep fade may not be accurate. However the typical specification designs, [22], of a cellular system impose the probability of successfully transmitting a packet to be high. It can be expected that the computed results represent a close estimation.

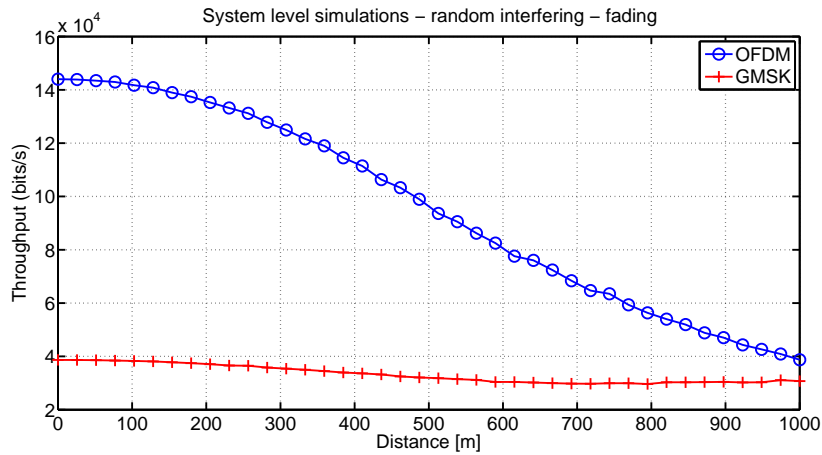


Figure 5.24: *Throughput for OFDM and GMSK, randomly placing the source of the interference signal through a fading channel.*

5.4 Throughput comparison for a system using orthogonal versus shared resources

This section details a comparison between the throughput achieved when both systems coexist in the same bandwidth and the throughput achieved when both systems have orthogonal resources. The purpose of this section is to illustrate the gain in throughput obtained if the coexistence of both systems in the same bandwidth was possible.

The results of this comparison are shown in Figure 5.25 for a AWGN channel and Figure 5.26 for a fading channel. In each case the throughput is calculated by adding the simulated throughput of each system. According to Figures 5.25 and 5.26 there is a loss in throughput when the resources are shared. It is left for discussion in Section 5.5.3 to discuss if the results featured in the aforementioned figures justify the applicability of the SIC technique for a real world scenario and support the initial proposal of using a SIC technique to achieve the coexistence of two different systems under the same frequency.

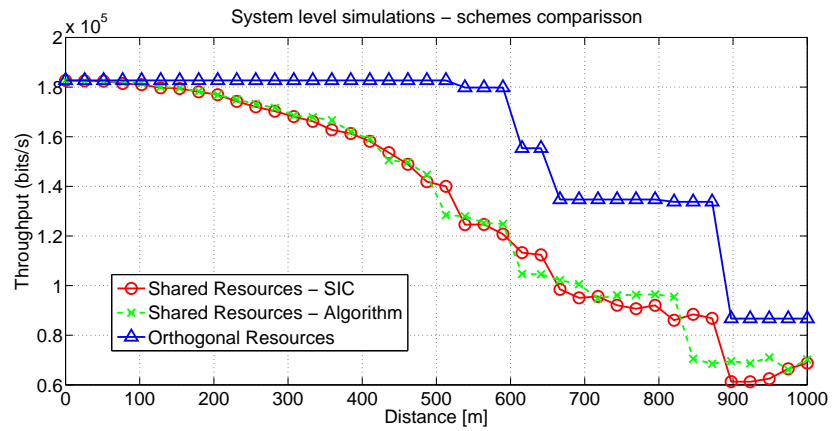


Figure 5.25: *Throughput for orthogonal and shared resources systems over AWGN channel.*

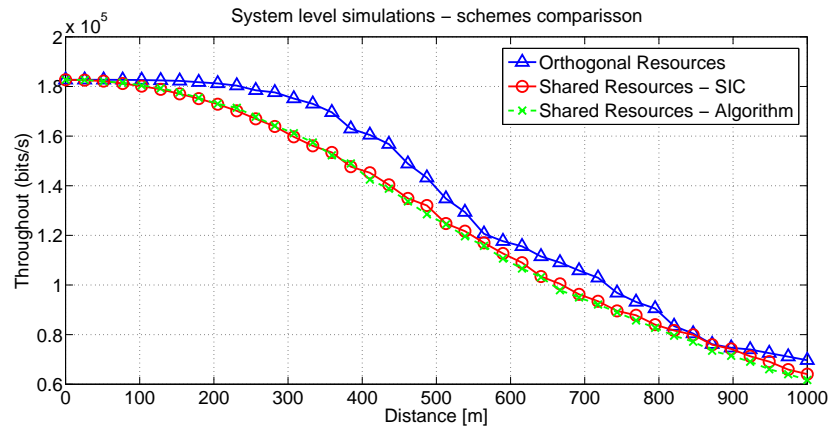


Figure 5.26: *Throughput for orthogonal and shared resources systems over fading channel.*

From Figures 5.25 and 5.26 can be extracted that there is no noticeable gain in the throughput achieved by the algorithm compared to the simple SIC. In this chapter the FSR comparisons shown so far have been studied only for a high SNR. However it is expected to have non desirable SNR due to fading or for large distances. In Figure 5.27 is shown the frame success rate achieved by SIC and the iterative algorithm for low SNR.

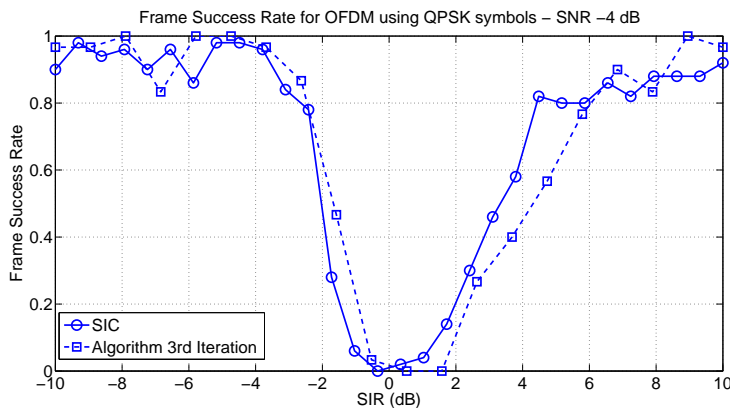


Figure 5.27: *FSR for OFDM applying the proposed algorithm and SIC for a SNR of -4 dB.*

From 5.27 it is extracted that there is no difference in the FSR for a low SNR. This fact explains the iterative algorithm behaviour for the curves shown in Figures 5.25 and 5.26.

5.5 Simulations using the guidelines of the METIS project

The METIS project [32] provides guidelines for the simulation of different scenarios defined in accordance to the expected use cases of the newly deployed radio access technologies. It includes among others an environmental model and a propagation model from which a simulation model can be built.

The scenario considered of relevance to this project is the so called "urban dense scenario". The main characteristics of this scenario are:

- Equally sized square buildings of different heights according to an uniform distribution.
- Equally sized streets.
- A eNodeB should be situated on the top of one of the buildings.

The propagation models provided by the METIS project include:

- A propagation model for a eNodeB situated on a building rooftop that computes the outdoor to outdoor and outdoor to indoor propagation losses.
- A propagation model for a transmitter situated much below the mean building height that computes the outdoor to outdoor and outdoor to indoor propagation losses.

Two different systems GSM and LTE will be considered throughout these simulations. The relevant parameters for both systems are shown in Table 5.4.

Parameter	Value
eNodeB Sensitivity	-114 dBm
D2D Sensitivity	-107 dBm
eNodeB Reception gain	16 dB
eNodeB Diversity gain	5 dB
eNodeB LNA gain	5 dB
Cable losses	3 dB
GSM MS transmitting power	33 dBm
LTE UE Transmitting power	24 dBm
Scenario Resolution	3 meters
Floor height	3.5 meters

Table 5.4: *Parameters of the simulation.*

5.5.1 System performance from the eNodeB perspective

In order to measure the system performance from the eNodeB perspective the scenario depicted in Figure 5.28 is simulated using the parameters of Table 5.4. It should be born in mind that both systems have been set to transmit with the maximum allowed power to take into account the worst case scenario in terms of interference. The scenario is composed of four buildings with a maximum height of 12 floors. The eNodeB is placed on the roof of one of the buildings. The D2D pairs are uniformly placed inside that building one floor at a time. The GSM devices are uniformly scattered around the ground level of the whole scenario. It should be born in mind that a GSM device can also be placed inside of a building but only in the ground floor.

The first step is to compute the path loss from the eNodeB. The results for different floors are shown in Figure 5.29.

Assuming that the channel is symmetrical the link budget from the UEs to the eNodeB can be computed taking into account the parameters shown in Table 5.4 obtained from [33] and [34]. From the link budget, the SNR and the the SIR can be computed. Making use of the results from Figure 5.17 on page 38 the frame success rate is calculated as a function of the SNR and the SIR.

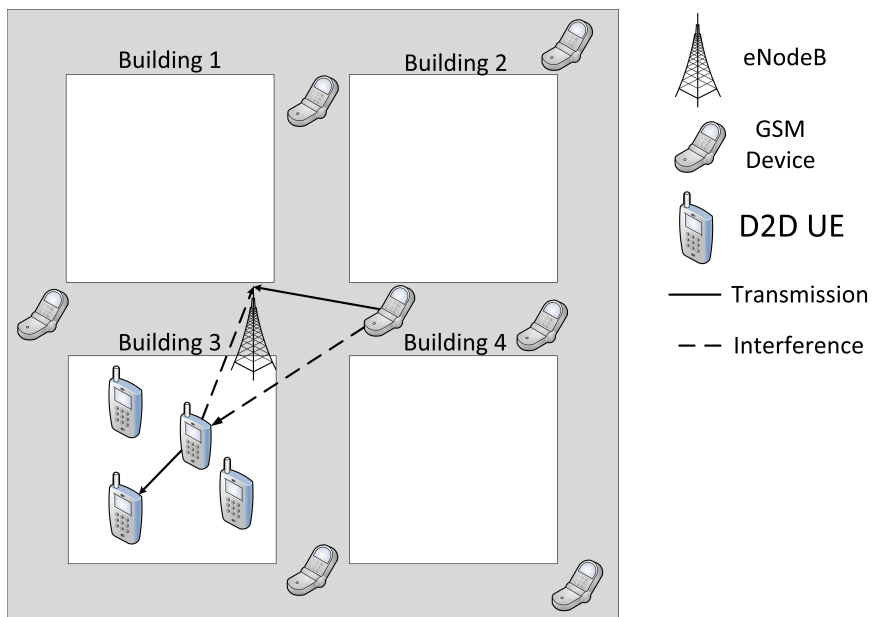
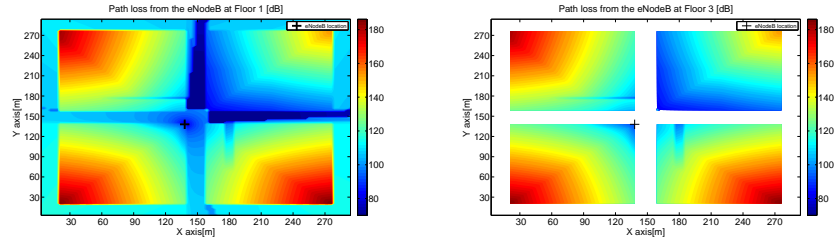


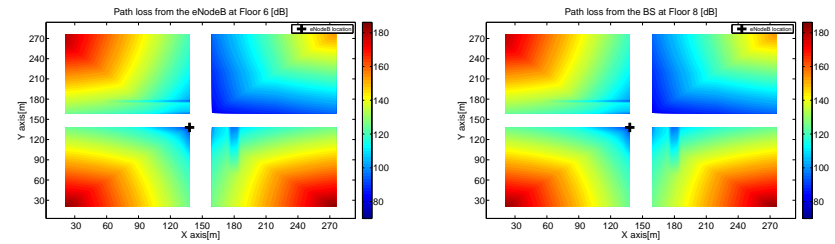
Figure 5.28: *Simulation Scenario from the eNodeB point of view.*

Performance of a legacy GSM system

The objective of this section is to measure the performance of a legacy system in the scenario described in Figure 5.28 when no interference from other systems is considered. The GSM users are randomly scattered in the scenario exclusively in the ground floor, the parameters used for this simulation are shown in Table 5.4. The results can be seen in Figure 5.30



(a) Losses computed from the eNodeB to the ground floor. (b) Losses computed from the eNodeB to the 3rd floor.



(c) Losses computed from the eNodeB to the 6th floor. (d) Losses computed from the eNodeB to the 8th floor.

Figure 5.29: Computed losses from the eNodeB to the different floors in the scenario.

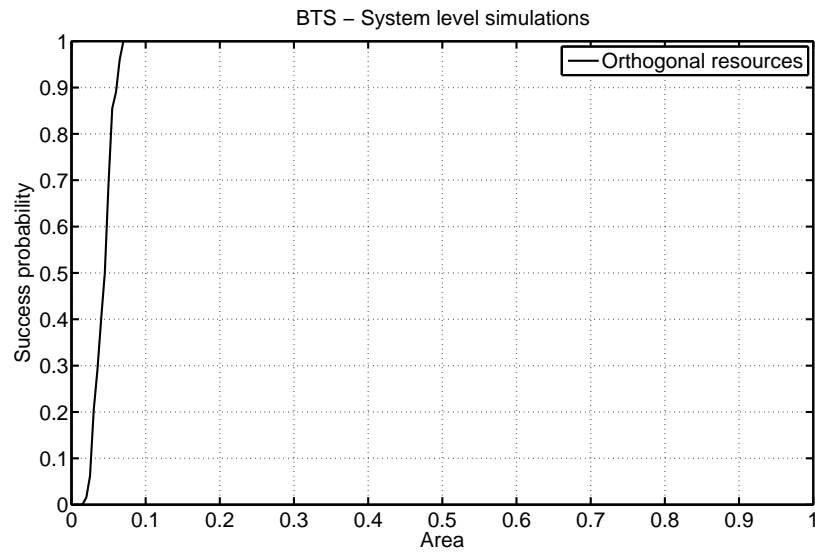


Figure 5.30: Success probability for the GSM system using a channel in exclusivity.

Figure 5.30 exhibits that even when no interference is accounted for, the system is not capable of servicing the whole scenario.

Performance of a system not using interference cancellation

The objective of this section is to measure the performance of an unmodified system in which two different radio access technologies coexist in the same frequency. The results are shown in Figure 5.31.

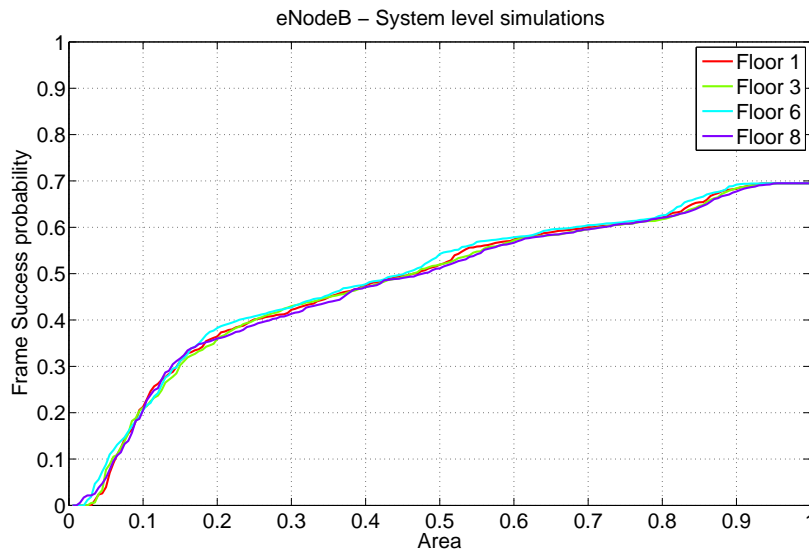


Figure 5.31: *Success probability for the GSM system sharing a channel with a D2D system with no Interference Cancellation.*

Figure 5.31 indicates that the interference from the D2D system is severe and affects the legacy GSM system enough to render it unusable.

Performance of a system using interference cancellation

The objective of this section is to measure the performance of a system that uses interference cancellation to allow the coexistence of two different radio access technologies in the same frequency. The results are shown in Figure 5.32

Figure 5.32 shows that there is not a discernible difference in performance throughout the different floors.

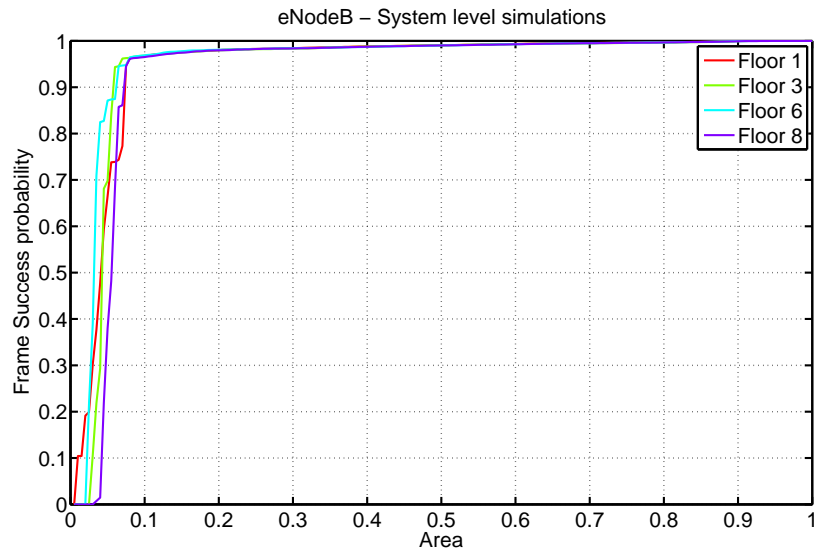


Figure 5.32: *Success probability for the GSM system sharing a channel with a D2D system with Interference Cancellation.*

Performance gain for a system using Interference cancellation

This section aims to show the gain achieved by a system in which two different radio access systems use the same frequency and employs an interference cancellation scheme compared to a system of the same characteristics that does not employ interference cancellation. This comparison can be observed in Figure 5.33.

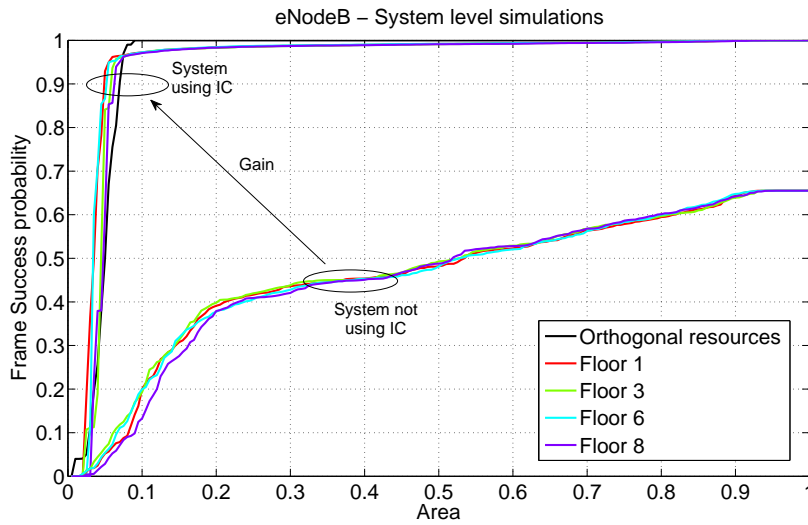


Figure 5.33: Comparison of the Frame success probability for a GSM system sharing a channel with a D2D system using/not using an Interference Cancellation scheme.

In Figure 5.33 it can be observed the enormous gain obtained by using the proposed interference cancellation technique.

5.5.2 System performance from the perspective of the D2D UE

In this section the performance of a D2D system is analysed. The simulation scenario from the perspective of the D2D UE is shown in Figure 5.34. The GSM users are randomly located in the ground floor, in the proximity of one of the buildings. The D2D users are located in incremental floors of that same building.

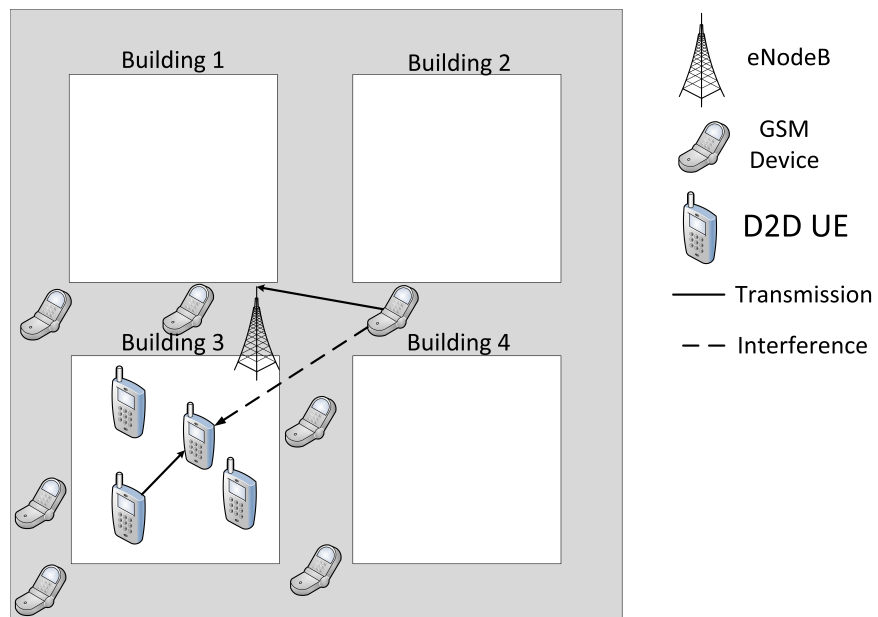
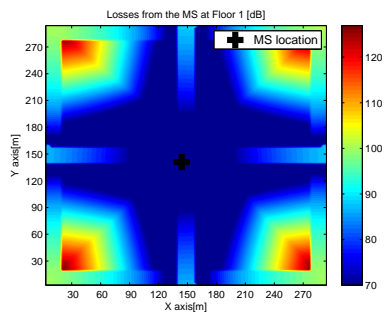
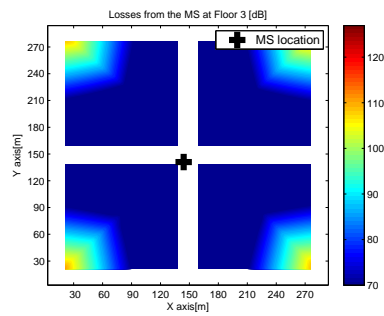


Figure 5.34: *Proposed Scenario from the D2D UE point of view.*

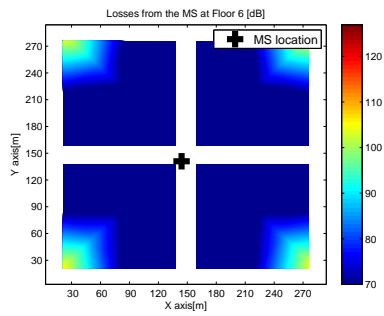
The propagation model from [32] is used to compute the Path Loss from the Mobile Station (MS) to the D2D UE where the interference cancellation takes place. The results are exhibit in Figure 5.35.



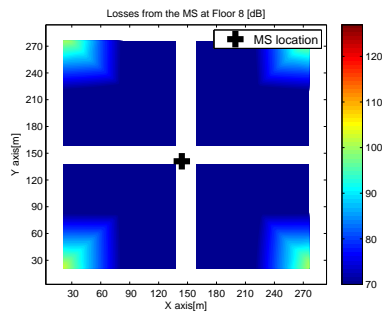
(a) Losses computed from the MS to the ground floor.



(b) Losses computed from the MS to the 3rd floor.



(c) Losses computed from the MS to the 6th floor.



(d) Losses computed from the MS to the 8th floor.

Figure 5.35: Computed losses from the MS to the different floors in the scenario.

Additionally the indoor propagation model from [32] is used to compute the path loss from the transmitting D2D UE to the receiving D2D UE and from the GSM MS to the receiving D2D UE. To compute the path loss between D2D UEs both Line-of-sight (LOS) and non LOS conditions with up to five interfering walls between the D2D UEs are considered. The link budget is computed considering the parameters from Table 5.4 and from it the SNR and the SIR are obtained. Making use of the results from Figure 5.16 on page 37 the frame success probability is obtained.

Performance of a D2D system

The objective of this section is to measure the performance of a D2D system in the scenario described in Figure 5.34. The results can be seen in Figure 5.36

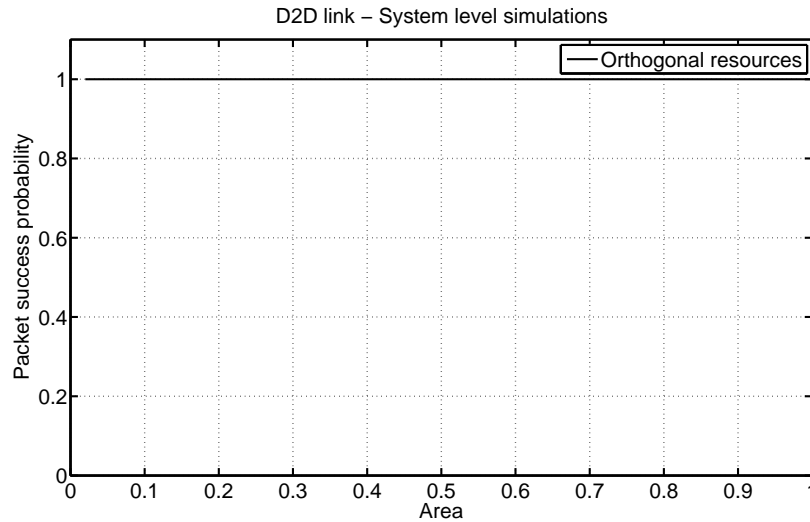


Figure 5.36: *Success probability for the D2D system using a channel in exclusivity.*

From Figure 5.36 it can be extracted that the D2D system works perfectly under the simulated conditions.

Performance of a system not using interference cancellation

The objective of this section is to measure the performance of an unmodified D2D system coexisting with a legacy GSM system in the same frequency. The results are shown in Figure 5.37.

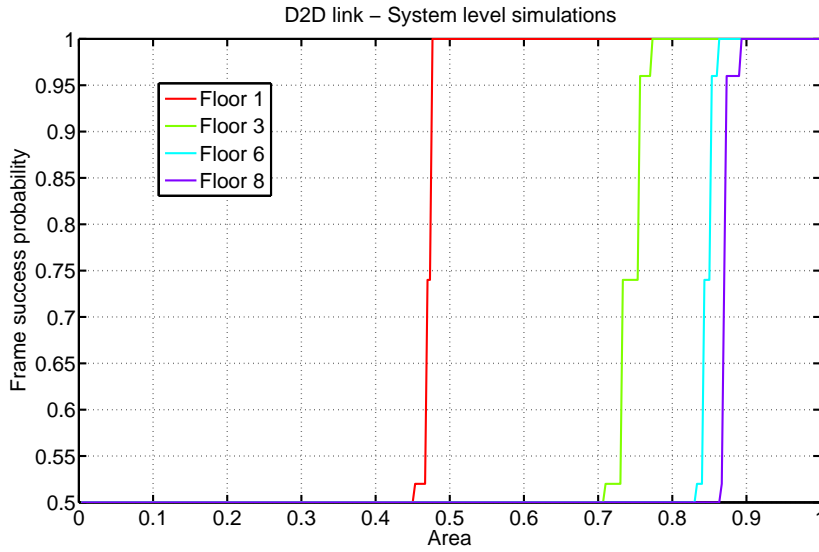


Figure 5.37: Success probability for the D2D system sharing a channel with a GSM system with no Interference Cancellation.

From Figure 5.37 it can be concluded that the best performance is achieved when the D2D UEs are located on the ground floor where the losses for the GSM MS are higher according to the model provided in [32].

Performance of a system using interference cancellation

The objective of this section is to measure the performance of an unmodified D2D system coexisting with a legacy GSM system in the same frequency for the scenario depicted in Figure 5.34. The results are shown in Figure 5.38. In Figure 5.38 it can be observed that there is not a significant difference in the system performance throughout the different floors.

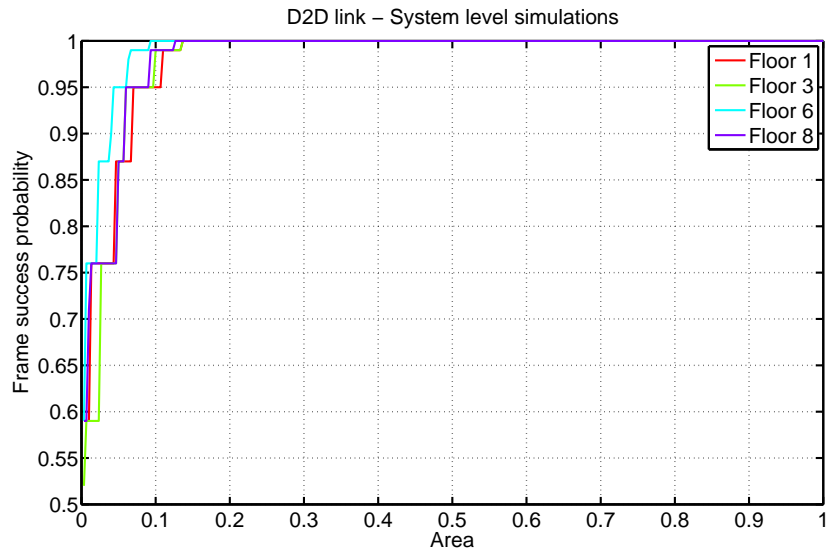


Figure 5.38: Success probability for the D2D system sharing a channel with a GSM system with no Interference Cancellation.

Performance gain for a system using Interference cancellation

This section aims to illustrate the gain achieved by a system in which two different radio access technologies use the same frequency and employs an interference cancellation scheme against a system of the same characteristics that does not employ interference cancellation. This comparison can be observed in Figure 5.39.

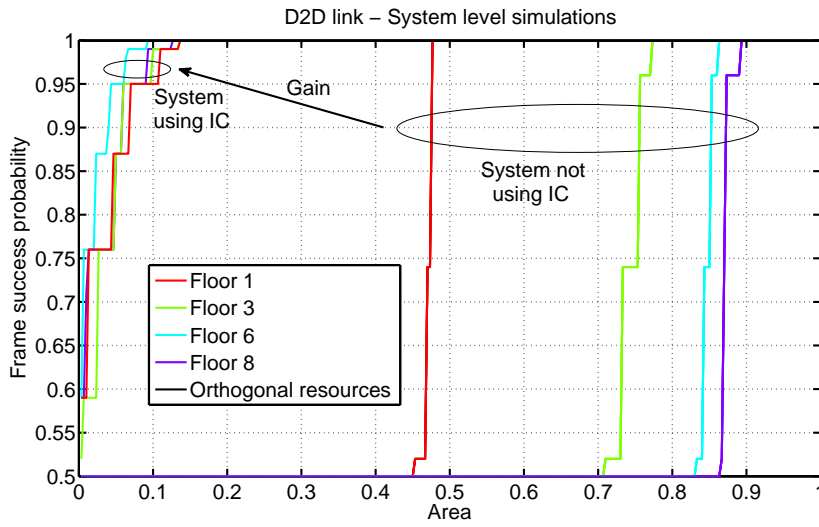


Figure 5.39: Comparison of the Success probability for a D2D system sharing a channel with a GSM system using/not using an Interference Cancellation scheme.

In Figure 5.39 it can be observed the remarkable gain obtained by using the proposed interference cancellation technique.

5.5.3 Results discussion for the METIS simulations

The results of this Section show that the coexistence of two different radio access technologies in the same frequency is achievable. The analysis from both ends of the communication link reflect that the trade-off for such possibility is a subtle decrease in the achievable quality of service.

Chapter 6

Implementation

This chapter addresses the description of the experiments carried out for this Thesis. The feasibility of an implementation for the interference cancellation scheme previously proposed will be analysed. The ultimate goal is to test the possibility of two different signals coexisting in the same frequency in a real scenario. As detailed in Chapter 4 the signals under study will be a GMSK modulated signal which it is used by the GSM system and a OFDM coded signal that it is used by the LTE system. A detailed account of the interference cancellation process and its results will be provided as well as a comparison with the simulation results from Chapter 5.

6.1 Hardware requirements

This section details the hardware requirements for implementing the proposed interference cancellation scheme, the hardware chosen and its properties.

For the implementation of the interfering cancellation scheme described in Chapter 4, access to the raw radio signal is required. Thus, the chosen hardware should provide access to the digital In-phase and Quadrature samples. Additionally to resemble as close as possible to the GSM system, the main signal characteristics of this system as detailed in Table 6.1 will be taken into consideration. Therefore taking into consideration the channel width, the chosen hardware should be capable of bandpass sampling of at least two times the higher bandwidth taken into account, in this case 400 KSamples/s.

A SDR platform should fit adequately for the previously mentioned requirements. In particular, an USRP2 and a NI USRP-2920, capable of sampling up to 10 MS/s, and equipped with RFX900 daughterboards, were used to carry out the experiment.

GSM system signal characteristics	
Modulation	GMSK
Frequency band	900 MHz and 1800 MHz
Channel width	200 KHz
Data rate	270.833 kbit/s (for all 8 GSM channels)

Table 6.1: *Relevant signal characteristics of the GSM system [4].*

6.2 Software tools

Software Defined Radio fundamentals: The Wireless Innovation Forum defines Software Defined Radio as: "a radio in which some or all of the physical layer functions are software defined".

As detailed in [35] there are several signal processing environments available to implement the desired baseband functionality in SDR being the most popular:

- MATLAB: a numerical computing environment that provides algorithms and tools for analog and digital signal processing.
- GNU Radio: a free and open-source software development toolkit that provides signal processing blocks to implement software defined radios.[36]
- IT++: a C++ library of mathematical, signal processing and communication classes and functions.[37]

The work discussed in this chapter makes use of of MATLAB for post-processing tasks and GNU Radio for implementing the basic transceiver functionality and for signal modulation and demodulation.

6.3 Setup Description

To implement the scenario of this Thesis, shown in Figure 2.2 on page 7, three USRPs are needed. The first USRP working as a receiver, the second USRP working as the transmitter for the desired signal and the third USRP working as the transmitter for the interfering signal. A graphical representation of this setup is shown in Figure 6.1.

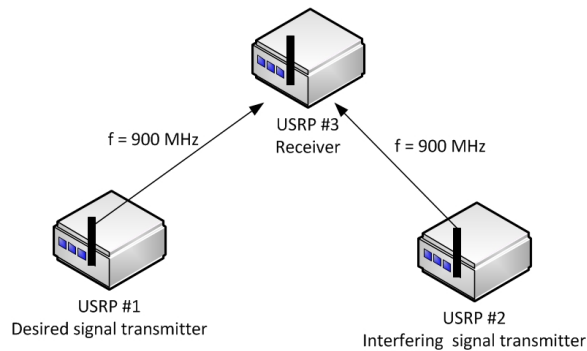


Figure 6.1: *Sketch of the ideal implementation setup.*

In order to establish a reference case, the performance of the two communication links is measured individually as shown in Figure 6.2.

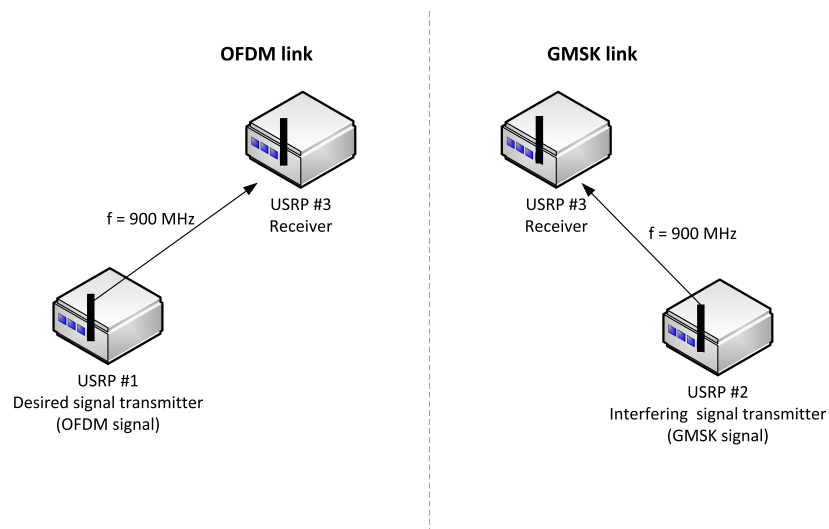


Figure 6.2: *Sketch of the setup used to establish a reference case. For both links the PSR is measured at the receiver.*

The Packet Success Rate (PSR) of the setup shown in Figure 6.2 is measured for the GMSK link and the OFDM link using the following purpose specific signal processing blocks included in GNU Radio:

- For the GMSK link:
 - In the transmitter, the narrowband benchmark_tx.py module is used to modulate and transmit a GMSK signal.
 - In the receiver, the narrowband benchmark_rx.py module is used to receive, demodulate and measure the packet throughput of the transmitted GMSK signal.

- For the OFDM link:
 - In the transmitter, the OFDM benchmark_tx.py module is used to modulate and transmit a OFDM signal.
 - In the receiver, the OFDM benchmark_rx.py module is used to receive, demodulate and measure the packet throughput of the transmitted OFDM signal.

The parameters selected for both links aim to maximize the PSR. The results of the tests show that the average PSR for the OFDM link is 80% and for the GMSK link is 100%.

One of the basic requirements for interference cancellation is receiving correctly the interfering signal. Therefore, the experiment will be focused on canceling a live GMSK interfering signal. The parameters of the GMSK link are shown in Table 6.2.

Furthermore as the PSR of OFDM link does not meet the minimum requirements for a reliable communication even in absence of interference, the signal received from the OFDM communication link will be substituted by an OFDM signal generated in MATLAB whose characteristics are shown in Table 6.2, the improvement of the OFDM receiver will be considered out of the scope of this Thesis. Both signals will be added in MATLAB to obtain the mixed signal to be analyzed.

Parameter	Value
Transmitting USRP	USRP2
Receiving USRP	NI-USRP2920
Sampling Rate	10^6 samples per second
Samples per Symbol	4
Digital attenuation	4 dB
Transmitted power	23 dBm
Receiver gain	40 dB
Receiver antenna	VERT2450 [38]
Receiver - Transmitter distance	0.7 meters
OFDM signal parameters	
Parameter	Value
Modulation	QPSK
Number of subcarriers	12
IFFT size	2048
Cyclic Prefix length	160

Table 6.2: *OFDM and System simulation parameters*

Therefore the two communication links that constitute the setup will be implemented in the following way:

- The GMSK link consists on a transmitter (USRP2) and a receiver (NI USRP-2920) communicating over a wireless link according to the parameters shown in Table 6.2. It should be noticed that the same data burst is transmitted through the 8 time slots simulating the GSM uplink. A picture of the setup for the GMSK link can be seen in Figure 6.3.
- The OFDM link will be implemented with a MATLAB generated signal whose characteristics are shown in Table 6.2.

A scheme of the implementation setup can be observed in Figure 6.4.



Figure 6.3: *Picture of the implemented GMSK link.*

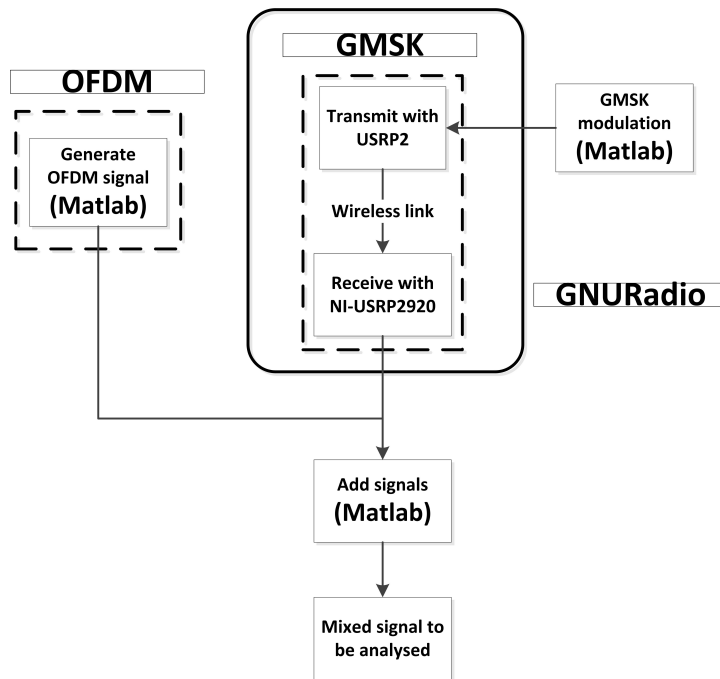


Figure 6.4: *Scheme of the implemented setup.*

6.3.1 GMSK modulation and demodulation

The GMSK transmission and reception is performed in GNU Radio, using the functions `gmsk-mod` and `gmsk-demod`. The modulator and demodulator are implemented as follows:

- The GNU radio GMSK modulator is composed of a non return to zero encoder, a Gaussian filter and a frequency modulator [39]. The modulator block diagram is shown in Figure 6.5.

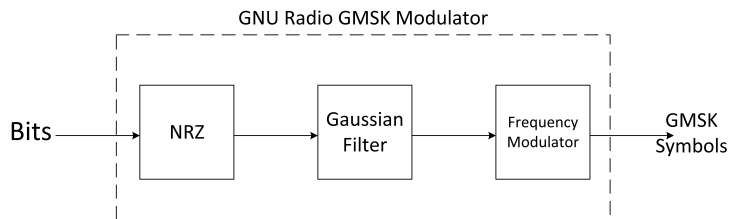


Figure 6.5: *GNU Radio GMSK Modulator*.

- The GNU radio GMSK demodulator includes the following blocks; a quadrature demodulator, a clock synchronization block using Mueller and Muller technique which is further explained in 6.3.2, and a slicer for symbol decision [39]. The block diagram is shown in Figure 6.6.

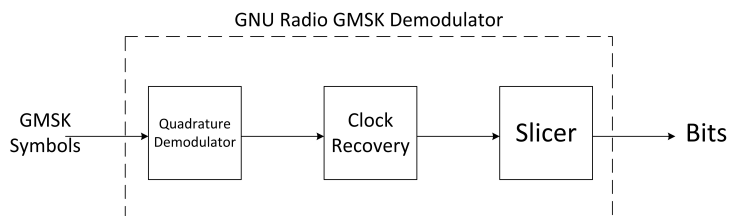


Figure 6.6: *GNU Radio GMSK Demodulator*.

6.3.2 Synchronization considerations

This section has been adapted from [40] [41] [42] and [24].

Synchronization plays a major role in the design of a digital communication system. In this subsection will be shown some of the major issues that affect to synchronization purposes. There are two main aspects to be taken into account, timing recovery and frequency recovery. Timing recovery works at a symbol level, and its purpose is to achieve symbol synchronization. Frequency recovery algorithms aims to remove the residual frequency offset produced by the hardware imperfections.

- **Timing Synchronization:** There are two main categories of timing synchronizers depending on their operating principles, error-tracking and feed forward. "Error-tracking synchronizers use the principle of the Phase-Locked Loop (PLL) to extract a sampling clock which is in close synchronism with the received signal" [24]. On the other hand, feed forward synchronizers measure the instantaneous timing error. Moreover, if a synchronizer uses the receiver decisions to help a timing estimation then it is called decision-directed. Otherwise is called non-data-aided.

- **Frequency Synchronization:** Frequency error between the transmitter and receiver local oscillators will result in a demodulated signal with a residual frequency offset. This residual frequency generates a spinning in the demodulated symbol. In order to accurately demodulate a symbol this effect needs to be removed.

In this experiment the implemented timing synchronizer is a Mueller and Muller [39]. Mueller and Muller is a discrete error-tracking, a typical block diagram is shown in Figure 6.7.

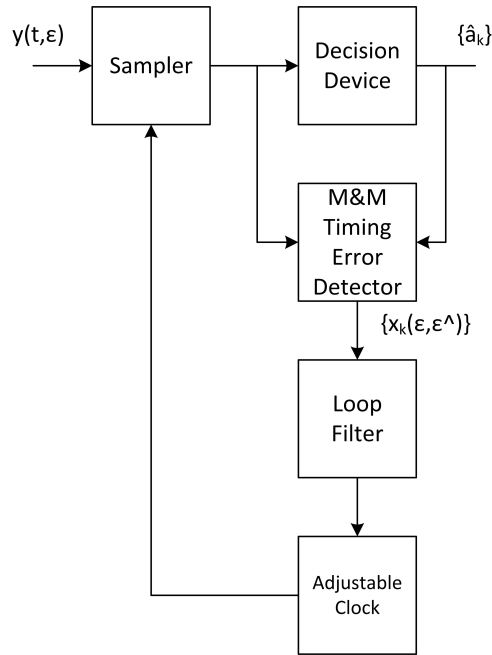


Figure 6.7: *Block Diagram of a receiver with a Mueller and Muller synchronizer [24].*

The timing error detector outputs the following sequence:

$$x_k(\epsilon, \hat{\epsilon}) = \hat{a}_{k-1}y(kT - \hat{\epsilon}T; \epsilon) - \hat{a}_k y(kT - T + \hat{\epsilon}T; \epsilon) \quad (6.1)$$

where T is the symbol period, ϵ is the timing error, $\hat{\epsilon}$ is the estimated timing error and a_k is the decided symbol. Figure 6.8 features an example of the error value in Mueller and Muller.

6.3.3 Bandwidth and Rate considerations

In order to adapt the modulated and transmitted GMSK signal to emulate a GSM signal behavior in relation with the LTE symbols, the transmission rate has to be changed. Taking into account that the GSM symbol rate is 270833

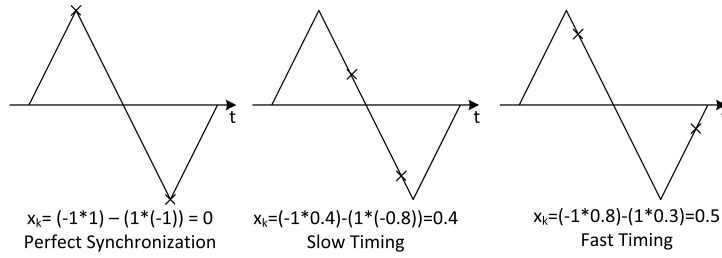


Figure 6.8: *Example of error calculation in Mueller and Muller.*

symbols per second [4] and 14000 symbols per second and per subcarrier for the LTE case [25]. This means that in a OFDM symbol period there are:

$$\frac{\text{GMSK symbols per second}}{\text{OFDM symbols per second}} = 19.3452 \text{ GMSK symbols} \quad (6.2)$$

From [25] it is known that the LTE symbol length is the ifft size plus the cyclic prefix size, in our case:

$$\text{ifft size} + \text{cyclic prefix size} = 2048 + 160 = 2208 \quad (6.3)$$

Therefore each GMSK symbol should have;

$$\frac{2208}{19.3452} \approx 113[\text{samples/symbol}] \quad (6.4)$$

Since the number of samples per symbol used to transmit the GMSK was only 4, the received GMSK signal needs to be up sampled to match the desired value. The up sampling process was achieved in MATLAB through the function `resample().m`.

6.4 Interference cancellation process

In order to successfully perform the SIC process, the interfering signal needs to be demodulated, modulated, and then subtracted from the received one. The process of demodulation and modulation will be called regeneration.

6.4.1 Interference regeneration

As previously detailed the raw GMSK I-Q samples received in the NI-USRP2920 are post-processed in MATLAB to perform the interference cancellation. The post-processing is carried out in two different stages:

1. Signal acquisition.
 - (a) Generating an OFDM signal within MATLAB.

- (b) Adjusting the power of the received GMSK signal in the USRP-2920 to sweep a range of SIR values of -20 dB to 5 dB.
 - (c) Adding the GMSK and OFDM signals.
2. Signal regeneration and subtraction.
- (a) Demodulating the GMSK signal.
 - (b) Regenerating the GMSK signal either from the demodulated bits obtained in the previous step (No side information case) or from the transmitted bits, assuming there were no errors in the communication link (side information case).
 - (c) Adjust the frequency of the regenerated signal so it fits the frequency offset of the received one.

The efficiency of the process will be measured with the achieved OFDM Bit Error Rate (BER). Afterwards the GSM signal is regenerated and removed from the received signal in MATLAB. The implementation scheme is described in figure 6.4.

6.4.2 Amplitude matching

In order to scale the regenerated signal amplitude, the root mean square power of the received GMSK signal is estimated as;

$$rms = \frac{1}{\sqrt{N}} \sum_{i=1}^N |Rx_i|^2 (V) \quad (6.5)$$

Where N is the number of samples per slot and Rx_i are the samples of the received signal. Next, the regenerated signal is multiplied by the following ratio;

$$ratio = rms / rms_{reg} \quad (6.6)$$

The received signal and the regenerated one are shown in Figure 6.9.

6.5 Initial interference cancellation scheme

The interference cancellation block diagram is shown in Figure 6.10. The slot synchronization is achieved by correlating the received signal with the training sequence. Afterward the interfering signal is demodulated and modulate as explained in 6.3.1. Finally, the desired signal is obtained by subtracting the regenerated signal to the received one.

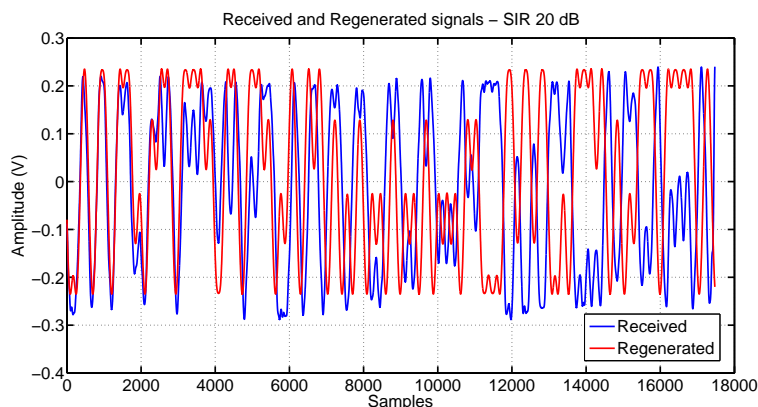


Figure 6.9: Received and regenerated GSMK slot for a SIR of 10 dB.

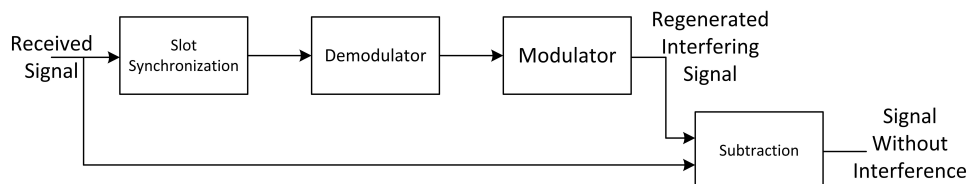


Figure 6.10: Interference Cancellation Block Diagram with side information

6.5.1 Initial interference cancellation results

It can be observed in Figure 6.9 that even though the achieved BER is 0 since side information is assumed, in the figure the regenerated signal does not match the received one. Since all the received symbols are successfully demodulated it would have been expected for the regenerated signal to match the received one. Taking into account that GSMK is a continuous phase modulation where all the symbols have the same amplitude, and that all the bits are successfully decoded, this leads to a phase error between the regenerated and received signal. Therefore some extra process at the interference cancellation scheme must be done.

6.6 Proposed interference cancellation scheme

As argued in the previous section, there were some discrepancies between the regenerated and received signals. Figure 6.11 features the phase difference between the signals. It can be observed that the phase difference is lineal and continuously increasing. This effect is caused by the local oscillators deviation, as explained in Subsection 6.3.2. A typical receiver is able to suppress this impairment in the signal, but to achieve a successful interference cancellation the regenerated signal needs to be impaired with

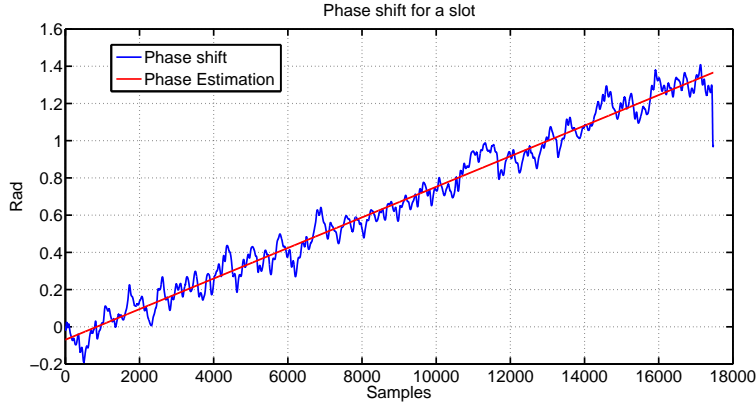


Figure 6.11: *Phase difference between the received and regenerated GMSK slot for a SIR of 20 dB.*

the same frequency shift.

6.6.1 De-compensation of the sampling clock shift

As previously argued it is fundamental for interference cancellation to estimate the frequency shift in the received signal, as can be observed in Figure 6.11. The phase shift is estimated by fitting a straight line that minimizes the least square error. In this simulation the MATLAB function `polyfit().m` has been used to estimate the phase. The estimated phase shift needs to be added to the regenerated signal as follows:

$$\hat{R}eg[k, \hat{\phi}] = Reg[k, \phi_{reg}]e^{j\hat{\phi}} \quad (6.7)$$

Where ϕ_{reg} is the regenerated signal phase, $\hat{\phi}$ is the estimated phase and $Reg[k, \phi_{reg}]$ is the regenerated signal.

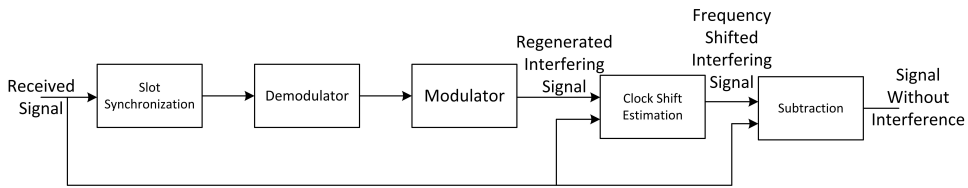


Figure 6.12: *Block Diagram of the proposed interference cancellation scheme.*

6.6.2 Proposed interference cancellation scheme results

The results of the proposed interference cancellation scheme are exhibited in Figures 6.13 and 6.14. Both figures represent the achieved bit success rate.

Additionally, for both figures:

- The blue curve represents the bit success rate obtained when applying the SIC technique.
- The red curve shows the bit success rate for the acOFDM simple detection.
- The black curve shows the achieved bit success rate for GMSK.

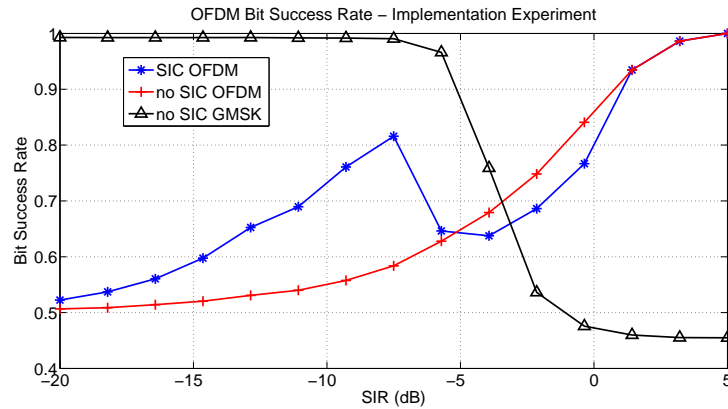


Figure 6.13: *Bit Success Rate for an antenna separation of 70 cm.*

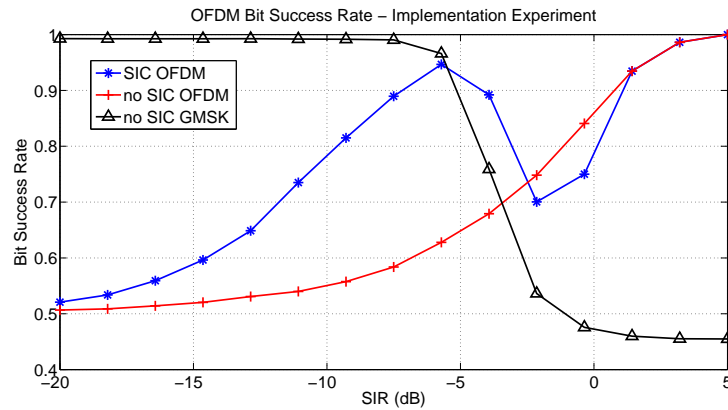


Figure 6.14: *Bit Success Rate for an antenna separation of 70 cm assuming side information.*

From the results featured in Figures 6.13 and 6.14 it can be inferred that for low SIR levels the GMSK subtraction is not accurate enough since the obtained success rate is close to 0.5. It is also observed that when the SIR starts increasing, the success rate increases as well reaching a maximum at 0.8 when no side information is available. The behaviour of the

simple detection curves resembles the results shown in Chapter 5 on page 22.

Figure 6.15 depicts the ratio between the rms of the result of subtracting the received and the regenerated signals and the rms of the transmitted OFDM signal. The relative rms shows how accurate the subtraction is, in case of a perfect subtraction the relative rms would be 0.

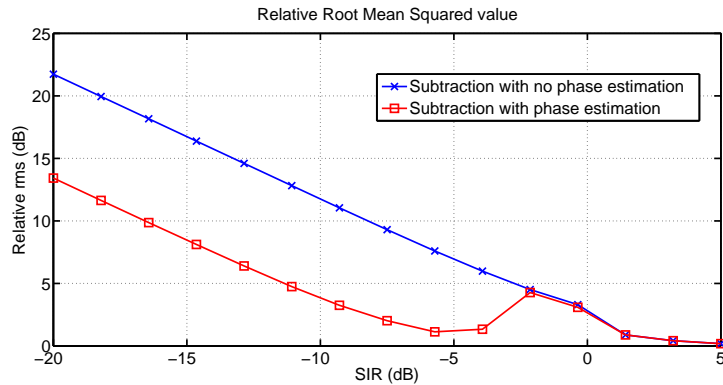


Figure 6.15: *Relative rms between the subtracted and original OFDM signals for phase estimation IC and simple IC cases.*

6.7 Experimental results discussion

From the results featured in Figures 6.13 and 6.14 it is extracted that the bit success rate does not reach higher than 0.95. Two reasons are identified for this behaviour:

- The experiment conditions were not the optimum ones.
- The amplitude matching may be including an error that masks the OFDM signal.
- The phase shift estimation is not accurate enough and needs to be improved.

In order to study the first reason, new measurements were taken, with an equivalent setup to that of Section 6.3 but with the antennas placed 20 cm apart. The results are shown in Figures 6.16 and 6.17.

It can be observed that the bit success rate obtained in the last set of measurements is higher than the one obtained in the first set. However the results still do not fit the expected values from 5 on page 22. It can be observed from the results that do not assume side information, Figures 6.13 and 6.16, that the bit success rate decays when the SIR is close to 0 dB. This decay is expected because the demodulated bit success rate decreases on par

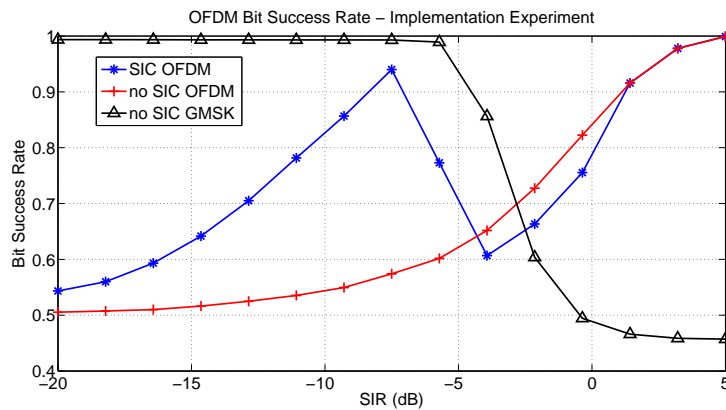


Figure 6.16: *Bit Success Rate for an antenna separation of 20 cm.*

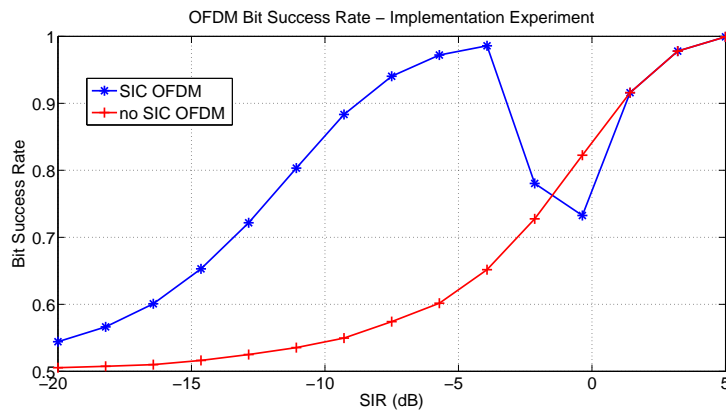


Figure 6.17: *Bit Success Rate for an antenna separation of 20 cm with access to side information.*

with the SIR as a consequence of the phase shift estimation errors leading to an unsuccessful subtraction. In contrast, this decay does not occur when side information is assumed as in Figures 6.14 and 6.17. If the phase shift estimator behaviour is studied for a SIR close to 0 dB, as depicted in Figure 6.18, it is observed that the estimation is not correct confirming the previous statements. Nevertheless, this reasoning does not justify the low bit success rate for low SIR levels. Similarly as done in Figure 6.14, in Figure 6.19 it is represented the ratio between the rms of the result of subtracting the received and the regenerated signals and the rms of the transmitted OFDM signal for the case where the antennas are placed 20 cm apart. It can be noticed that the rms ratio linearly decreases when the SIR level increases, without taken into account the zones close to a SIR of 0 dB which have already been explained before. This means that the subtraction error is constant with relation to the received signal amplitude. To achieve an error

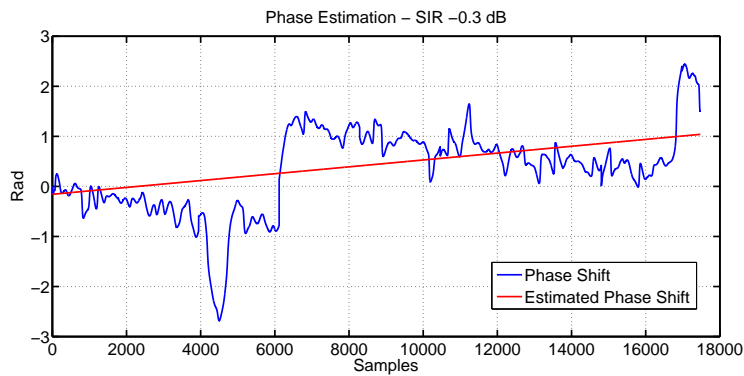


Figure 6.18: Phase shift estimator performance for a SIR level of 0.3 dB taking into account side information.

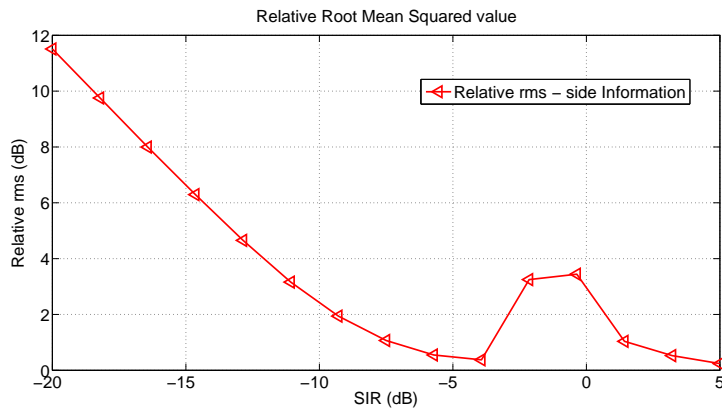


Figure 6.19: rms ratio between, the received and regenerated signal subtraction, and the OFDM. Taking into account side information.

reduction, that yields an increased bit success rate, the power and phase estimation methods need to be improved. However further improvement in the implemented algorithms is left for future works.

Chapter 7

Conclusion

7.1 Summary

As introduced in Chapter 1 network operators can cope with the demand from emerging technologies like M2M or communications while optimizing the required investment by smartly planning the roll-out of new technologies. The results from the work conducted support the possible continuation of the exploitation of the legacy networks. The benefits of the coexistence of different technologies should not be disregarded as a nearly optimal approach to serve the increasingly atomic market that results from the prevalence of the communications needs in every kind of industry. By offering a transparent solution to the end user, oblivious to the backbone of the network, operators can continue operating and profiting from their amortized legacy infrastructures, offer custom tailored solutions at moderate costs and discourage new competitors from serving the otherwise abandoned users of the legacy systems.

Throughout this Thesis an additional approach to both traditional cellular network planning and resource allocation has been proposed, implemented, tested and measured. The novel proposal described not only aligns with the latest research, such as [23], but goes beyond by proving the possibility for two different radio access technologies to coexist in the same frequency under loose restrictions.

Chapter 2 defines the scenario to be studied as well as the challenges and delimitations considered. The radio access technologies chosen are GSM for the legacy system and LTE for the D2D system. The objective of this thesis is stated as "the development of a Single Antenna Interference Cancellation (SAIC) algorithm, its implementation and its impact in a network".

Chapter 3 overviews the state of the art related to interference management. Different proposals are discussed and an solution based on an improved receiver with advanced interference cancellation capabilities is selected as the best fit for the scenario discussed in Chapter 2.

Chapter 4 analyses the scenario described in Chapter 2 and proposes a spatial segmentation as a result of the different SIR levels experienced at both ends of the communication link. This segmentation allows for the definition of three working areas in which the interference can be handled differently. For each of these areas an interference cancellation technique is proposed. The subsequent work focuses in two of these areas for which the viability of the spectral coexistence between two systems is examined.

Chapter 5 provides a full account for the performance of the proposed interference cancellation technique by simulating a communication link and examining it from three different perspectives: physical level, link level and system level. The guidelines from the METIS project are followed to build a simulation that closely resembles the real conditions experienced by a cellular network. Both ends of the communication link are studied and the results of applying interference cancellation exhibit an enormous gain in all cases. Overall, it has been proved that a D2D system can successfully coexist with a legacy D2I system with a small decrease in the performance of the latter as a trade-off.

Chapter 6 details the implementation of the proposed interference cancellation technique. Experimental results demonstrate that there is a considerable gain between the initial approach and the proposed technique. However the performance of the implemented technique is substantially worse than the simulation results from Chapter 5 forecast.

7.1.1 Research contributions

Throughout this document it has been proven:

- The feasibility of an interference cancellation technique for a live GMSK signal.
- The successful coexistence of two systems, GSM and LTE, through opportunistic interference cancellation with a decrease in throughput and coverage area as the trade-off.

7.1.2 Expected applications

In section 5.5.3 on page 59 it is exposed a possible application in which a frequency could be reused within a high building for short range communications. However there are several potential applications where the proposed method in this document could be applied according to [6] such as:

- Distributed Resource Allocation: The D2D will sense the spectrum and select the available resources without the control of the eNodeB.

- Cooperative Communications: Cooperation between D2D can enhance the available range and the overall network throughput.
- Network Coding: Linear coding of multiple packets at the transmitter can improve the communication flows between D2D.

7.2 Future outlook

There are plenty of possible extensions to the work conducted. The coexistence between GSM and LTE is used as the base for the investigations but the plethora of wireless access technologies commercially available gives room to study the performance of alternative systems to LTE that could lead to a performance improvement. Furthermore, it has been considered exclusively a SAIC technique but given the Multiple Input Multiple Output (MIMO) capabilities of the eNodeB and recent terminals an important future extension is to investigate the possible enhancement to the interference cancellation results. Regarding some of the concepts explained in Chapter 6 the following extensions are suggested:

- The phase shift estimator could be improved by including small phase fluctuations.
- Applying coding would improve the received bit success rate. Although, if instead of applying coding depending on the channel state information, could be applied taking into account the SIR, the bit success rate robustness would be increased.
- An adaptive system could be developed making use of the proposals from the previous points.

Appendices

Appendix A

Cellular Networks

This appendix addresses the basic concepts of a cellular network. The concepts discussed in this appendix include the characteristics of the mobile radio channel, an introduction to TDD and FDD and a brief description of cellular network planning. This Appendix is adapted from [4].

A.1 Channel Considerations

In order to fully understand the basics of a cellular network it is indispensable to examine the impact of the channel in the system. This section will briefly explain the main concepts used to model the channel for the simulations of Chapter 5 on page 22.

Under ideal conditions the Free Space Path Loss is used to predict the received signal strength, when both transmitter and receiver have a clear, unobstructed LOS. The received signal power decays with the square of the propagation path length. The path loss produced by the channel at a distance d_1 can be expressed as:

$$L = 10\log_{10} \left[G_t G_r \left(\frac{\lambda}{4\pi d_1} \right)^2 \right] dB \quad (\text{A.1})$$

Where G_t and G_r are the transmitting and receiving antenna gains in the direction of propagation and λ is the selected wavelength. Channel losses are frequency dependent, generally increasing with the inverse of the frequency. However this equation does not apply to a typical cellular scenario. A well studied case is the simple two ray scenario, shown in Figure A.1 on the facing page. In this case, the path loss can be described as:

$$L = 10\log_{10} \left[\left(\frac{h_1 h_2}{d_2^2} \right)^2 \right] dB \quad (\text{A.2})$$

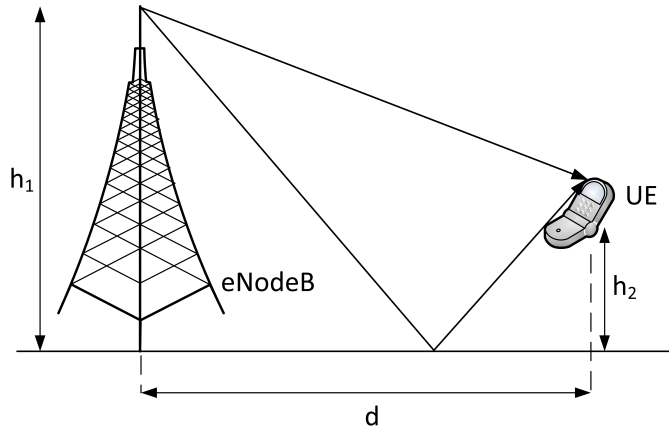


Figure A.1: *Illustration of the 2 ray path model.*

From equation A.1 it can be extracted that the path loss decay is bigger than d^2 . In real world scenarios the path loss decay is usually modelled as a function of the distance as:

$$L = d^{-\alpha} \quad (\text{A.3})$$

where α is the attenuation constant, normally defined as $2 \leq \alpha \leq 5$. In multipath channels all the different components carry a different phase, due to the different propagation path lengths, dispersion, and reflection with different materials among other reasons. The addition of all the components with a random phase can result in the cancellation of the signal at the receiver. This effect is known as fading.

Attending to the power of the received multipath components fading can be classified as:

- Rayleigh fading: all the multipath components have a similar power.
- Ricean fading: one of the multipath components is clearly stronger than the others, for example in the case of LOS communication.

Fading can also be classified as slow fading, usually related to shadowing, and fast fading related to multipath.

Fading is as well frequency selective, therefore if the working bandwidth is small enough to have a flat frequency response the channel is known as frequency-nonselective. If the working bandwidth is large enough to experience different levels of fading the channel is known as frequency-selective.

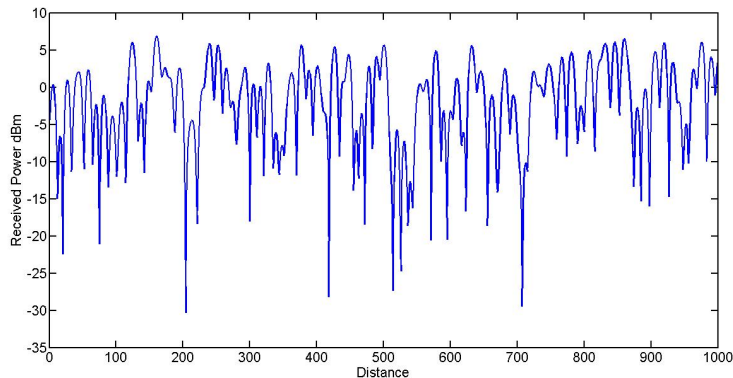


Figure A.2: *Typical Rayleigh fading.*

A.2 Frequency Division Duplex and Time Division Duplex

A communication system is said to be full duplex if it is capable of simultaneous reception and transmission. A half duplex system can achieve full duplex functionality if the switch between transmission and reception is fast enough to be unnoticeable for the user. Traditionally there are two techniques to achieve this capability, FDD and TDD.

A.2.1 Frequency Division Duplexing

FDD divides the working frequency band in two parts, assigning different frequencies for the transmitter and the receiver. There must be a frequency gap large enough to avoid the transmitter and the receiver interfering each other.

A.2.2 Time Division Duplexing

TDD manages to achieve a duplex communication by assigning different times to transmission and reception as shown in Figure A.4 and by switching between both modes quickly enough to be unnoticeable for the user. TDD is a good alternative to FDD because the implementation complexity is reduced. However during the interval T shown in Figure A.4 only half of the time is used for transmission, therefore the TDD rate must be roughly two times higher than the one in FDD to achieve the same bit rate.

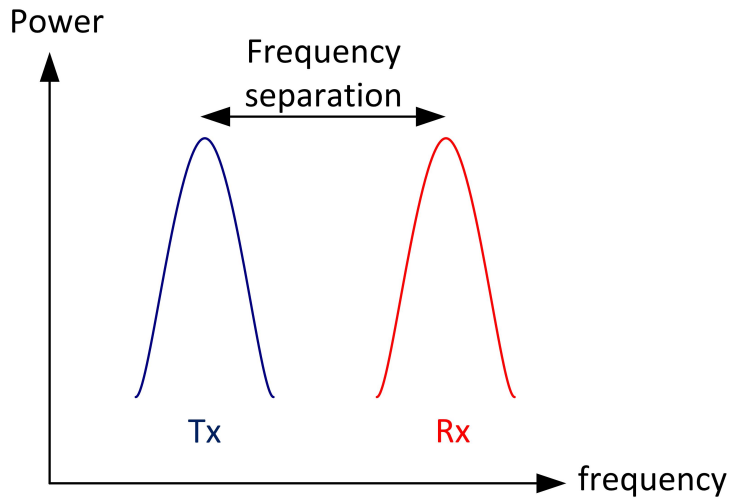


Figure A.3: *Frequency Division Duplex Scheme.*

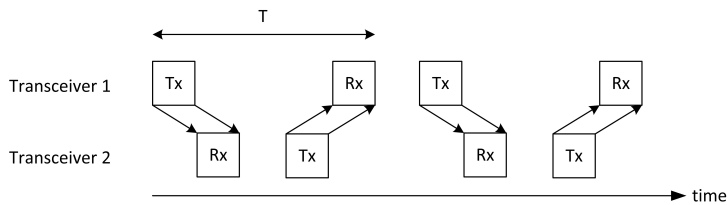


Figure A.4: *Time Division Duplex Scheme.*

A.3 Multiple Access Techniques

In a cellular system, the available spectrum is shared by the users. To avoid collisions between users the resources are divided and granted on demand. Different techniques are available to divide the system resources such as Frequency Division Multiple Access (FDMA), TDMA and Code Division Multiple Access (CDMA) that are explained in the following subsections.

A.3.1 Frequency Division Multiple Access

FDMA systems divide the total bandwidth available in sub-bands of equal bandwidth, channels. The system assigns a channel to each user. In figure A.5 a basic FDMA scheme is shown.

A.3.2 Time Division Multiple Access

In TDMA systems the user is cyclically allocated a finite transmission time (slot) and a frequency band. Usually in TDMA systems the total system bandwidth is divided in sub-bands. Each user is assigned with one time slot

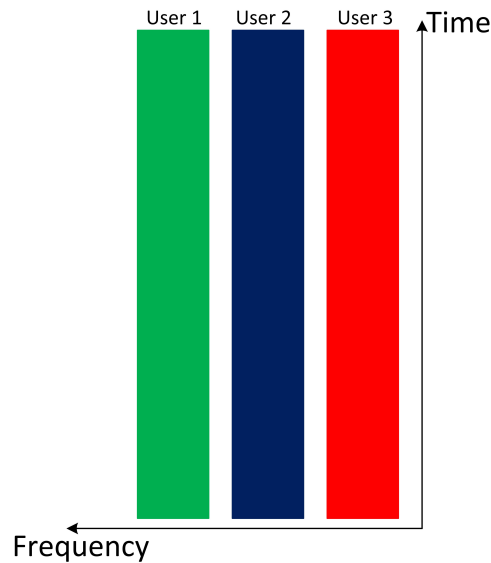


Figure A.5: *FDMA Channels scheme.*

and one sub-band as shown in figure A.6. Narrowband systems in order to avoid fading and achieve frequency diversity, the sub-band assignment is time-variant to statistically avoid fading. Collisions are avoided by using orthogonal hopping sequences.

A.3.3 Code Division Multiple Access

CDMA systems assign an entire frequency band to multiple users. This seamless coexistence is possible by multiplying the signal to be transmitted by different orthogonal codes. Afterwards, the signal of interest can be recovered by multiplying the received signal by the right code, otherwise the signal will behave as noise. The main drawback of this technique is the so-called near-far effect, that occurs when the power of one of the non desired signals is too high for the receiver to recover the desired signal. To avoid this situation a power control protocol is usually implemented.

A.4 Cellular Network planning

Mobile radio networks are dimensioned taking into account that:

- The number of users is several times higher than the maximum capacity of the system.
- The spectrum available is limited.

A generally accepted solution to cope with the latter limitation is to spatially reuse the frequencies. The main concepts related to frequency reuse are [43];

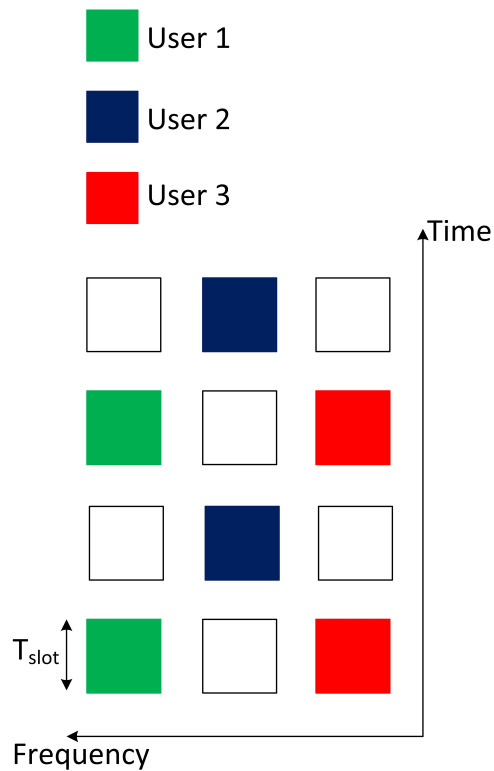


Figure A.6: *TDMA Channels scheme.*

- The area of interest is divided into cells of different shape, most commonly hexagonal.
- The cells are grouped into clusters. Every cluster is assigned all the frequencies available. The total bandwidth is divided into N channel sets where N is the cluster size i.e. the number of cells in the cluster.
- The cell clusters are spatially repeated. Each cell of the cluster is assigned a unique set of channels not assigned to any other cell in the cluster.
- The channel assignment follows an iterative process, determined by the minimum reuse distance.
- The process in which a connected device moves from one cell, where it is making use of a channel, to another and gets new resources assigned without losing its connection, is called handover.

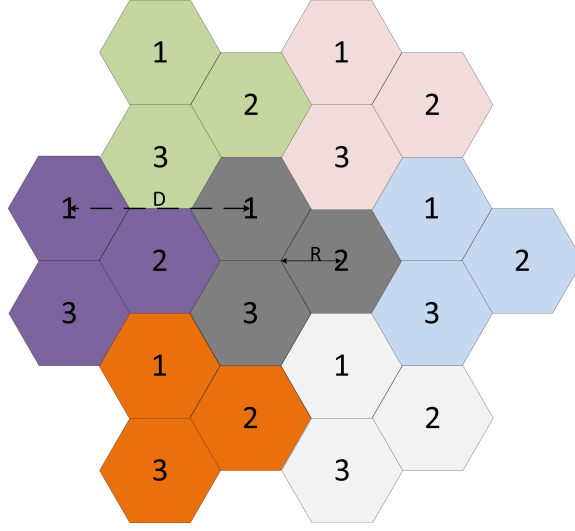


Figure A.7: Cluster Scheme: example of frequency allocation and clusters.

A.4.1 Signal to Noise Ratio and Signal to Interference Ratio considerations

The interference produced by the cell at a reuse distance D can be described as:

$$SIR = \frac{DesiredSignalPower}{InterferingSignalPower + NoisePower} \quad (A.4)$$

The interference can be considered from the base station or from the device point of view. If considering the interference from the device point of view, placing the device in the corner of a cell at a distance R from the base station and assuming that the interfering transmitters are placed equidistantly and transmit with the same power, the signal to interference ratio can be expressed as;

$$SIR = \frac{P_{tx}R^{-\alpha}}{\sum_{i=1}^6 P_{tx}D^{-\alpha} + N} = \frac{P_{tx}R^{-\alpha}}{6P_{tx}D^{-\alpha} + N} \quad (A.5)$$

If the noise power is ignored the next expression can be derived:

$$SIR \approx \frac{1}{6} \left(\frac{R}{D} \right)^\alpha \quad (A.6)$$

Therefore it can be inferred that the signal to interference ratio is dependent on the ratio of the cell radius R and the reuse distance D [4].

Appendix B

Basic Principles of GSM Physical Channel

This Appendix outlines the GSM physical channel characteristics relevant to the work conducted. The main concepts explained are: the GMSK modulation, the access scheme and the burst structure. This chapter has been adapted from [4].

B.1 GMSK

The GSM makes use of the GMSK modulation. GMSK is derived from MSK which is a continuous phase frequency in which the maximum frequency deviation is minimized. The modulation procedure comprehends three functions, as shown in Figure B.1. First, the data bits are differentially

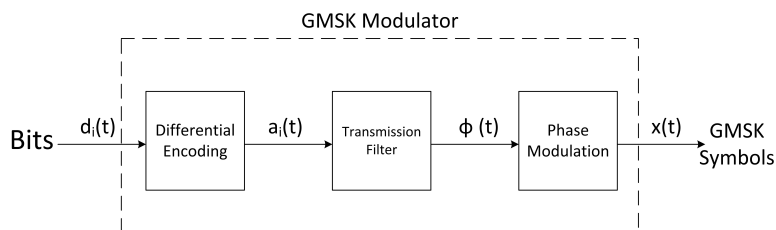


Figure B.1: *GMSK modulator*.

encoded:

$$\hat{d}_i = (d_i + d_{i-1}) \bmod_2 \quad (\text{B.1})$$

$$a_i = 1 - 2\hat{d}_i \quad (\text{B.2})$$

Where d_i is the i -th bit to be transmitted, a_i is the modulation data which weighs a Dirac pulse. In order to create the modulation phase $\varphi(t)$, the

pulses are filtered. The impulse response of the transmission filter is defined as the convolution of a rectangular pulse and a Gaussian filter defined by the impulse response $h(t)$, $g(t)$ can be expressed as:

$$g(t) = \frac{1}{\sqrt{2\pi}\sigma} e^{-\frac{t^2}{2\sigma^2 T^2}} \otimes \text{rect}(t/T) \quad (\text{B.3})$$

being σ and $\text{rect}(t/T)$;

$$\sigma = \frac{\sqrt{\ln 2}}{2\pi BT} \quad (\text{B.4})$$

$$(\text{B.5})$$

$$\text{rect}(t/T) = \begin{cases} 1/T & \text{for } |t| < T/2 \\ 0 & \text{for } |t| \geq T/2 \end{cases}$$

where T is the bit duration, B is the 3 dB bandwidth of the Gaussian filter and the product BT is set to 0.3 in GSM. Therefore it can be derived that the phase function can be written as:

$$\varphi(t) = \sum_i a_i \pi \eta \int_{-\text{inf}}^{t-iT} g(u) du \quad (\text{B.6})$$

being η the modulation index, set to 1/2 in GSM.

Finally the modulated GMSK signal can be expressed as:

$$x(t) = \sqrt{\frac{2E_c}{T}} \cos(2\pi f_0 t + \varphi(t) + \varphi_0) \quad (\text{B.7})$$

where E_c is the bit energy, f_0 is the carrier frequency and φ_0 is a random phase offset assumed to be stable through the whole data burst.

B.2 Multiple Access Scheme

GSM makes use of FDD, the available bandwidth for each band is 25 MHz. Each band is divided in channels of 200 KHz. The access scheme is a combination of TDMA and FDMA. Each user is assigned with one sub-band and a time slot as shown in figure B.2.

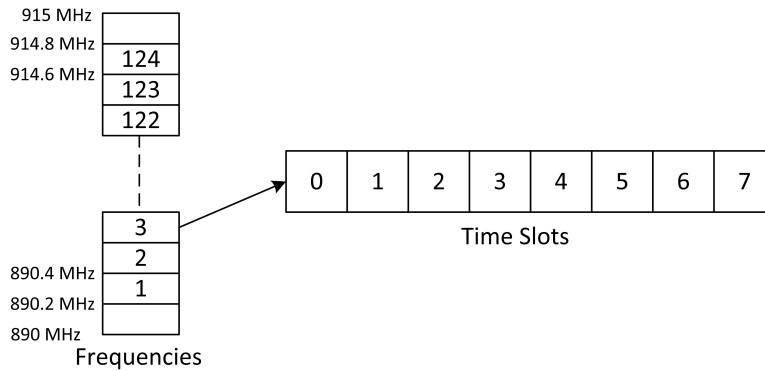


Figure B.2: *GSM Access Scheme for the uplink in the 900 MHz band.*

B.2.1 GSM Data Burst

Although there are five different types of burst defined in GSM, in this Thesis only the normal data burst has been simulated. Thus, this subsection will be focused exclusively in the normal burst. One normal burst is allocated per slot. As depicted in Figure B.3, a normal burst is composed of:

8.25 guard bits to avoid slots interference.

Two blocks of three tail bits set to zero whose main function is to help in the demodulation process.

Two blocks of 57 coded data bits

Two blocks of 1 bit to distinguish a traffic burst from a signalling burst.

A block of 26 bits of training sequence used to estimate the channel and for synchronization purposes.

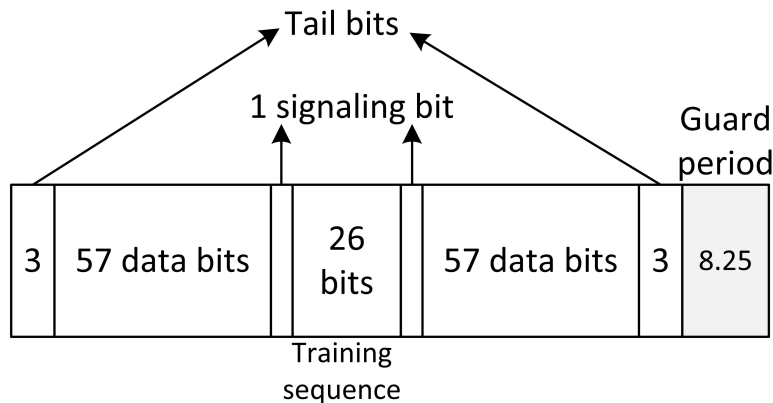


Figure B.3: *GSM Normal Data Burst.*

Appendix C

Basic Principles of LTE Physical Channel

This appendix addresses the basics of the LTE standard for wireless communications. The goal is to provide a brief background that supports the assumptions and concepts discussed throughout this Thesis. The main LTE characteristics explained are: the transmission scheme used in LTE, the different modulations, frame structure, and a brief explanation of the downlink physical channel. The contents of this Appendix have been adapted from [25] and [44].

C.1 Principles of OFDM

OFDM transmissions are based on the FDMA principles, each user being allocated a certain frequency range to transmit in order to share the channel. In OFDM each user is granted access to a set of subcarriers spread over a wide bandwidth. To avoid the Inter Symbol Interference (ISI) the subcarriers should be orthogonal to each other as shown in Figure C.2. Assuming that N_{Sc}^{Rb} subcarriers have been assigned to an user, the

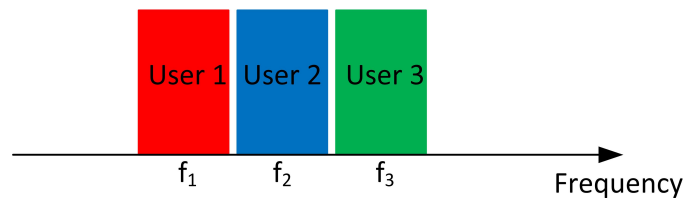


Figure C.1: *FDMA example.*

transmitted signal $x(t)$ in the interval $mT_u < t < (m + 1)T_u$, being T_u the

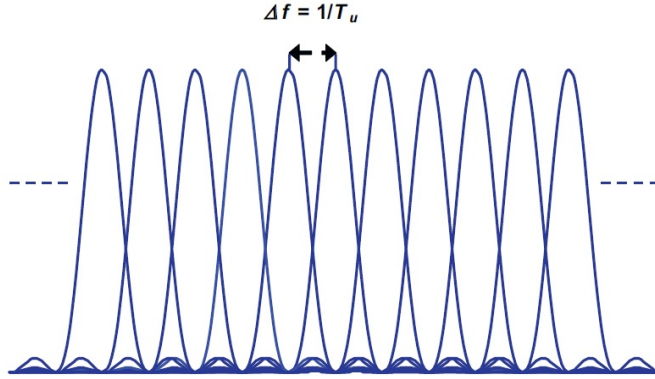


Figure C.2: OFDM subcarrier Spacing [29].

subcarrier period, would be noted as:

$$x(t) = \sum_{k=0}^{N_{Sc}^{Rb}-1} X_k(t) = \sum_{k=0}^{N_{Sc}^{Rb}-1} a_k^{(m)} e^{j2\pi k \Delta f t} \quad (C.1)$$

Where $X_k(t)$ is the k th modulated subcarrier with frequency Δf , and $a_k^{(m)}$ the k th complex symbol to be transmitted. Consequently N_{Sc}^{Rb} symbols can be transmitted in parallel. Figure C.3 depicts a typical OFDM modulator. Finally, to prevent ISI in OFDM and reduce the receiver complexity, a cyclic

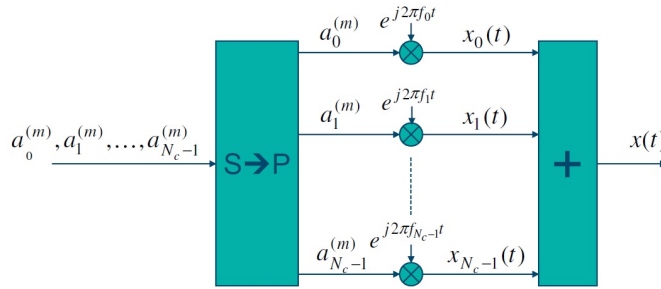


Figure C.3: OFDM Modulator [29].

prefix is added to $x(t)$.

C.1.1 Peak average power ratio (PAPR)

A well known drawback of OFDM is the Peak average power ratio (PAPR). The PAPR is defined as follows:

$$\text{PAPR} = \frac{|\text{OFDM}_{\max}|^2}{\text{rms}(\text{OFDM})^2} \quad (C.2)$$

Where OFDM_{\max} is the peak value of the OFDM transmission, and $\text{rms}()$ is the root mean squared value. The PAPR is a major challenge in OFDM transmitters since the sum of many narrowband signals in time domain can result in high values at some points compared to the mean signal power. This leads to a high power consumption in linear amplifiers and a reduced operation range. In [29] some possible solutions for the PAPR are briefly explained:

- Tone Reservation: A portion of the subcarriers are reserved. Instead of transmitting data, the reserved subcarriers are modulated in order that the Peak-to-Average Power Ratio (PAPR) is minimized. On the other hand, reserving a subset of subcarriers result into bandwidth reduction, and the calculations to compute the correct modulation to reduce the PAPR are complex.
- Prefiltering or Precoding: "Linear processing is applied to the symbol sequence before the OFDM modulation" [29].
- Selective Scrambling: Different scrambling codes are applied to the bit sequence and modulated afterwards. Only the coded sequence with the lower PAPR is transmitted. The receiver must try all the scrambling codes in order to find the right bit sequence.

C.2 Frame structure

This subsection explains the structure of a LTE frame. There are two types of frame structures available in LTE, one applicable to FDD, and one applicable to TDD. Since the TDD features of LTE have not been taken into account in this Thesis, only the FDD frame will be explained. The smallest unit available in a LTE frame is $T_s = 1/(15000 * 2048)$. All the other parameters are given in function of T_s . The downlink and uplink transmissions in LTE are organized in radio frames with a duration of $T_f = 307200T_s = 10$ ms. Each radio frame is composed of 10 subframes, which are formed by two consecutive slots of duration $T_{slot} = 0.5$ ms. The radio frame structure is illustrated in Figure C.4.

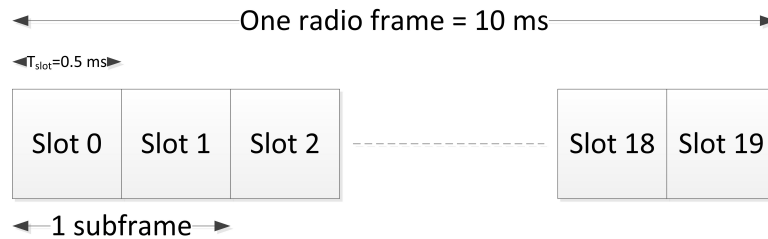


Figure C.4: *TDD-LTE frame structure.*

C.3 Downlink Transmissions

This subsection outlines the available resources in a LTE downlink transmission. A resource element is the smallest resource unit in LTE, shown in Figure C.5. A resource element makes reference to a symbol mapped in one subcarrier. The number of symbols per slot (N_{symb}^{Dl}) depends on the cyclic prefix length and subcarrier spacing. The number of subcarriers (N_{Sc}^{Rb}) may also be variant [25]. In this Thesis the number of symbols per slot has been set to seven and the number of subcarriers per resource block is set to 12. A downlink transmission may be composed by several resource blocks. The modulations allowed are BPSK, QPSK, 16QAM and 64QAM. Throughout this work only the last three modulation schemes have been evaluated.

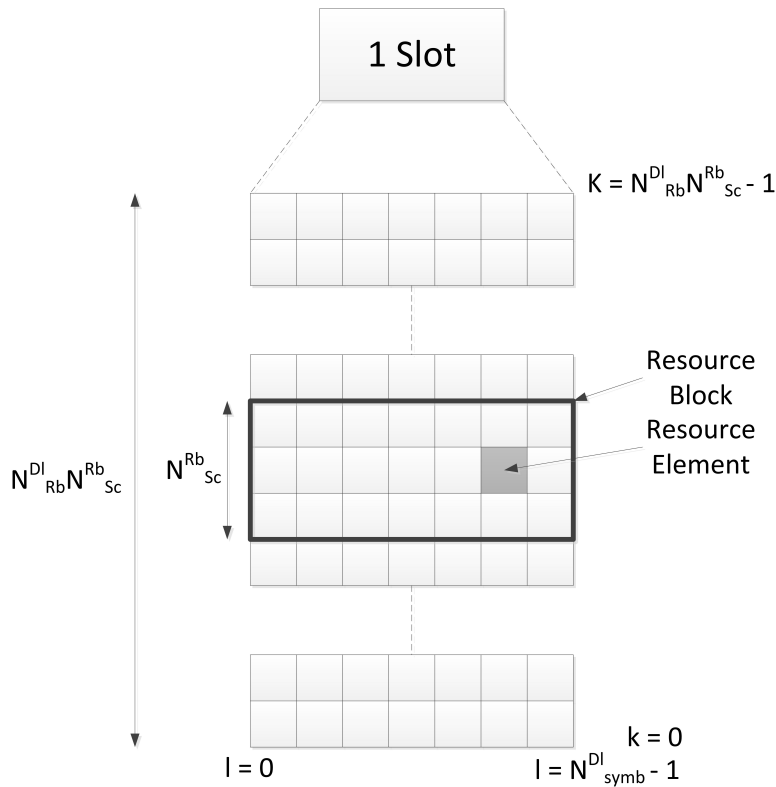


Figure C.5: Resources Scheme in LTE.

C.3.1 Throughput calculations

In this section the LTE throughput calculations are described according to the concepts previously explained. The number of LTE slots in a second can

be computed as:

$$N_{slot} = \frac{1}{T_{slot}} = 2000 \quad (C.3)$$

Taking into account the number of symbols per slot, and the N_{Sc}^{Rb} subcarriers the throughput would be:

$$Thr = 7 * N_{slot} * N_{Sc}^{Rb} * \log_2(M) \quad (C.4)$$

Where M is the modulation order of the mapped symbols.

Appendix D

USRP2 Architecture

This appendix describes the Universal Software Radio Peripheral (USRP) radio used in the experiment detailed in Chapter 6. It has to be remarked that two different USRP's were used: an USRP2, and a NI-USRP 2921. Both radios have similar features and architecture. Since the purpose of this Appendix is to provide a basic understanding of the tools utilized in the experiment only the USRP2 will be described. A more detailed description of the NI-USRP 2921 can be found in [45].

The concepts explained in this Appendix have been adapted from [46].

D.1 USRP2 Basic Description

The USRP2 is based in "a low-IF architecture which combines elements from a traditional super-heterodyne analog complex down-conversion architecture and the more recent digital domain down-conversion technology" [46]. Figure D.1 features a typical low-IF receiver. The "Stage 1" converts the radio frequency to a low intermediate frequency. The stage 2 digitally converts the low-IF to a zero center frequency and also filters the image frequency.

A USRP2 can be divided in two main components, the daughterboard and the FPGA.

D.1.1 Daughterboard

The daughterboard processes the radio frequency and converts it to the USRP working band. There are a large variety of daughterboards compatible with the USRP. The RFX900 daughterboard was used for the experiment described in Chapter 6. "The RFX900 is a high-performance transceiver designed specifically for operation in the 900 MHz band. With a typical power output of 200 mW, and noise figure of 8 dB. Jumper settings can

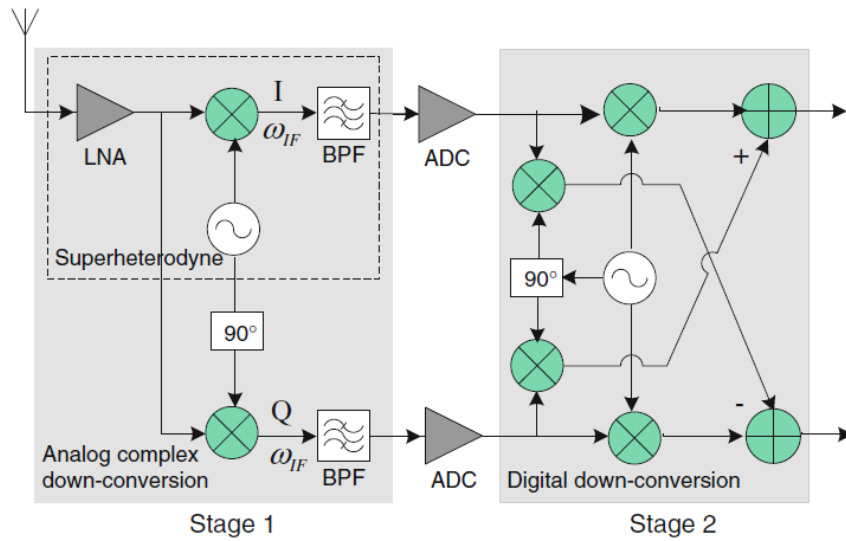


Figure D.1: Typical low-IF receiver architecture [46].

bypass an on-board Surface Acoustic Wave (SAW) filter to allow operation in a wider frequency range." [47].

D.1.2 Field Programmable Gate Array (FPGA)

The FPGA performs the digital processing. The FPGA is typically composed of:

- A complex down converter that is in charge of shifting the signal to zero frequency.
- A decimator, implemented as a four cascade integrator-comb filter.
- A half-band filter.

List of Abbreviations

3GPP 3rd Generation Partnership Project

AWGN Additive White Gaussian Noise

BS Base Station

BEP Bit Error Probability

BER Bit Error Rate

BPSK Binary Phase-Shift Keying

C/I Carrier to Interferer Power Ratio

CDF Cumulative Distribution Function

CDMA Code Division Multiple Access

CEPT European Conference of Postal and Telecommunications Administrations

CIR Carrier to Interferer plus noise Ratio

CM-SAIC Constant Modulus Single Antenna Interference Cancellation

D2D Device to Device

D2I Device to Infrastructure

DIR Dominant to Rest Interferer Ratio

eNodeB Evolved Node B or E-UTRAN Node B

FDD Frequency Division Duplex

FDMA Frequency Division Multiple Access

FCC Federal Communications Commission

FEP Frame Error Probability

FOSS Free and Open-Source Software

GERAN GSM EDGE Radio Access Network

GMSK Gaussian Minimum Shift Keying

GPRS General Packet Radio Service

GSM Global System for Mobile Communications

IoT Internet of Things

ISI Inter Symbol Interference

ISM Industrial Scientific and Medical

LOS Line-of-sight

LTE Long Term Evolution

METIS Mobile and wireless communications Enablers for the Twenty-
twenty Information Society

MIMO Multiple Input Multiple Output

M2M Machine to Machine

MS Mobile Station

MTC Machine-Type Communications

OC-D2D operators controlled D2D

OFDM Orthogonal Frequency Division Multiplexing

OFDMA Orthogonal Frequency Division Multiple Access

OTT Over The Top

PAPR Peak-to-Average Power Ratio

PDF Probability Density Function

PER Packet Error Rate

PLL Phase-Locked Loop

PSK Phase Shift Keying

PSR Packet Success Rate

QAM Quadrature Amplitude Modulation

QOS Quality Of Service

ROI Return over Investment

RRH Remote Radio Head

SAIC Single Antenna Interference Cancellation

SIR Signal to Interference Ratio

SIC Successive Interference Cancellation
SNR Signal Noise Ratio
SSR Symbol Success Rate
SUD Single user decoding
TSC Training Sequence
UE User Equipment
UTRAN Universal Terrestrial Radio Access Network
US United States
SINR Signal to Interfering Noise Ratio
USRP Universal Software Radio Peripheral
SER Symbol Error Rate
SDR Software Defined Radio
TDD Time Division Duplex
TDMA Time Division Multiple Access
FPGA Field Programmable Gate Array
FSR Frame Success Rate
QPSK Quadrature Phase Shift Keying
EDGE Enhanced Data Rates for GSM Evolution

List of Figures

2.1	Transition from D2I system to a D2D system. Figure adapted from [6].	6
2.2	Reference scenario: a legacy device coexisting with a D2D link in the same frequency uplink.	7
3.1	Transmission Power level to packet recognized at the receiver (PRR) [20].	13
4.1	Representation of the different SIR zones for the reference scenario of Figure 2.2 on page 7.	14
4.2	Example of zone delimitation as a function of the SIR.	15
4.3	Example of sharing spectrum for LTE and GSM.	16
4.4	OFDMA and GMSK in frequency.	19
4.5	Algorithm flowchart.	21
5.1	Bit success rate for GMSK with one GMSK interfering signal over a AWGN channel.	24
5.2	Bit success rate for OFDM with one GMSK interfering signal over a AWGN channel.	26
5.3	Bit success rate for GMSK with one OFDM interfering signal over a AWGN channel.	26
5.4	Bit success rate for a OFDM signal using QPSK modulated subcarriers under the interference of a GMSK signal over a AWGN channel after applying SIC.	27
5.5	Bit success rate for a GMSK signal under the interference of a OFDM signal using QPSK modulated subcarriers over a AWGN channel after applying SIC.	28
5.6	Bit success rate for a OFDM signal using 64-QAM modulated subcarriers, under the inference of a GMSK signal over a AWGN channel after applying SIC.	29
5.7	Bit success rate for a GMSK signal under the interference of a OFDMA signal using 64-QAM modulated subcarriers over a AWGN channel after applying SIC.	30

5.8	Bit success rate for OFDM with one GSMK interfering signal over a AWGN channel using the proposed algorithm	31
5.9	Bit success rate for GSMK with one OFDM interfering signal over a AWGN channel using the proposed algorithm.	31
5.10	Bit success rate for GSMK with one OFDM interfering signal with 12 subcarriers over a AWGN channel using the proposed algorithm.	32
5.11	Bit success rate for GSMK with one OFDM interfering signal with 12 subcarriers over a AWGN channel using the proposed algorithm.	33
5.12	FSR for OFDM over a AWGN channel.	35
5.13	FSR for GSMK over a AWGN channel.	35
5.14	FSR for OFDM over a AWGN channel with a OFDM interfering signal.	36
5.15	FSR for GSMK over a AWGN channel with a GSMK interfering signal.	37
5.16	FSR for OFDM over a AWGN channel with a GSMK interfering signal using the proposed algorithm.	37
5.17	FSR for GSMK over a AWGN channel with a OFDM interfering signal using the proposed algorithm.	38
5.18	Simulated System Level Scenario from the device point of view.	39
5.19	Simulated System Level Scenario from the Base Station point of view.	40
5.20	Throughput for OFDM and GSMK over a AWGN channel.	41
5.21	Throughput for OFDM and GSMK over a fading channel.	41
5.22	Throughput for OFDM and GSMK for a deterministically placed interfering source.	43
5.23	Throughput for OFDM and GSMK, randomly placing the source of the interference signal when the channel is considered AWGN.	44
5.24	Throughput for OFDM and GSMK, randomly placing the source of the interference signal through a fading channel.	45
5.25	Throughput for orthogonal and shared resources systems over AWGN channel.	46
5.26	Throughput for orthogonal and shared resources systems over fading channel.	46
5.27	FSR for OFDM applying the proposed algorithm and SIC for a SNR of -4 dB.	47
5.28	Simulation Scenario from the eNodeB point of view.	49
5.29	Computed losses from the eNodeB to the different floors in the scenario.	50
5.30	Success probabilitiy for the GSM system using a channel in exclusivity.	50

5.31	Success probability for the GSM system sharing a channel with a D2D system with no Interference Cancellation.	51
5.32	Success probability for the GSM system sharing a channel with a D2D system with Interference Cancellation.	52
5.33	Comparison of the Frame succes probabilitiy for a GSM system sharing a channel with a D2D system using/not using an Interference Cancellation scheme.	53
5.34	Proposed Scenario from the D2D UE point of view.	54
5.35	Computed losses from the MS to the different floors in the scenario.	55
5.36	Success probability for the D2D system using a channel in exclusivity.	56
5.37	Success probability for the D2D system sharing a channel with a GSM system with no Interference Cancellation.	57
5.38	Success probability for the D2D system sharing a channel with a GSM system with no Interference Cancellation.	58
5.39	Comparison of the Succes probabilitiy for a D2D system sharing a channel with a GSM system using/not using an Interference Cancellation scheme.	59
6.1	Sketch of the ideal implementation setup.	62
6.2	Sketch of the setup used to establish a reference case. For both links the PSR is measured at the receiver.	62
6.3	Picture of the implemented GMSK link.	65
6.4	Scheme of the implemented setup.	65
6.5	GNU Radio GMSK Modulator.	66
6.6	GNU Radio GMSK Demodulator.	66
6.7	Block Diagram of a receiver with a Mueller and Muller synchronizer [24].	67
6.8	Example of error calculation in Mueller and Muller.	68
6.9	Received and regenerated GMSK slot for a SIR of 10 dB. . .	70
6.10	Interference Cancellation Block Diagram with side information	70
6.11	Phase difference between the received and regenerated GMSK slot for a SIR of 20 dB.	71
6.12	Block Diagram of the proposed interference cancellation scheme.	71
6.13	Bit Success Rate for an antenna separation of 70 cm.	72
6.14	Bit Success Rate for an antenna separation of 70 cm assuming side information.	72
6.15	Relative rms between the subtracted and original OFDM signals for phase estimation IC and simple IC cases.	73
6.16	Bit Success Rate for an antenna separation of 20 cm.	74
6.17	Bit Success Rate for an antenna separation of 20 cm with access to side information.	74

6.18	Phase shift estimator performance for a SIR level of 0.3 dB taking into account side information.	75
6.19	rms ratio between, the received and regenerated signal subtraction, and the OFDM. Taking into account side information.	75
A.1	Illustration of the 2 ray path model.	81
A.2	Typical Rayleigh fading.	82
A.3	Frequency Division Duplex Scheme.	83
A.4	Time Division Duplex Scheme.	83
A.5	FDMA Channels scheme.	84
A.6	TDMA Channels scheme.	85
A.7	Cluster Scheme: example of frequency allocation and clusters.	86
B.1	GMSK modulator.	87
B.2	GSM Access Scheme for the uplink in the 900 MHz band.	89
B.3	GSM Normal Data Burst.	89
C.1	FDMA example.	90
C.2	OFDM subcarrier Spacing [29].	91
C.3	OFDM Modulator [29].	91
C.4	TDD-LTE frame structure.	92
C.5	Resources Scheme in LTE.	93
D.1	Typical low-IF receiver architecture [46].	96

List of Tables

5.1	Parameters of the simulation.	24
5.2	Parameters of the reference cases simulation.	25
5.3	Parameters of the simulation.	34
5.4	Parameters of the simulation.	48
6.1	Relevant signal characteristics of the GSM system [4].	61
6.2	OFDM and System simulation parameters	64

Bibliography

- [1] P. Bhat, S. Nagata, L. Campoy, I. Berberana, T. Derham, G. Liu, X. Shen, P. Zong, and J. Yang, "Lte-advanced: an operator perspective," *Communications Magazine, IEEE*, vol. 50, no. 2, pp. 104–114, February 2012.
- [2] L. Lei, Z. Zhong, C. Lin, and X. Shen, "Operator controlled device-to-device communications in lte-advanced networks," *Wireless Communications, IEEE*, vol. 19, no. 3, pp. 96–104, June 2012.
- [3] GSMA, "GSMA Public Policy Position: Spectrum Auctions," October 2012.
- [4] J. Eberspacher, H.-J. Vogel, and C. Bettstetter, *GSM Switching, Services and Protocols*. Wiley, 2001.
- [5] ETSI, "Feasibility study on single antenna interference cancellation (SAIC) for GSM networks." February 2012.
- [6] P. Phunchongharn, E. Hossain, and D. Kim, "Resource allocation for device-to-device communications underlying lte-advanced networks," *Wireless Communications, IEEE*, vol. 20, no. 4, pp. 91–100, August 2013.
- [7] K. Doppler, M. Rinne, C. Wijting, C. Ribeiro, and K. Hugl, "Device-to-device communication as an underlay to lte-advanced networks," *Communications Magazine, IEEE*, vol. 47, no. 12, pp. 42–49, Dec 2009.
- [8] P. Hoeher, S. Badri-Hoeher, W. Xu, and C. Krakowski, "Single-antenna co-channel interference cancellation for tdma cellular radio systems," *Wireless Communications, IEEE*, vol. 12, no. 2, pp. 30–37, April 2005.
- [9] N. Miridakis and D. Vergados, "A survey on the successive interference cancellation performance for single-antenna and multiple-antenna ofdm systems," *Communications Surveys Tutorials, IEEE*, vol. 15, no. 1, pp. 312–335, First 2013.

- [10] D. Son, B. Krishnamachari, and J. Heidemann, "Experimental study of concurrent transmission in wireless sensor networks," in *Proceedings of the 4th International Conference on Embedded Networked Sensor Systems*, ser. SenSys '06. New York, NY, USA: ACM, 2006, pp. 237–250. [Online]. Available: <http://doi.acm.org/10.1145/1182807.1182831>
- [11] Y.-U. Jang and E.-R. Jeong, "Opportunistic power control for successive interference cancellation," *Communications Letters, IEEE*, vol. 15, no. 3, pp. 296–298, March 2011.
- [12] J. Andrews and T. Meng, "Optimum power control for successive interference cancellation with imperfect channel estimation," *Wireless Communications, IEEE Transactions on*, vol. 2, no. 2, pp. 375–383, Mar 2003.
- [13] W.-J. Choi, K.-W. Cheong, and J. Cioffi, "Iterative soft interference cancellation for multiple antenna systems," in *Wireless Communications and Networking Conference, 2000. WCNC. 2000 IEEE*, vol. 1, 2000, pp. 304–309 vol.1.
- [14] R. Ramesh, H. Arslan, A. Hafeez, and D. Hui, "Single antenna interference cancellation for 8psk signals in egrps," in *Vehicular Technology Conference, 2009. VTC Spring 2009. IEEE 69th*, April 2009, pp. 1–5.
- [15] H. Trigui and D. T. M. Slock, "Cochannel interference cancellation within the current gsm standard," in *Universal Personal Communications, 1998. ICUPC '98. IEEE 1998 International Conference on*, vol. 1, Oct 1998, pp. 511–515 vol.1.
- [16] X. long Meng, Z. Liu, and W.-L. Jiang, "A single antenna interference cancellation algorithm based on fictitious channels filtering," in *Signal Processing (ICSP), 2012 IEEE 11th International Conference on*, vol. 1, Oct 2012, pp. 179–182.
- [17] A. Hafeez, D. Hui, and H. Arslan, "Interference cancellation for edge via two-user joint demodulation," in *Vehicular Technology Conference, 2003. VTC 2003-Fall. 2003 IEEE 58th*, vol. 2, Oct 2003, pp. 1025–1029 Vol.2.
- [18] M. Pukkila, G. Mattellini, and P. Ranta, "Constant modulus single antenna interference cancellation for gsm," in *Vehicular Technology Conference, 2004. VTC 2004-Spring. 2004 IEEE 59th*, vol. 1, May 2004, pp. 584–588 Vol.1.
- [19] C. Masouros, T. Ratnarajah, M. Sellathurai, C. Papadias, and A. Shukla, "Known interference in the cellular downlink: a performance

- limiting factor or a source of green signal power?" *Communications Magazine, IEEE*, vol. 51, no. 10, pp. 162–171, October 2013.
- [20] K. Whitehouse, A. Woo, F. Jiang, J. Polastre, and D. Culler, "Exploiting the capture effect for collision detection and recovery," in *Embedded Networked Sensors, 2005. EmNetS-II. The Second IEEE Workshop on*, May 2005, pp. 45–52.
- [21] M. E. Şahin, I. Guvenc, and H. Arslan, "An iterative interference cancellation method for co-channel multicarrier and narrowband systems," *Physical Communication*, vol. 4, no. 1, pp. 13 – 25, 2011. [Online]. Available: <http://www.sciencedirect.com/science/article/pii/S1874490710000297>
- [22] "Digital cellular telecommunications system (phase 2+); radio transmission and reception (gsm 05.05)," March 1996.
- [23] X. Lin and H. Viswanathan, "Dynamic spectrum refarming with overlay for legacy devices," *Wireless Communications, IEEE Transactions on*, vol. 12, no. 10, pp. 5282–5293, October 2013.
- [24] H. Meyr, M. Moeneclaey, and S. A. Fechtel, *Digital Communications Receivers, Synchronization, Channel Estimation and Signal Processing*. Wiley, 1998.
- [25] "3GPP TS 36.211 version 11.4.0 Release 11: Evolved Universal Terrestrial Radio Access (E-UTRA); physical channels and modulation," October 2013.
- [26] S. Ghnimi, A. Rajhi, and A. Gharsallah, "Ber performance of gmsk modulation under radio mobile propagation environments," in *Mediterranean Microwave Symposium (MMS), 2011 11th*, Sept 2011, pp. 305–308.
- [27] L. Rugini and P. Banelli, "Ber of ofdm systems impaired by carrier frequency offset in multipath fading channels," *Wireless Communications, IEEE Transactions on*, vol. 4, no. 5, pp. 2279–2288, Sept 2005.
- [28] P. Prakasam and M. Madheswaran, "Automatic modulation identification of qpsk and gmsk using wavelet transform for adaptive demodulator in sdr," in *Signal Processing, Communications and Networking, 2007. ICSCN '07. International Conference on*, Feb 2007, pp. 507–511.
- [29] E. Dahlman, S. Parkvall, and J. Skold, *4G LTE/LTE-Advanced for Mobile Broadband*. Elsevier, 2011.

- [30] C. B. Schlegel and L. C. Perez, *Trellis and Turbo Coding*. Wiley-IEEE, 2004.
- [31] G. T. G. M. 46, “RACH intensity of time controlled MTC devices,” 2010.
- [32] M. F. Jose F. Monserrat, “Mobile and wireless communications Enablers for the Twenty-twenty Information Society - deliverable d6.1,” 2013.
- [33] H. Holma and A. Toskala, *WCDMA for UMTS: HSPA Evolution and LTE*. John Wiley and Sons, 2010.
- [34] —, *LTE for UMTS: OFDMA and SC-FDMA based radio access*. John Wiley and Sons, 2009.
- [35] M. Kjellsson, “USRP Implementation Strategies,” Master’s thesis, KTH Electrical Engineering, 2010. [Online]. Available: <http://www.ee.kth.se/php/modules/publications/reports/2010/IR-SB-XR-EE-SB%202010:006.pdf>
- [36] “GNU Radio Wiki.” [Online]. Available: <http://gnuradio.org/redmine/projects/gnuradio/wiki>
- [37] “It++ documentation.” [Online]. Available: <http://itpp.sourceforge.net/4.3.1/>
- [38] L. com Global Connectivity, “Hyperlink wireless 2.4 ghz to 5.8 ghz 3 dbi tnc-male tri-band rubber duck antenna.” [Online]. Available: <http://L-com.com>
- [39] F. Ge, C. Chiang, Y. Gottlieb, and R. Chadha, “Gnu radio-based digital communications: Computational analysis of a gmsk transceiver,” in *Global Telecommunications Conference (GLOBECOM 2011)*, 2011 IEEE, Dec 2011, pp. 1–6.
- [40] M. on Pun, M. Morelli, and C. C. J. Kuo., *Multi-Carrier Techniques For Broadband Wireless Communications: A Signal Processing Perspectives*. London, UK: Imperial College Press, 2007.
- [41] “Implementing an OFDM transceiver by Software Defined Radio,” 2009. [Online]. Available: https://www.troopers.de/wp-content/uploads/2011/10/TR12_TelcoSecDay_Welte_Mobsec.pdf
- [42] M. Berner, “Timing and Carrier recovery,” 2005.
- [43] A. Goldsmith, *Wireless Communications*. Cambridge University Press, 2005.

- [44] H. Holm and A. Toskala, *LTE for UMTS - Evolution to LTE-Advanced*. Wiley, 2011.
- [45] National Instruments, “NI USRP-2920, NI USRP-2921 Universal Software Radio Peripherals.” [Online]. Available: <http://www.trinergy.co.th/pdf/usrp.pdf>
- [46] S. Peng and Y. Morton, “A usrp2-based reconfigurable multi-constellation multi-frequency gnss software receiver front end,” *GPS Solutions*, vol. 17, no. 1, pp. 89–102, 2013. [Online]. Available: <http://dx.doi.org/10.1007/s10291-012-0263-y>
- [47] E. Research, “Rfx900 750-1050 mhz rx/tx.” [Online]. Available: <https://www.ettus.com/product/details/RFX900>

List of Corrections